TOPICAL REVIEW

Self-assembled peptide nanostructures for functional materials

To cite this article: Melis Sardan Ekiz *et al* 2016 *Nanotechnology* **27** 402002

IOP Publishing Nanotechnology
Nanotechnology 27 (2016) 402002 (37pp) doi:10.1088/0957-4484/27/40/402002

Topical Review

Self-assembled peptide nanostructures for functional materials

Melis Sardan Ekiz, Goksu Cinar, Mohammad Aref Khalily and Mustafa O Guler

Institute of Materials Science and Nanotechnology, National Nanotechnology Research Center (UNAM), Bilkent University, Ankara, 06800 Turkey

E-mail: moguler@unam.bilkent.edu.tr

Received 29 April 2016, revised 18 June 2016
Accepted for publication 5 July 2016
Published 31 August 2016

Abstract

Nature is an important inspirational source for scientists, and presents complex and elegant examples of adaptive and intelligent systems created by self-assembly. Significant effort has been devoted to understanding these sophisticated systems. The self-assembly process enables us to create supramolecular nanostructures with high order and complexity, and peptide-based self-assembling building blocks can serve as suitable platforms to construct nanostructures showing diverse features and applications. In this review, peptide-based supramolecular assemblies will be discussed in terms of their synthesis, design, characterization and application. Peptide nanostructures are categorized based on their chemical and physical properties and will be examined by rationalizing the influence of peptide design on the resulting morphology and the methods employed to characterize these high order complex systems. Moreover, the application of self-assembled peptide nanomaterials as functional materials in information technologies and environmental sciences will be reviewed by providing examples from recently published high-impact studies.

Keywords: peptide, nanomaterials, self-assembly, nanofiber

(Some figures may appear in colour only in the online journal)

1. Introduction

Molecular self-assembly is an emerging and powerful tool in the synthesis of functional nanoscale structures as a bottom-up fabrication method. It is defined as the spontaneous organization of molecules into stable, well-defined structures under equilibrium conditions through noncovalent interactions. Self-assembly is ubiquitous in many biological systems and results in the formation of a variety of complex biological structures found in nature. These complex and elegant examples inspire scientists to create similar artificial systems by using the building blocks of life, such as amino acids, lipids, nucleic acids and saccharides. In most cases, thermodynamically stable structures are formed through enthalpic and entrophic interactions that involve both the assembling subunits and the surrounding solvent molecules [1]. Naturally, many key developments have paved the way for progress in this sophisticated field, such as the discovery of close-packed forms of amphiphilic molecules, the arrangement of monolayers by long chain hydrocarbon amines and the distribution of ordered monolayers of alkanethiolate molecules on gold substrates [2].

In this review, we describe peptide synthesis strategies, peptide self-assembly and the relation of the peptide design to the corresponding self-assembled nanostructures. In addition to the synthesis and functionalization of peptide nanostructures, we also provide an overview of the characterization techniques that have been developed for understanding the interactions between individual peptide subunits and their effect on the physical and chemical properties exhibited by the self-assembled system. The peptide nanostructures are considered to be attractive candidates for a broad range of

biomedical applications, and have already been reviewed extensively [3–6]. Here we present recent applications of peptide-based nanomaterials by providing specific examples such as peptide-templated inorganic nanomaterials, semiconducting peptide nanowires and catalytic peptides.

2. Peptides: synthetic approaches

Peptides consisting of natural or synthetic amino acids are interesting building blocks for the construction of supramolecular assemblies. These simpler structures aid us in understanding more complex systems present in nature. Scientists employ a variety of approaches in the synthesis of peptide building blocks and strive for the production of the peptide of interest while minimizing or eliminating other possible by-products. Synthetic approaches utilized for the fabrication of peptide molecules can be classified into three main classes: solid phase strategies, ring-opening polymerization techniques and genetic engineering [7, 8].

Solid phase peptide synthesis (SPPS) is the most widely used method for the synthesis of small to medium size peptides. In this technique, the peptide sequence is grown, step-by-step, on an insoluble polymeric resin through the sequential addition of individual amino acids. Deviations from the intended amino acid sequence are prevented through use of modified amino acids with unreactive N-termini, which can be activated only after treatment with a deprotecting agent [9]. Amino acids used for the couplings bear orthogonal protecting groups. The orthogonal chemistry approach enables two or more protecting groups to be used concurrently without affecting each other in situations where one of the functional groups requires manipulation. General features associated with these protecting groups can be considered as (i) their ease of introduction into the functional group; (ii) their stability in different reaction conditions; and (iii) their safe removal at the end of the synthetic process [10]. Prior to the coupling, there is a need to activate the carboxylic group of the last amino acid in the sequence by using phosphonium, aminium, uronium or carbodiimide-based reagents that catalyse the formation of amide bonds. Although carbodiimide derivatives lead to an increase in the degree of racemization during the activation of amino acids, this effect can be minimized by using additives, especially N-hydroxy derivatives, which suppress the formation of N-acylurea by shifting the reaction towards the formation of the active ester form of the amino acid [11]. At the end of the synthesis, the peptide is cleaved from the resin with an acid treatment.

Microwave-assisted SPPS is another option for synthesizing longer peptides with increased reaction rates and purities. Typically, coupling reagents and additives used in microwave-assisted SPPS are identical to those applied in conventional SPPS, and peptide couplings are carried out at temperatures in the range 50 °C–80 °C unless amino acids carry a potential risk of epimerization [12]. Setbacks encountered in solution phase synthesis, such as time consuming isolation and purification of intermediate peptides, are overcome with SPPS. With the SPPS strategy, it is possible to control not only the amino acid sequence but also the C- and N-terminal functionality of the created peptide [13]. Therefore, this technique is eligible for the synthesis of linear, branched, dendritic or cyclic peptides [14, 15]. In addition, different chemical moieties, such as fatty acids, lipids, saccharides, nucleotides, polymers, drugs, aromatic units and dyes can be incorporated into the peptide backbone through linkage chemistry while the peptide is still on the resin. - Further progress in peptide synthesis is native chemical ligation, which bypasses the limitations of SPPS with respect to the size and solubility of the peptides, and entails the chemoselective conjugation of two unprotected peptides (an α-thioester-containing peptide and an N-terminal cysteine-ended peptide) through thioester linkage. These peptides are first individually synthesized using SPPS, and subsequently linked to each other in the solution phase to create large-sized peptides and even complex proteins [16].

On the other hand, the preparation of high molecular weight monodisperse polypeptides with precisely defined primary structures can be achieved by protein engineering, also called genetic engineering. This strategy allows the synthesis of not only structural proteins but also *de novo* designed proteins as a result of the cellular expression of artificial genes [17]. In contrast to chemical synthesis methods, this technology can be considered as a biological tool for the preparation of peptide-based materials, and involves insertion of a synthetically designed gene into a circular DNA plasmid to produce the desired polypeptide or protein in bacterial or eukaryotic expression systems [18]. One of the advantages of this methodology is that a broad range of nonproteogenic amino acids or functional groups can also be integrated for the preparation of artificial proteins [19].

Polypeptides with high molecular weights, narrow polydispersity and retained chiral integrity can be synthesized by the ring-opening polymerization of amino acid N-carboxyanhydrides (NCA) in a controlled manner [20]. For the polymerization, there are two widely accepted mechanisms: normal amine and the activated monomer mechanisms. In both mechanisms, a range of nucleophiles and bases such as amines and metal alkoxides are used for the initiation of polymerization [21]. Although NCA polymerization suffers from a lack of control over the exact primary peptide sequence, in contrast to SPPS or genetic engineering, it allows the synthesis of polypeptides in high yields and large quantities [22]. In some cases, side reactions that occur during NCA polymerization may result in failure in the production of homo and block polypeptides, which can be prevented by introducing various metal- and organo-catalysts [20]. In addition, some applications require using high purity monomers to obtain optically pure polypeptides with predictable molecular weights and low polydispersity.

Several other chemical methodologies have been developed to synthesize peptide- and protein-based hybrids. Anchorage of two components has been achieved through thiol–maleimide or alkyne–azide couplings as well as by imine and hydrazone linkages, atom transfer radical polymerization and chemoselective peptide ligation methods [8, 23, 24]. Although each strategy has its own limitations,

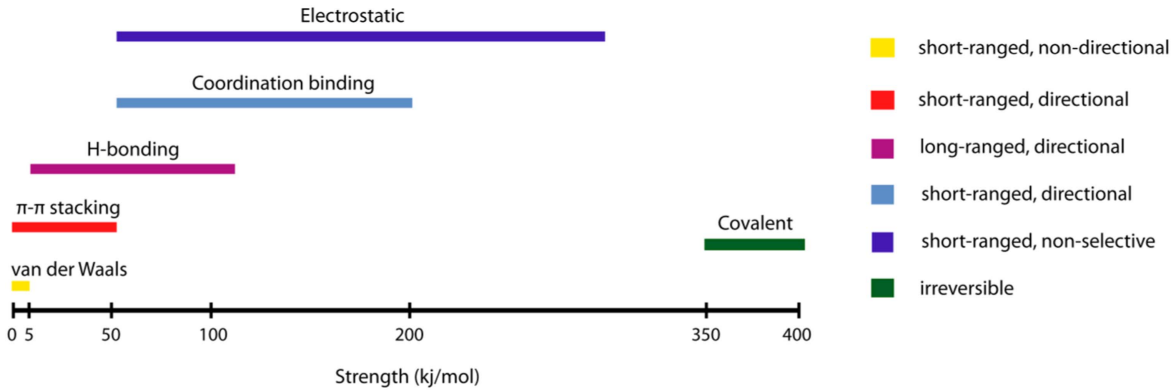

Figure 1. Strength and properties of the noncovalent interactions involved in self-assembly.

with recent advances in synthetic strategies, sophisticated peptidic architectures can be created by using these versatile chemical tools.

3. Self-assembly of peptides

Amino acids serve as a diverse biochemical toolbox for the construction of peptide-based materials, exhibiting a broad range of physicochemical properties with regards to their charge, hydrophobicity, size and polarity. Consequently, peptide materials containing different amino acid sequences can be designed to serve a variety of biological functions. This diversity is further enriched by the introduction of nonproteinogenic groups into the peptide backbone. Since the synthesis methods, structures and properties of peptides are well known, peptide-based materials can also be utilized as model systems to gain insight into biological self-assembly mechanisms in nature [25]. Peptide self-assembly is mainly governed by noncovalent interactions. These interactions not only drive the self-assembly process but also stabilize the secondary structure of peptides and proteins [26].

3.1. Forces driving peptide self-assembly

Noncovalent interactions such as hydrogen bonding, hydrophobic, electrostatic and van der Waals interactions, π–π stacking and coordination bonds are the main contributors of molecular self-assembly (figure 1) [27, 28]. While nonpolar amino acids, including aliphatic (e.g. alanine, leucine, valine) and aromatic (e.g. tyrosine, phenylalanine) amino acids, are mainly responsible for hydrophobic clustering through hydrophobic interactions and π–π stacking, respectively, polar amino acids result in either hydrogen bonding or electrostatic interactions depending on whether they have uncharged (e.g. serine, asparagine) or charged (e.g. lysine, histidine, glutamic acid) residues [29]. In addition to individual amino acids, the peptide backbone itself provides considerable stability through hydrogen bonds. Although these interactions are individually weak, the cooperative action of binding residues across multiple self-assembling subunits can enable formation of stable assemblies. The cooperative binding also ensures a degree of sequence-specificity in the self-assembling system [30].

Naturally occurring hydrogen bonding patterns, such as those found in β-sheets, α-helices, and coiled coils, are utilized in the design of a number of peptide sequences to form higher order structures as a result of self-assembly. The stabilization of multiple peptide backbone arrangements occurs through hydrogen bonding interactions between the backbone amide and carbonyls and results in the formation of β-sheets. These structures may be in parallel or antiparallel arrangements depending on the direction of the strands. Peptides are typically designed to contain repeating amino acid residues for hydrophobic and hydrophilic regions, which ensure that the hydrophobic part will be buried within the self-assembled structure while the hydrophilic region, which often contains functional sequences, is exposed to the aqueous environment [31]. Unlike β-sheets, α-helices are formed by individual peptide chains where backbone amide components are intramolecularly hydrogen bonded. This arrangement leads to the presentation of the amino acid side chains on the surface of each helix and further facilitates the accessibility of amino acid side chains to the solvent. In some cases, these single α-helices can assemble by coiling together and form so-called coiled coils. Peptide sequences responsible for coiled coil formation generally bear a repeat motif consisting of seven residues. These *heptad* motifs can be derived using generalized wheel diagrams that denote the positions and biochemical properties of amino acids at each location. The rules governing the formation of coiled coil structures are well-studied and conceived. In this section of the review, we present a relatively brief discussion for the H-bonding patterns exploited in peptide self-assembly, however, there are comprehensive reviews in the literature [32, 33].

3.2. Factors triggering self-assembly

There is a growing interest in creating dynamic systems that assemble and disassemble in response to external cues. Since noncovalent interactions are delicate interactions, they have a great tendency to respond to alterations in environmental conditions such as pH, light, temperature, ionic strength, and solvent polarity [34]. Among these, pH switch is the most facile approach for controlling and directing the self-

assembly [35–39]. A number of peptides are inherently sensitive to pH change due to the introduced charged amino acids, leading to a structural transformation. Apart from pH stimuli, light-triggered systems designed by van Hest and Stupp groups were developed by using a photocleavable group bearing peptide amphiphiles, and morphological transitions were observed for both cases in response to light [40–42]. Furthermore, polymerizable diacetylene unit containing peptide molecules were shown to respond to UV light irradiation to acquire one-dimensional nanostructures by the -Tovar group [43]. On the other hand, thermally triggered peptide-based materials causing a change in the self-assembly of the nanostructure have been reported by several groups [44–49]. In addition to thermal energy, the Ulijn group has demonstrated that ultrasound energy can assist the reorganization of supramolecular nanostructures by temporarily disrupting noncovalent interactions in the peptide system and subsequently allowing their reformation in more thermodynamically favourable positions [50]. In addition, the effect of ionic strength and metal ions on the self-assembly mechanism of peptide molecules were examined by the addition of different type of cations into the peptide-based systems. While charged amino acids are mainly responsible for salt-induced self-assembly, as in the case of ionic-complementary peptides [51], β-hairpin peptides [52], ultrashort peptides [53] and peptide amphiphiles [54, 55], histidine residues have been predominantly used in the metal-binding domain due to the affinity of the imidazole ring to several coordination metal ions [56–59]. In addition to the above-mentioned external stimulus factors, solvent polarity can also exert a profound effect on the supramolecular nanostructures. A solvent controlled structural transition was observed for several peptides due to the changed interactions between the hydrophobic domain of the peptide and solvent molecules [60–63]. The self-assembly mechanism can be alternatively induced by enzyme catalysed reactions. Structural switches can be employed in a controllable manner by using enzymes specific to peptide sequences [64–68].

4. Design–nanostructure relation in peptide-based systems

The number, type, and sequence of amino acids can be manipulated to design self-assembling peptides. When amino acids are considered individually, they have their own specific characteristics. For instance, glycine imparts flexibility to the peptide structure, as it lacks a side chain and does not carry steric hindrance, while the proline ring constrains the number of conformations that the peptide backbone can adopt, resulting in a high degree of conformational rigidity [69, 70]. Cysteine, on the other hand, can be chemically or intermolecularly modified via thiol–maleimide chemistry or disulphide bridging, respectively. Moreover, tyrosine, serine and threonine are utilized in further chemical and enzymatic modifications through their hydroxyl groups. Depending upon the chemical modifications of the C- or N-terminus, the properties of peptide building blocks can also be modulated. There are two other major parameters affecting the structure of peptide-based systems, the secondary structure and noncovalent interactions, which were mentioned in the previous section. Peptides supported by α-helical or β-sheet features allow the construction of various different nanostructures [71, 72]. While peptide secondary structures are often sufficient to ensure the formation of kinetically and thermodynamically stable structures, conformational interactions can also be supported through linker residues that are covalently conjugated to peptide building blocks [73]. In this section, we discuss the structural features of peptide materials and highlight representative studies of self-assembled systems composed of peptide building blocks. This section is divided into three parts, which discuss the importance of design in the resulting self-assembled nanostructures of different classes of peptides, namely peptides composed of only amino acids, peptides modified by the attachment of hydrophobic acyl chains and peptide containing hybrid systems.

4.1. Peptides composed of only amino acids

Peptides highlighted in this section typically contain both hydrophobic and hydrophilic amino acid domains, as amphiphilic peptide designs readily self-assemble into well-organized nanostructures. The distribution and number of hydrophobic and hydrophilic amino acids in the peptide sequence determine the final structure, including nanofibre, nanotape, nanorod, nanovesicle, nanotube and micelle, of the self-assembling peptides. Depending on the nature of the hydrophobic domain, the aggregation propensity and, similarly, the critical aggregation concentration (CAC) of the peptides can be modulated, which is very important for the stability of the assembly in an aqueous environment [74]. Table 1 summarizes the sequences of the peptides discussed in this section, the morphology of the nanostructures they form, and additional information regarding the structural features they exhibit.

The Zhang group has designed several short (7–8 amino acid) peptides and described them as a new class of surfactant-like peptides (SLPs) [75]. In their design, six consecutive hydrophobic residues (A_6, V_6 or L_6) were attached to a head group with one or two aspartic acid residues, and charges on the N-termini were blocked by acetyl groups to prevent positive charge formation in the hydrophobic tail. The self-assembly of these peptides resulted in the formation of nanotubes or vesicles measuring ~30–50 nm in diameter. The type of nanostructure formed was affected by the hydrophobicity of the tail but not by the number of integrated charged residues. They also reported that similar peptides with two different positively charged (K and H) head groups exhibited analogous structures in transition electron microscopy (TEM) [96]. By using a similar design, the influence of the hydrophobic tail length on the formed nanostructure was investigated by Lu's group with A_3K, A_6K, and A_9K peptides [76]. These peptides exhibited structural transition as their hydrophobic tail extended due to the change in packing within the nanostructure. While A_3K self-assembled into unstable peptide sheet stacks, A_6K and A_9K formed long

Table 1. Recently reported peptide designs composed of only amino acids.

Peptide sequence	Structure	Details	References
X_6D_n (X = A, V, L and n = 1, 2)	Nanotube/vesicle	30–50 nm in diameter	[75]
Ac-A_mK-A_m (m = 3, 6 and 9)	Sheet/fibre—worm-like micelle/rod	Hydrophobic peptide region—structural transition relation	[76]
I_mK, L_mK (m = 3–5)	Micelle/nanofiber	Sequence dependent structural change	[77]
X_6K_2 (X = I, L and V)	Flat ribbon/ rod-like structure	Concentration dependent structural change	[78]
Ac-GAVILRR-Am	Nanodonut	Outer and inner diameters: 105 ± 12 nm and 22 ± 10 nm, respectively	[79]
$A_{12}R_2$	Twisted fibrils	Diameter of fibrils 5–6 nm, pitch size of a twist ~10 nm	[80]
$P_{10}R_3$-Am	Vesicle	Hydrodynamic radius (R_H) = 74 nm	[81]
Ac-PSPCFKFEP-Am	Nanofiber	(β-sheet + β-turn)	[82]
A_6H	Nanotape	Twisted nanotapes 38.3 ± 8.0 nm thick	[83]
X_6K_n (X = A, L and V; n = 1–5)	Nanotube/vesicle	Hydrophobicity-structure relation	[84]
Ac-$A_2V_2L_3WE_n$-COOH (n = 2 or 7)	Nanovesicle	Roughly 120 nm in diameter	[85]
EFL_4FE	Nanotube	Diameter of tubes = 20–30 nm	[86]
Ac-EFFAAE-Am/Ac-KFFAAK-Am	Nanofiber	Co-assembled system	[87]
Ac-X_3-C and oxidized forms Ac-X_3C-CX_3-Ac (X = A, V and I)	Nanosphere/fibre	Effect of dimerization on self-assembly	[88]
Ac-RARADADARARADADA-Am	Nanofiber	10–20 nm in diameter	[89]
Ac-FKFEFKFE-Am, Ac-KEFFFFKE-Am	Nanoribbon/nanotape	Sequence and concentration dependent structural change	[90]
*X*K*X*K*X*K*X*KV^{D}PPTK*X*K*X*K*X*K*X*-Am (X = Val, Abu, Nva, Nle, Phe and Ile)	Nanofiber	Average fibril width = 3.2–3.5 nm	[91]
cyclo-[(Q^{D}AE^{D}A)$_2$]	Nanotube/nanoparticle	Nanotube diameter ≈1 μm	[92]
cyclo-[(Q^{D}L)$_4$]	Fibre/bundle	Formation of fibres from nanotubes	[93]
cyclo[(WR)$_n$] (n = 3–5)	Vesicle	Ring size-vesicle size relation	[94]
Ac-K_2(QX)$_6K_2$-Am (X = L, F, W and Y)	Nanofiber	Multidomain peptides with ABA block motif	[95]

fibrillar worm-like micelles with uniform diameters of 8 ± 1 nm and short nanorods with smaller diameters of around 3 ± 1 nm, respectively. The morphological diversity of peptide nanostructures stems from the equally diverse nature of the interactions between their constituent amino acids, with both hydrophobic and hydrophilic residues imparting characteristic properties to the overall structure. To gain insight into this cooperative effect, Han *et al* synthesized a variety of peptides containing three to five consecutive leucine or isoleucine residues attached to one polar lysine residue [77]. They systematically studied the role of hydrogen bonding and its cooperative effect with hydrophobic interactions by changing the number and the type of the hydrophobic residues. As expected, an increase in the number of hydrophobic residues gave rise to a decrease in the CAC values of both L_mK and I_mK. Since isoleucine had a higher propensity to form β-sheet conformation, the I_mK series formed long nanofibers through the combination of hydrogen bonding and hydrophobic interactions, whereas L_3K self-assembled into spherical micelles. Moreover, the rest of the L_mK series exhibited nanofiber morphology due to the domination of intermolecular hydrogen bonding by additional leucine residues. In the case of I_mK assemblies, the diameter of the nanofibers gradually decreased as the number of isoleucine residues increased, stemming from the change in chain packing. In another comparative study conducted by Baumann and coworkers, I_6K_2, L_6K_2 and V_6K_2 peptides were prepared in an aqueous salt solution (2 mM NaCl) to investigate the concentration dependence of the aggregation [78]. Although the secondary structures of all three peptides remained steady over the wide range of concentrations, morphological inspection of the self-assembled peptide structures revealed that peptides showed variance in their nanostructures as their concentrations changed. While peptides prepared at lower concentrations tended to form rod- and sheet-like structures with different cross sections, the average rod length and ribbon/sheet area could be tuned by varying the concentration. The effect of the molecular geometry on the nanostructure formation and its relation to the concept of surfactant packing parameter were further analysed by Khoe *et al* [79]. A cone-shaped molecular structure (Ac-GAVILRR-Am) was synthesized using five subunits of increasing size and hydrophobicity, starting with small glycine and alanine residues and ending with two bulky arginine residues that function as a cationic head group. Above its CAC, it self-assembled into both vesicular and donut-shaped nanostructures. Experimental results, together with model fittings, demonstrated that donut-shaped nanostructures had outer and inner diameters of 110 and 25 nm, respectively. Additionally, the diameter of the spherical nanovesicles

were estimated to be around 41.5 nm, the same as the diameter of the average thickness of the donut-shaped structures. The cationic arginine head group was also used in another SLP design to integrate twelve alanine residues [80]. This oligomeric peptide was synthesized via the NCA polymerization method rather than the standard solid phase peptide synthesis method to prevent the aggregation problem encountered in the couplings of multiple identical amino acids. 2wt% samples were analysed in cryo-TEM and it was revealed that electrostatic repulsion between terminal arginine residues, together with hydrogen bonding of alanine residues, resulted in the formation of twisted fibrils. In another study, a proline-rich sequence was used instead of alanine-rich domains and one additional arginine residue was conjugated to the hydrophilic segment [81]. The change in the type of amino acid completely changed the self-assembly mechanism, leading to the formation of quite different supramolecular nanostructures. Owing to the fact that a pyrrolidine ring in proline is responsible for the conformational constraints, this block polypeptide formed stiff helical rod structures, known as polyproline type II (PPII) helices, in aqueous solution. In contrast, arginine residues provided flexibility to the structure. These two components created a rod-coil system that is capable of self-assembling into vesicular nanoaggregates with a unimodal distribution of hydrodynamic radii. Proline residues were used in another study at both N- and C-termini of a nine-residual peptide to reduce the hydrogen bonding network in the β-sheet structure at the strand ends, and to bend the peptide chain by forming turns, favouring the formation of interfibrillar structure [82]. Additionally, the hierarchical arrangement of these supramolecular aggregates exhibited a concentration dependent manner.

Unlike the above-mentioned SLPs, Castelletto *et al* introduced for the first time a histidine attached hexaalanine sequence, which had the ability to chelate to transition metal ions, particularly zinc cations, through its imidazole side chain [83]. They compared the structural differences between A_6H assemblies prepared in water and a $ZnCl_2$ containing solution at neutral and acidic pHs, and observed that while aqueous assemblies self-assembled into short sheets at pH 7, A_6H dissolved in $ZnCl_2$ solution formed pseudo-crystalline particles containing plate/tape-like sheets. This work examined the effect of the number and type of integrated hydrophobic residues on the resulting supramolecular nanostructure but not the length of the head group. Liu *et al* extended the hydrophilic amino acid chain length of X_6, where *X* was alanine, valine or leucine, by introducing one to five lysine residues [84]. Extending the hydrophilic chain length changed the surfactant-like character of peptides to a more block-type arrangement. Morphological analysis pointed out that alteration in the hydrophilicity varied the morphology of the peptide assemblies. Peptides with a longer hydrophilic segment but identical hydrophobic tail had a higher CAC, leading to the formation of vesicles rather than nanotubes. Accordingly, peptides having good solubility as well as very high CAC above the working concentration range failed to form any regular self-assembled structures. In another study done by van Hell *et al*, an approach previously used by the Zhang group [79] was adopted to synthesize cone-shaped amphiphilic peptides [85]. A conical shape was provided by the addition of amino acids having bulkier side chains near the charged glutamate residues at the C-terminus. However, here, two different peptides were synthesized with different lengths of hydrophilic domains ($Ac\text{-}A_2V_2L_3WE_{2/7}\text{-}COOH$). They formed nanovesicles of comparable size with a diameter of approximately 120 nm, irrespective of the number of glutamate residues found in the head group.

By contrast to the classical design of traditional amphiphilic peptides, the double-headed architecture of bolaamphiphiles, composed of a hydrophobic core and two hydrophilic moieties flanking both ends of the core, have received growing interest for their ability to form different self-assembled nanostructures [97–99]. Recently, the Hamley group reported that they designed a linear octapeptide (EFL_4FE) self-assembled into nanotubes with diameters of 20–30 nm at high concentrations (1wt%), whereas they tended to form sheet-like structures at lower concentrations [86]. In another study conducted by our group, co-assembly of oppositely charged Ac-EFFAAE-Am and Ac-KFFAAK-Am peptides at physiological pH resulted in the formation of nanofibers [87]. Recently, the Cui group devised several phenylalanine containing bolaamphiphiles, (EFFFFE, KFFFFK and EFFFFK), whose terminal charges were modulated to investigate the effect of electrostatic interactions on the resulting polymorphic nanostructure [100]. This led to the twisting of the β-sheet tapes and accordingly the formation of fibrils, twisted ribbons and belts.

Self-assembly can also be induced by utilizing specific chemical functionalities found in the peptide backbone. For instance, amphiphilic gemini peptides, formed as a result of linking two cysteine containing single chain peptides with disulphide bond through oxidation, were designed, and its self-assembly behaviour was compared with that of the corresponding single chain counterparts [88]. Furthermore, three different hydrophobic amino acids (alanine, valine and isoleucine) were chosen to tune the molecular hydrophobicity of the peptides and to study its effect on the self-assembly together with dimerization. As the hydrophobicity of the single chain peptides increased, spherical aggregates became larger by as much as 5.5 ± 2.2 nm, and even short fibrils with heights of 6.0 ± 1.5 nm were initiated in the case of the strongly hydrophobic I_3C peptide. After oxidation, additional constraints in molecular conformation were observed due to the gemini geometry, further enhancing intra- and intermolecular interactions and supporting the self-assembly process. All three gemini peptides formed thin fibres with heights of approximately 1 nm and length of submicrometers. Hauser *et al* previously demonstrated the synthesis of ultrashort (tri- to heptamer) natural peptides and detailed their self-assembly mechanisms [101, 102]. This group has also used cysteine in a heptapeptide design (Ac-LIVAGKC-Am) to crosslink the system through disulphide bridging in addition to non-covalent interactions [103].

Amphiphatic peptides arranged in an alternating fashion were firstly developed by the Zhang group [89, 104, 105]. The ionic self-complementary peptides formed stable β-strand

and β-sheet structures that further self-assembled into well-ordered nanofibres due to electrostatic interactions. Although Zhang *et al* classified complementary ionic sides into various moduli based on the alternation of the charges, the $(XZXZ)_n$ motif, where *X* and *Z* represented polar and nonpolar amino acids, respectively, is the most frequently exploited sequence to direct self-assembly [106, 107]. Beta-sheets are generally arranged into bilayer structures where the hydrophobic side chains are localized in the interior part and the hydrophilic side chains are exposed to the aqueous medium. Lee *et al* dissected the effect of sequence pattern variation on the self-assembly of amphiphatic peptides by using the frequently studied Ac-$(FKFE)_2$-Am peptide as a model [90]. They compared the self-assembly behaviour of all four related sequences to that of a model peptide. The alteration in the amino acid groupings and the disruption of the alternating pattern not only decreased the self-assembly ability but also changed the morphology of the resulting materials. On the other hand, Ramachandran *et al* worked with two oppositely charged amphiphatic peptides (KVW10 and EVW10) presenting either cationic or anionic amino acids to create a co-assembled system driven by charge neutralization [108]. While the individual peptide solutions did not have any fibrillar structures, nanofibrous network formation was observed upon mixing of oppositely charged peptide solutions. Schneider *et al* designed a series of amphiphatic peptides consisting of two-sided alternating nonpolar valine and polar lysine residues flanking a type II β-turn promoter sequence (-V^DPPT-) [109, 110]. This turn-inducing sequence elicited a slight kink in the peptide skeleton and directed the self-assembly of molecules into bilayer β-sheet fibrils together with a contribution of alternating amino acid residues. In some cases, when some alterations were made in the amino acids, fibril lamination was observed, which is the main consequence of the disruption of hydrogen bonding pattern as well as β-hairpin conformation. Recently, Micklitsch *et al* also investigated the influence of nonpolar amino acid units in the hydrophobic face of the hairpin on self-assembly behaviour and fibril morphology [91]. Six different amino acids were selected based on the varying content of hydrophobicity, β-sheet propensity and aromaticity. Although the type of amino acid used in the peptide design did not show a significant influence on the local morphology of the fibrils, the residue type became an important factor when fibrils underwent higher order assembly.

Alternating sequences have been also used in cyclic peptide design to form nanotubular structures. While the assembly of cyclic peptides was first proposed by De Santis *et al* [111], the Ghadiri group first demonstrated that controlled acidification of an even-numbered pH responsive heterochiral cyclic peptide resulted in the formation of nanotubes [112]. The assembly of extended tubular structures is predominantly driven by intermolecular hydrogen bonding between cyclic peptide rings where carbonyl and amide bonds are perpendicularly oriented to the plane of the ring, while amino acid side chains generate the exterior walls of the nanotube. It was recently reported that the morphology of the self-assembled nanostructures of a cyclo-$[(Q^DAE^DA)_2]$ peptide was controlled by changing pH, reaction and sonication time. Also, the size of resulting cyclic peptide nanotubes and nanoparticles were shown to be tuned by monitoring multiple parameters such as peptide concentration and PEG modification [92]. Rubin and coworkers showed that cyclo-$[(Q^DL)_4]$ peptide monomers assembled into large, rod-like structures with diameters up to 2 μm and lengths of tens to hundreds of micrometres were composed of thousands of individual nanotubes with a diameter of 2 nm [93]. Unlike heterochiral cyclic peptides, surfactant-like cyclic peptides first developed by the Parang group can also form self-assembled nanostructures in an aqueous environment depending on the hydrophobicity/charge balance in the peptide sequence [94]. Among the cyclic peptides, cyclo $[WR]_n$ peptides formed vesicle-like structures whose diameters increased as the ring size increased. For a more detailed background on the design principles of cyclic peptides and related examples, we direct readers to recently published reviews [15, 113, 114].

Another class of peptide assemblies described by Hartgerink group is multidomain peptides (MDPs) [115, 116]. The side chains of the peptides are arranged in an ABA block motif, where a B block composed of alternating hydrophilic and hydrophobic amino acid residues is the major motif driving the self-assembly, and peripheral A blocks employ -charged amino acids to control the self-assembly through electrostatic interactions. The extended β-sheet conformation of the peptides leads to creating a facial amphiphile. Packing of two of the hydrophobic faces against each other forms a 'hydrophobic sandwich', which further elongates through antiparallel β-sheet hydrogen bonding. Although the length of the fibres depended on the design of the ABA motif, the width and height of the fibres were 6 nm and 2 nm, respectively. The self-assembly of MDPs was further explored by introducing aromatic amino acid residues into the core and it was concluded that hydrogen bonding pattern changed depending on the type of substituted aromatic amino acid without affecting the basic nanofiber morphology [95].

4.2. Peptide amphiphiles

The second class of self-assembling peptide molecules reviewed in this section is peptide amphiphiles (PAs), also called lipidated peptides or lipopeptides, which are composed of two main regions, a hydrophobic alkyl tail and a hydrophilic peptide sequence. These molecules are naturally present in living organisms, which have important roles as initiators in the signal transduction pathways [117, 118] and in the host defence mechanisms of bacteria [119]. The lipidic parts of these molecules are believed to take part in protein–protein and protein–lipid interactions and provide a link to the cellular membrane [118].

Amphiphilicity is the main triggering factor for the self-assembly of PA monomers into well-defined supramolecular nanostructures and the stability of the resulting assemblies can be further improved by enhancing the amphiphaticity of the PAs. Self-assembly is mediated by a variety of different noncovalent interactions, such as electrostatic interactions

Table 2. Recently published studies using peptide amphiphile architectures.

Peptide amphiphile	Structure	Details	References
$C_{16}H_{31}O$-$V_3A_3E_3$	Nanofiber	Salt-induced nanofiber formation	[130, 131]
$C_{16}H_{31}O$-F_3E_3	Twisted/helical ribbon	Time/sequence dependent morphological transformation	[132]
$C_{16}H_{31}O$-$(VE)_2$, $C_{16}H_{31}O$-V_2E_2, $C_{16}H_{31}O$-$(EV)_2$, $C_{16}H_{31}O$-E_2V_2	Nanobelt/nanofiber/nanoribbon	Structural variation in isomeric peptide amphiphiles	[133]
$C_{16}H_{31}O$-$(VE)_n$ (n = 2, 4 and 6)	Nanobelt	Dimensions of belt structure versus number of amino acid	[134]
$C_{16}H_{31}O$-$WA_4KA_4KA_4KA$	Worm-like micelle/nanofibers	Time dependent morphological transition	[135]
$C_{16}H_{31}O$-A_4LSQETFSDLWKLLPEN	Worm-like micelle	Secondary structure-supramolecular structure relation	[136]
$C_{16}H_{31}O$-KTTKS	Flat tape-like/twisted structure/spherical micelle	pH tuned morphology	[35]
$C_{12}H_{23}O$-GAGAGAGY	Nanofiber/twisted nanoribbon	pH tuned morphology	[137]
$C_{16}H_{31}O$-IAAAEEEE-Am	Nanofiber	pH and concentration dependent self-assembly	[138]
$C_{16}H_{31}O$-KKFFVLK	Nanotube-helical ribbon/twisted tapes	Thermo-reversible transition	[45]
$C_{12}H_{23}O$-VFDNFVLK-Am and $C_{12}H_{23}O$-VVAGE (mixture)	Nanofiber	Nanofiber diameter ≈10–20 nm	[139]
$C_{12}H_{23}O$-P_4R_4-Am, $C_{12}H_{23}O$-$P_4K_2R_8$-Am	Nanosphere	Diameter ≈15–45 nm	[140]
KLWVLPKCK$_2$A$_2$V$_2$K($-OC_{12}H_{23}$)-Am KLWVLPKCK$_2$K($-OC_{22}H_{41}$)-Am	Nanofiber/nanosphere	Importance of β-sheet forming region on self-assembly	[141]
$C_nH_{(2n-1)}O$-VRGDV (n = 10, 12, 14 and 16)	Nanofiber	Tail length versus self-assembly at different pH	[142]
$C_{16}H_{31}O$-H_6-$(OEG)_4$-Am, $(OEG)_4$-H_6K(-$OC_{12}H_{23}$)-Am	Nanofiber/nanosphere	Position of aliphatic tail-control on morphology	[39]
$C_{24}H_{47}O$-GANPNAAG (diacetylene units on C_{24} chain: 4,6- 10,12- or 16-18-positions)	Nanofiber	Temperature versus fibre stability	[143]
di$C_{16}H_{31}O$-EQLESIINFEKLTWE-Am	Cylindrical micelle	8.0 ± 2.3 nm in diameter, polydisperse in length	[144]
qC_8-Tat, dC_8-Tat, mC_8-Tat	Nanofiber	Mean diameter of nanofiber ≈15 nm	[145]

between charged amino acids, hydrogen bonding, π–π stacking and hydrophobic interactions. These interactions may lead to the formation of nanostructures with diverse morphologies, including fibres, micelles, nanotapes, nanotubes and nanosheets [70]. As described by the Israelachvili group, the balance between hydrophobic and electrostatic interactions needs to be taken into account when determining the geometry of amphiphiles with minimum free energy [120]. Since an alteration in the hydrophilic segment can lead to a change in the critical packing parameter [121], it can affect the morphology of the overall assembly [122, 123]. Also, Velichko *et al* investigated the contribution of hydrophobic interactions and hydrogen bonding to the morphology of the resulting PA assemblies by molecular simulation techniques and created a phase diagram displaying distinct morphologies with respect to the corresponding variables [124]. Experimental results were also in good agreement with those obtained by computational analysis. While a high content of intermolecular hydrogen bonds between peptide blocks favoured the formation of cylindrical PA nanofibers in solution, PA molecules lacking hydrogen bonds had a tendency to form micellar structures [125, 126]. Tsonchev *et al* performed Monte Carlo simulations to demonstrate the role of electrostatic interactions in the self-assembly of PA nanofibers [127]. Later, the proposed self-assembly mechanism was further studied by Lee *et al* and Fu *et al* through molecular dynamic simulations and it was revealed that individual PAs initially formed spherical micelles, and they transformed into long thin fibres by merging with one another due to hydrophobic interactions [128, 129]. The PA assemblies can be engineered to display various morphologies and fulfil various functions by modifying the peptide building blocks. The type of hydrophobic group, the choice of amino acids and the secondary structure formed by the system affect the morphology of the final PA assembly. Recently published studies presenting the design of PAs are discussed in this section (table 2).

The Stupp group demonstrated that a $C_{16}H_{31}O$-$V_3A_3E_3$ PA, in which hydrophilicity of the peptide domain increased towards the C-terminus, self-assembled into elongated fibres

after neutralization by pH adjustment or by the salt-mediated screening of charged glutamic residues. Although both formulations exhibited similar morphologies, salt-induced PA nanofibers formed stronger intra- and interfiber crosslinks through calcium mediated ionic bridges [130]. Additionally, highly aligned fibrils were obtained using the same design by either injecting a heated PA solution into a saline solution or dragging the same solution through a film of calcium salt solution [131]. The lamellar plaque structure generated during the heat treatment transformed into bundles of nanofibers upon cooling. They also observed an unexpected morphological transformation from twisted ribbons into energetically more stable helical ribbons in $C_{16}H_{31}O$-F_3E_3 PAs after aging them at room temperature for a month [132]. To clarify the reason behind this phenomenon, a similar peptide was synthesized by replacing phenylalanine residues with alanine residues and it was observed that the newly designed peptide formed 7–9 nm diameter cylindrical fibrils and did not exhibit any change after being aged, indicating that this conformational change is due to the aromatic stacking rearrangement and stems from the existence of the phenyalanine residues. Another critical parameter causing the morphological change in the nanostructure is the concentration. Cui *et al* designed an alternating hydrophobic and hydrophilic amino acids containing PA, $C_{16}H_{31}O$-VEVE [146]. In the customized molecular design, laterally grown PAs self-assembled into one-dimensional ultralong and wide nanobelts, with widths of the order of 150 nm and height between 10 and 20 nm, presenting peptide epitopes at the surfaces. With a decrease in concentration, a morphological transition from large nanobelts to twisted nanoribbons was observed by TEM. The same peptide domain was also used in another study, together with its isomeric counterparts, to investigate the importance of peptide side chain interactions in the morphology of the resulting supramolecular assembly [133]. Each peptide amphiphile isomer displayed a different one-dimensional nanostructure, such as nanobelts, nanofibres, twisted and helical ribbons and nanotubes, due to the switch in the amino acid order. While alternating sequence bearing molecules, VEVE and EVEV, exhibited flat morphologies as nanobelts and twisted ribbons, respectively, VVEE and EEVV peptide segments led to the formation of two distinct types of nanofibers. In addition to the amino acid order, the effect of the number of valine-glutamic acid (VE) dimeric repeats on the shape and dimension of the supramolecular nanostructures was also systematically studied [134]. As the length of the peptide sequence increased, a shift from flat to cylindrical structures was observed. This effect was attributed to a higher tendency to form twisted β-sheets by longer sequences.

In addition to the discussed nanostructures, the Tirrell group demonstrated two different peptides self-assembling into worm-like micelles due to their α-helix propensities [135, 136]. In the first design, lysine residues were symmetrically distributed around the helical structure to provide individual helices in the micellar state [135]. The results acquired from cryo-TEM, IR and circular dichroism (CD) revealed that time dependent morphological transition from spherical to worm-like micelles was observed after days, and they were eventually transformed into long nanofibrillar structures with an outer diameter of ∼10 nm. In the second design, they explored the influence of hydrophobic amino acid residues on the self-assembly of PAs by conjugating four alanine residues between the palmitic acid and oligopeptide sequence [136]. The inclusion of hydrophobic alanine residues has resulted in major changes in the morphology of the PA structures, which formed worm-like micelles rather than nanoribbons, and were rich in β-sheets rather than α-helices.

Nanostructured features of the PAs can be manipulated by varying the external parameters such as pH, temperature or ionic strength. The effect of pH and temperature on the self-assembly behaviour of $C_{16}H_{31}O$-KTTKS was investigated in two separate studies [35, 147]. Whilst an increase in the temperature gave rise to the formation of micellar structures rather than extended tape structure due to the disruption of hydrogen bonding, a gradual decrease in pH transformed nanotapes into twisted fibrils at pH 4 and spherical micelles at pH 2. Similarly, pH dependent morphological alteration was reported for $C_{12}H_{23}O$-GAGAGAGY PAs [137]. Cylindrical nanofibers observed at pH 9 transformed into twisted ribbons at pH 4, most likely due to the neutralization of carboxylic acid, and subsequently the weakening of electrostatic interactions, leading to the stacking of the β-sheet laminates. Furthermore, Ghosh *et al* demonstrated that the tendency of PAs to respond to pH change can be programmed by changing the position of single hydrophobic amino acid residue in a short amphiphilic peptide [138]. As isoleucine moved away from the alkyl tail, nanofiber formation was favoured over spherical micelles due to the enhanced propensity for β-sheet formation. In another study carried out by the Hamley group, thermo-responsive structural change was reported in PAs decorated with a KLVFF core motif that induced self-assembly through π–π stacking and hydrophobic interactions [45]. A reversible unwinding transition was observed between twisted tapes and nanotubes/ribbons in a temperature dependent manner.

Co-assembly of two oppositely charged PAs can also lead to some modifications in the self-assembled nanostructures due to the electrostatic interactions occurring between charged amino acid residues. Cylindrical nanofibers were observed by the Stupp group upon mixing oppositely charged palmitoylated peptides [148, 149]. Our group have also reported that lauric acid conjugated lysine and glutamic acid bearing peptides self-assembled into high aspect ratio, one-dimensional fibrillar nanostructures [54]. We also observed that short bioactive sequences exploited in the PA design did not alter the shape of the resulting supramolecular assemblies [139, 150, 151]. The Hamley group studied the co-assembly of oppositely charged PAs by mixing them at different ratios [152]. Co-assembly driven mainly by electrostatic interactions brought about enhanced β-sheet formation compared to samples prepared with a single component and resulted in the formation of nanotapes.

The shape of the nanostructure can be tuned by either varying or omitting the β-sheet forming domain [74, 140, 153]. Guler *et al* studied the importance of hydrogen bonding among the peptide segment in supramolecular

assemblies by a replacing trileucine sequence with triproline [74]. Due to the β-sheet breaking nature of proline residues, spherical aggregates were observed instead of the cylindrical nanofibers obtained with the former system. Mammadov *et al* [154] and Mumcuoglu *et al* [140] also used proline residues to form micellar structures by disrupting the β-sheet secondary structure to study the importance of nanostructural features in tuning the immune response and to develop an efficient delivery vehicle for the transfection of oligonucleotides, respectively. Recently, Moyer *et al* demonstrated that nanofibre formation was disrupted when a β-sheet forming region (A_2V_2) was removed from the peptide sequence. This truncated sequence self-assembled into nanospheres with diameters in the range 5–10 nm depending on the length of the tail region [141].

The conjugation of an alkyl group to a peptide segment was shown to enhance the thermal stability of the corresponding structure [14, 118]. The influence of alkyl tail length, its position and number on the self-assembly of PAs was investigated in detail by several research groups. The van Hest group examined the effect of alkyl tail length on the stability of β-sheet assemblies of GANPNAAG [155] and KTVIIE [156] peptides. As the length of the tail increased, the thermal stability of the PAs improved and the transition from β-sheet to random coil was observed at higher temperatures. Furthermore, Xu *et al* synthesized four PAs with different tail lengths by using the VRGDV sequence as the peptide domain and showed that PAs with shorter tail lengths did not maintain stability at higher pH due to weaker hydrophobic interactions [142]. On the other hand, the relationship between the site where the hydrophobic segment is attached to the peptide domain and the resulting nanostructure shape was investigated by incorporating an alkyl tail on either the N- or C-terminus of an oligo-histidine peptide sequence, and it was revealed that cylindrical and spherical morphologies were obtained at physiological conditions, respectively [39]. He *et al* reported that while two aliphatic tails attached to one side of the peptide sequence formed long fibrils, peptides conjugated from either side self-assembled into short twisted fibrils [157]. In addition, van del Heuvel *et al* showed that the stability of the self-assembled nanofibres can be controlled by changing the position of the diacetylene moiety on the hydrophobic tail without varying the length of the tail [143]. The Tirrell group introduced a dialkyl chain containing peptides [158] and investigated the effect of the length of double tail on the thermal stability of the collagen-like structure in the peptide amphiphile [159]. They further studied the effects of both the number and the length of alkyl tail on the nanostructured features of model collagen peptide amphiphiles by using a combination of small-angle neutron scattering and cryo-TEM [160]. In their design, dialkyl conjugated T-cell epitope bearing a peptide self-assembled into 8 nm diameter of cylindrical micelles [144]. In addition to the dialkyl tail bearing peptide amphiphiles, the Cui group designed three Tat-peptide conjugates with different numbers of octanoic acid tails [145]. It was reported that while single and double tail containing peptides could not form any well-defined nanostructures, four aliphatic tails attached one self-assembled into a fibrillar structure with a diameter of 15 nm, most likely due to enhanced intermolecular hydrogen bonding.

4.3. Peptides containing other hybrid systems

In this section, peptidic hybrid systems composed of various chemical groups besides peptides such as lipids, polymers, nucleobases, saccharides, aromatic groups, halogen elements, etc are elaborated to understand the key factors affecting the self-assembly behaviour of the related molecules. Table 3 depicts the self-assembled forms of recently reported hybrid peptide systems and gives additional information regarding their assembly properties. Peptides were modified not only by changing their amino acid sequences, but also by using capping molecules at the N- or C-termini or by inserting a linker between peptide domains. These modifications have been used both to investigate the mechanisms involved in self-assembly behaviour and to control the structural features of peptide assemblies for practical purposes [161–163].

Using aromatic moieties at the N-terminus of the peptide is another strategy for driving self-assembly by providing amphiphilicity to the structure. Unlike the assembly mechanism of aliphatic peptide amphiphiles, here aromatic moiety dominantly directs the self-assembly by its planar structure and resulting geometric restrictions due to the preferred stacking arrangements [181]. Vegners *et al* synthesized an aromatic peptide amphiphile, Fmoc-LD, which folded into filamentous micelles [182]. Various dipeptide combinations have been exploited together with the Fmoc (9-fluorenylmethoxycarbonyl) unit since then [67, 183–186]. Tang *et al* examined the self-assembly behaviour of Fmoc-dipeptides composed of a combination of phenylalanine and glycine residues and revealed that the flexibility of the overall structure as well as the resultant conformation were affected by the amino acid type and sequence, leading to the formation of structurally different assemblies [164]. In addition, Fmoc-dipeptides, Fmoc-tripeptides, and tetra- and pentapeptide derivatives were also presented, which exhibited nanofibrous or nanotubular structures [187–190]. In addition, the effect of a halogen substituent and the position of its substitution on the aromatic side chain of Fmoc-F were systematically studied by the Nilsson group [165]. Since the identity of halogen and its position on the benzyl ring affected the self-assembly process and the morphology of the self-assembled fibrillar structures, it was hypothesized that the mentioned variations lead to the perturbation in the energetics of the aromatic π–π interactions that drive self-assembly. The influence of the C-terminal modifications on fluorinated Fmoc-F derivatives (Fmoc-F_5-Phe-OH and Fmoc-3-F-Phe-OH) was further investigated by the same group [166]. The hydrophobicity and hydrogen bonding capacity of the C-terminus were adjusted by altering the carboxylic acid group of the C-terminal with the amide and methyl ester derivatives. Their assembly kinetics and resultant structural features were studied either one by one or in co-assembled form. They recently reported that the electronic nature of the substituent anchored

Table 3. Recently reported hybrid peptide systems.

Hybrid system	Structure	Details	References
Fmoc-FF, Fmoc-FG, Fmoc-GG, Fmoc-GF	Nanoribbon/fibre/sheet	Effect of glycine substitution on self-assembly	[164]
Fmoc-*n*-*X*-Phe (n = 2, 3 or 4 and X = F, Cl or Br)	Fibril	Observed fibril diameter = 16–45 nm	[165]
Fmoc-3-F-Phe-*X* and Fmoc-F_5-Phe-*X* (X = OH, NH_2 or OMe)	Fibril	Effect of C-terminal modification on self-assembly	[166]
Naphthalene-FF-taurine	Nanotube	Nanotube diameter = 9 ± 2 nm	[167]
Phenothiazine-GFFY	Nanofibre	Nanofiber diameter ≈ 25 nm	[168]
Pyrenebutyryl-ϵ-Ahx-VVAGH-Am	Nanofibre	Induced chirality	[169]
Boc-FF	Nanosphere	30 nm–2 μm	[170]
E_3-*X*-G-perylene diimide-G-*X*-E_3 (X = A_3 or $^DA_3$)	Nanofibre/fibre bundle	Bundle heights 15–45 nm	[171]
Terthiophene-*X*E (X = G, V, I and L)	Nanosheet/nanotube	Amino acid- nanostructure relation	[172]
D*XX*-quaterthiophene-*XX*D (X = G, A, V, I, F)	Nanofibre	Interactions of amino acids with π-electron core	[173]
Trigonal WTW	Nanosphere/nanofibre	Structural change upon pH change	[174]
mPEO_7-F_4-OEt	Nanotube	Mean wall thickness ≈7 nm	[175]
PEG-Pep-fluorophore-Pep-PEG	Micelle	Average hydrodynamic diameter ≈15–20 nm	[176]
CREKA-PEG_{2000}-DSPE	Micelle	Average hydrodynamic diameter of 17.0 ± 1.0 nm	[177]
KK(K-hepta thymine-K)G_3A_3K(-$OC_{16}H_{31}$)-Am	Nanofibre	Nanofibres with a diameter of 8 ± 1 nm	[178]
$C_{18}H_{35}$O-CTGACTGA-E_4-Am	Micelle	Spherical micelles with diameter of 5–30 nm	[179]
Nucleobase-F_n-glucoside (n = 1 or 2)	Nanofiber/nanoparticle	Nanofibers: 9–15 nm, nanoparticles: 18–27 nm	[180]

to the benzyl ring of Fmoc-F also exerted influence on the self-assembly [191].

Other than the Fmoc group, naphthalene [167, 192], phenothiazine [168], pyrene [169], carboxybenzyl [193], azobenzene [194, 195], naproxen [196] and benzimidazole [197] moieties were also utilized as aromatic capping at the N-terminus facilitating the self-assembly. The Xu group demonstrated that the incorporation of a non-proteinaceous amino acid, taurine and naphthalene into the peptide backbone resulted in the formation of nanotubes, nanofibers or nanoribbons depending on the assembly conditions, such as temperature, sonication and pH [167]. In another study, Ou *et al* showed that phenothiazine conjugated tetrapeptide (-GFFY) prepared at 0.2wt% formed uniform nanofibres with diameters of 25 nm [168]. On the other hand, pyrene was conjugated to the peptide sequence (VVAGH) with an ϵ-aminohexanoic acid linker by our group. The formation of the nanofibres, observed in TEM, was mainly driven by the solvophobic effect [169]. The assembly also led to helical organization of pyrene within the hydrophobic core and to acquiring chirality, which was verified by fluorescence spectroscopy and CD measurements.

Unlike aromatic capping groups, the tert-butoxycarbonyl (Boc) moiety was also anchored to short peptide sequences [170, 187]. The Gazit group studied the structural and mechanical properties of the Boc-FF peptide and a morphological characterization conducted by SEM and AFM revealed that Boc-FF peptide dissolved in organic solvent self-assembled into spherical structures whose diameters showed variation from 30 nm to 2 μm. The same sequence was also investigated in terms of the effect of solvent on the resultant morphology and a structural change was observed from spheres to nanotubes when water was used instead of ethanol as a diluent for the peptides prepared in HFIP [198].

Peptide π-electron rich systems are another well-studied class of hybrid peptide systems, and their self-assembled architectures exhibit different photophysical, electrical and mechanical properties. The π-electron rich systems can be integrated into peptide backbone in many different ways: as a side chain [199], as a linker between two peptide sequences [200] or as a capping molecule at the N-terminus [201]. While designing a peptide and π-electron construct, an amino acid sequence/π-electron system pair should be selected carefully in terms of its energetic contributions to the self-assembly in order to form supramolecular structures with improved electron transport properties [202, 203]. The Hodgkiss group examined the thermodynamic factors affecting the self-assembly of peptide–perylene diimide conjugates by altering the peptide hydrophobicity, charge density, length, stereocentre inversion and amphiphilic substitution [171]. The self-assembly of alanine-rich conjugates resulted in the formation of bundles with heights of 15–45 nm. Moreover, changes in peptide hydrophobicity and the insertion of an imide hexyl group resulted in the most prominent effect with respect to changes in thermodynamic properties. As another π-conjugated system, a terthiophene moiety was coupled to four different dipeptides by the Stupp group, which assembled into one-dimensional nanostructures [172]. The main consideration in their design was the selection of hydrophobic amino acids, based on van der Waals volume and

hydrophobicity values, to study the impact of steric hindrance and hydrophobic van der Waals interactions on the supramolecular structure. On the other hand, the Tovar group worked with peptide–π–peptide triblock molecules [204], and demonstrated that acidic solutions of quaterthiophene-peptide (D*XX*) conjugates prepared at 0.1wt% exhibited one-dimensional nanostructures [173]. Some variations in the width or persistence length of the nanostructure were obtained depending on the type of amino acid residue used adjacent to the π-core.

Peptides can also be functionalized on an organic template to provide symmetry in the structure and yield an ordered architecture. Different molecules such as tris(2-aminoethyl)amine (TREN) [205], 1,3,5-tris(aminomethyl)-2,4,6-triethylbenzene [206], and pentaazacyclopentadecane [207], were used to conjugate different peptides to these trigonal or pentagonal templates to afford nanoassemblies with different structures. The Kimizuka group designed a C_3-symmetric peptide conjugate (Trigonal WTW) where an iodoacetoamidated core was used for the coupling of an 8-mer tryptophane zipper-forming peptide, and its self-assembly resulted in the formation of nanospheres and nanofibres depending on the pH [174].

Amphiphilicity in the hybrid structure can alternatively be achieved by anchoring hydrophilic polymers to hydrophobic peptide segments, or vice versa, through different chemistries to afford copolymer conjugates of varied structures [208]. The nature of the polymer, the chemical heterogeneity of the peptide, the conjugation site, and the reaction medium can affect the structure, dynamics and function of the corresponding hybrid system. A number of polymer–peptide conjugates have been reported, where polymers with different composition, number and length of side chains were used to create different forms of nanostructures [209, 210]. Tzokova *et al* showed a $mPEO_7$–F_4–OEt conjugate via click chemistry and its self-assembly afforded nanotubes with a mean internal diameter of 3 nm and a mean wall thickness of roughly 7 nm [175]. While tetrapeptide domain provided the antiparallel β-sheet structure, PEO chains assisted to the stabilization of the structure. It is also possible to synthesize amphiphilic triblock polymer–peptide conjugates. The Mandal group designed an ABA type triblock conjugate composed of a hydrophobic peptide part and a hydrophilic PEG moiety at both ends of the peptide domain [176]. Micelle formation was observed when the hybrid system underwent aggregation in water and the diameter of resultant spherical micelles was found to be 15–20 nm based on TEM imaging. In addition to the polymer conjugation, phospholipids have been used to create peptide hybrids [177, 211–213]. Tirrell and coworkers reported a multicomponent system (peptide-PEG-DSPE) that self-assembled into micellar structures with an average hydrodynamic diameter of 17 $\pm$ 1 nm in an aqueous environment [177]. While the peptide domain served as the polar head group, PEG and DSPE were used as the spacer and tail, respectively.

Similar to lipids, nucleobases or saccharides can also be conjugated to the peptides [186]. A peptide nucleic acid (PNA)/peptide amphiphile conjugate, designed by the Stupp group, was constructed on a solid support and a poly-thymine PNA heptamer was built on the peptide amphiphile whose self-assembly resulted in the formation of uniform nanofibers with a diameter of 8 $\pm$ 1 nm [178]. Similar approach was later used by Zhang group to synthesize a series of peptide nucleic acid amphiphiles (PNAA) containing different hydrophobic and hydrophilic moieties [179]. The self-assembly driven mainly by the base pair stacking of PNAA duplexes and intermolecular noncovalent interactions led to the formation of spherical micelles with a diameter of about 5−30 nm. On the other hand, Xu *et al* preferred utilizing simple building blocks, basically a nucleobase, amino acid and saccharide, rather than using peptide nucleic acid derivatives or glyco amino acid units to generate molecular architectures with defined structures [180]. Supramolecular assemblies obtained by pH increment exhibited differences in morphology due to the number and type of presenting amino acid and nucleobase residues. Saccharide incorporated peptide conjugates were also developed, which can form uniform self-assembled nanostructures. They can be synthesized through a number of synthetic approaches, including the use of glycosylated amino acids [214], direct conjugation of the sugar to the peptide backbone or amino acid side chains through amino bonds [215], or the use of a linker molecule for indirect conjugation [216, 217].

5. Characterization of self-assembled peptide nanostructures

Characterization of the self-assembled nanoscale architectures can be done using sophisticated techniques due to their complex and dynamic nanoscale nature. Advances in materials characterization methods, in conjunction with recent developments in nanotechnology, have resulted in the development of advanced tools and approaches for the investigation of chemical, physical, electrical and mechanical properties. These techniques can be classified as spectroscopic, x-ray, microscopic, electrical and mechanical characterizations with various examples leading the material developments in different fields (figure 2).

5.1. Spectroscopic analysis

Spectroscopic methods are used to understand the chemical and physical characteristics of nanoscale peptide organizations, such as their bond properties, vibrational modes and covalent and noncovalent interactions. Although the basic principles of the spectroscopic techniques rely on the detection of the transitions on the molecules such as nuclear spin, molecular vibrations or electronic states, the detection methods for these transitions become different depending on the radiation source. The common spectroscopic techniques such as nuclear magnetic resonance (NMR), Fourier transform infrared spectroscopy (FTIR), Raman and CD spectroscopy have been widely used for the analysis of different self-assembled peptide nanostructures designed for various applications. NMR is a powerful technique enabling the

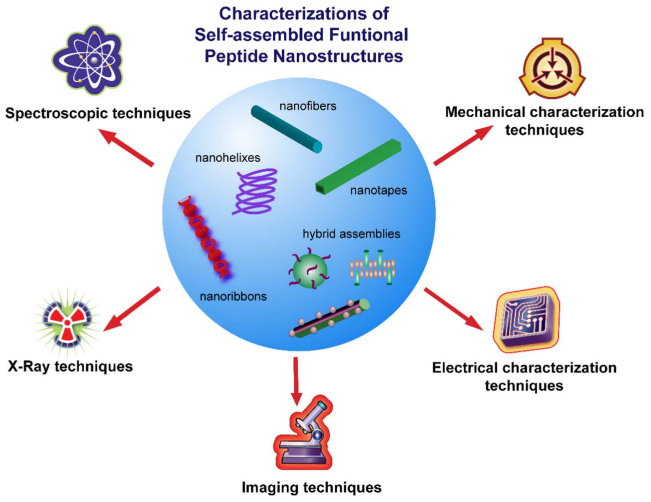

Figure 2. Common characterization techniques for a variety of self-assembled peptide nanostructures.

analysis of the peptide-based architectures at both liquid and solid conditions [218]. The self-assembly mechanism of Fmoc-protected peptide networks have been studied via 1D proton and 2D nuclear overhauser NMR spectroscopy (NOESY) in liquid and sol–gel transition states, and hydrophobic and intermolecular interactions were demonstrated to be particularly vital for nanostructure formation [219]. In another study, diffusion ordered NMR (DOESY NMR) spectroscopy [220] was conducted to follow the transitions on the structural organization of the peptide nanostructures due to the biocatalytic activity and hydrolysis of the assemblies in a liquid environment [221]. On the other hand, solution state NMR methods limit the characterization of more complex peptide assemblies in liquid environment with high resolutions. Magic-angle spinning (MAS) solid-state NMR (ssNMR) spectroscopy overcomes the limits of solution-based NMR techniques, enabling through-space interatomic distance and torsion angle measurements on isotopically labelled peptide molecules [222–224]. The packing of self-assembled palmitoyl PA nanostructures and their supramolecular organization have been identified by the incorporation of the data collected via ssNMR and rotational-echo double resonance NMR analysis [225] measuring the distances between ^{13}C and ^{15}N isotopically labelled PA molecules [226]. The molecular organization of ^{13}C-labelled self-assembled RADA-l peptide nanofibre matrices, developed as an extracellular matrix (ECM) mimicking microenvironment have been identified via the detailed analysis of a cross-polarization MAS (CPMAS) spectrum including the peak positions, line widths and dipolar couplings [227]. In addition, ssNMR measurements revealed the high resolution structural organization of the supramolecular peptide-based nanocarrier (figure 3) [228] and self-assembled monomorphic MAX1 fibrils within the hydrogel network [229].

Infrared (IR) spectroscopy deals with the electromagnetic spectrum change of peptides due to molecular vibrations and conformational changes within amide A (~3200–3300 cm^{-1}), amide I (~1600–1700 cm^{-1}), amide II (~1480–1580 cm^{-1}) and amide III (~1200–1300 cm^{-1}) bands in the mid-infrared region [230–232]. The shifts in the amide I band were analysed to monitor the structural changes as a result of the peptide self-assembly, which can be triggered via different factors such as UV irradiation [233], ultrasonication [234, 235], pH, ion addition or electrostatic interactions. In particular, the peaks in the amide I bands, which are correlated with C=O stretching of the self-assembled peptide nanostructures, contribute to the analysis of parallel or anti-parallel β-sheet [236, 237], α-helix, β-turn or random-coil secondary structure organization of the peptide assemblies. The effect of trifluoroacetic acid salt on cationic peptide nanostructures [238] can be determined on FTIR spectra within the amide I region [239]. In addition to transmission IR approaches, grazing angle IR, in which the sample is dried and placed almost parallel to IR beam [125], can be used to determine the preferred hydrogen bonding orientation within the peptide nanostructures [95]. The attenuated total reflectance (ATR) mode also enables the characterization of the self-assembled peptide nanostructures at the surfaces or within the solutions [240] without any pellet preparation or sample manipulation [241]. The collected ATR-FTIR spectrum of the pentapeptide assemblies has been reported to show the vibrational peaks associated with β-sheet secondary structure organization within the amide I band [242].

Although IR spectroscopy provides many advantages for the study of the self-assembly process and the structural organization of peptide nanostructures, the strong background of water molecules overlapping in the amide I region limits the analysis of the peptide samples prepared in physiological conditions [243, 244]. The use of deuterated solvents such as D_2O during the IR spectroscopy suppresses the background absorption in liquid conditions [245]. In the literature, the effect of ultrasonication on the reconfiguration of the peptide assemblies in D_2O was studied by analysing the changes in the amide I band [235]. Real time FTIR analysis of the peptide bolaamphiphiles in D_2O pointed to the β-sheet structural organization of the self-assembled nanostructures due to the progress of the enzymatic reactions [246]. The isotope-edited IR spectroscopy allows the site specific analysis of the peptide assemblies with high resolutions [247]. The co-assembly of two enantiomeric short amphipathic peptides into rippled β-sheet co-fibrils has been revealed via ^{13}C-labelled carbonyls in the peptide backbone (figure 4) [248]. Moreover, the analysis of isotope-edited high spectral resolutions, cross-peak couplings and solvent exposure through 2D line shapes were facilitated via 2D IR spectroscopy [249], in which the nonequilibrium conditions of the peptide conformations were monitored in real time [250] with submicrosecond [251] or picosecond resolutions [252]. This approach was also applied to study the salt bridges between oppositely charged amino acids: glutamate (Glu^-) and arginine (Arg^+) in solution with picosecond time resolution [253].

Similar to the vibrational IR techniques, the Raman scattering of the peptide assemblies assists the analysis of the structural properties in the assigned modes of molecular bonds found in the peptide architectures [254]. However,

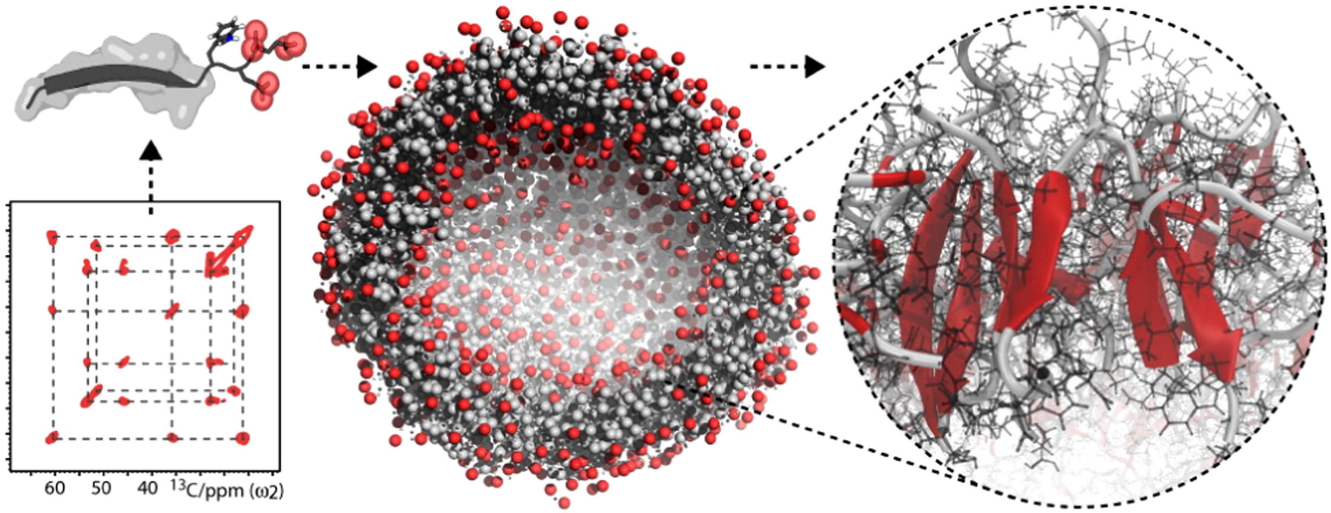

Figure 3. Detailed structural model of a self-assembled peptide-based nanocarrier developed in the light of ssNMR experiments. Adapted with permission from [228]. Copyright 2015 American Chemical Society.

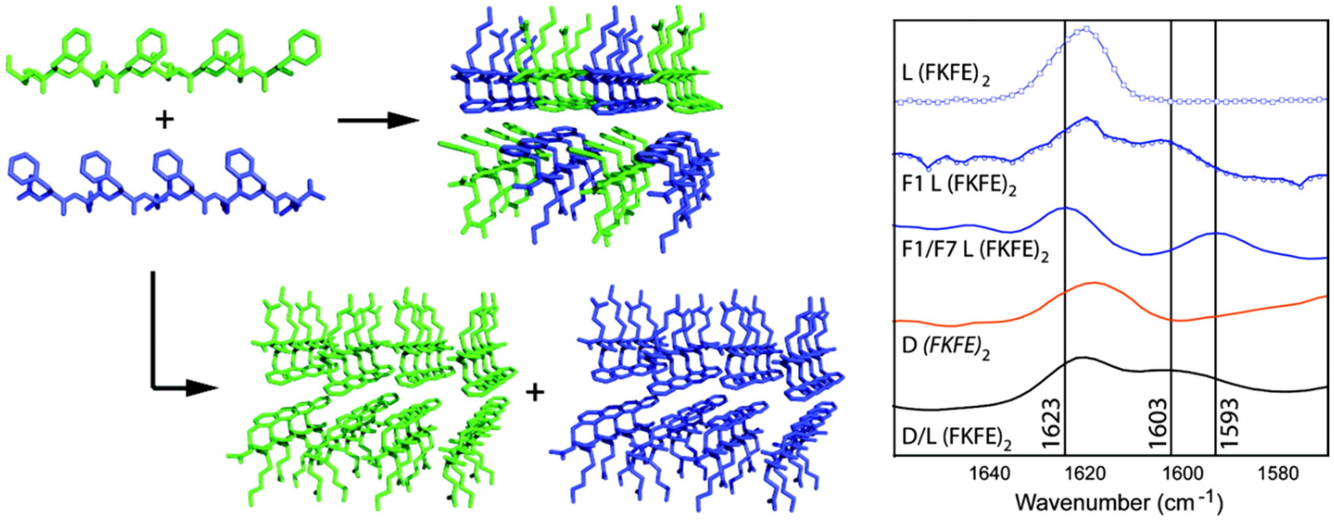

Figure 4. Schematic representation of self-assembly of enantiomeric, amphipathic peptides into co-assembled rippled β-sheet fibrils (right). Adapted with permission from [248]. Copyright 2012 American Chemical Society. The analysis of the IR spectra of unlabelled and ^{13}C-labelled L, D and mixed L- and D-Ac-(FKFE)$_2$-NH$_2$ fibrils (left) points to the alternating organization of the peptides with L and D chirality (top) instead of self-sorted enantiomeric ordering (bottom) within the extended β-sheets.

conventional Raman spectroscopy lacks the spatial resolution for detailed characterizations of the peptide nanostructures due low signal to noise ratios at dilute conditions, and different approaches have been developed to improve the scattering intensities for the analysis. UV resonance Raman spectroscopy, which enhances the frequencies in vibrational amide modes including amide III and C_α–H bands were applied to selectively monitor the secondary, tertiary or quaternary organization of the peptides in solution [255–258]. The relatively low Raman signal of the peptide assemblies was also increased via surface-enhanced Raman scattering (SERS) using the localized surface plasmon resonances of the metallic clusters in liquid or solid environments [259, 260]. In addition to the surface enhancement, tip-enhanced Raman scattering (TERS) enables the comprehensive characterization of the peptide nanostructures merging the scanning probe approach with vibrational spectroscopy [261, 262].

The chiral biomolecules including DNA, proteins and peptides interact with right- and left-handed photons differently, and that difference generates a non-zero CD signal depending on the conformation of the molecules [263]. CD spectroscopy functions at the near and far UV regions (180–320 nm) and provides information on the secondary structure of peptide assemblies [264], conformational changes that may occur following pH change [265], chirality of supramolecular peptide architectures [266] and interactions between toxic molecules [267], or metal ions [268] and self-assembling peptides. Recently, induced supramolecular chirality of achiral chromophores, whether covalently attached or noncovalently conjugated to the chiral PA molecules as a

result of self-assembly, have been studied using this technique in solution phase [169]. The β-sheet organization of asymmetric self-neutralizing amphiphilic peptide wedges, which enhances strong positive and negative peaks at 190 and 220 nm, respectively, was reported as a result of CD analysis of the supramolecular assemblies [269]. Blue shifted CD spectra of the peptide assemblies, with a positive maximum at 195 nm and two negative maxima at around 205 and 218 nm, showed formation of the super-helical peptide assemblies [270]. The conformational differences, such as twisting or disordered β-sheets in the assemblies, can be detected via shift in the CD spectra due to the π–π^* transitions within the peptide backbone [265, 271]. The effect of increased solution temperature on the secondary structures of the semiconductor functionalized peptide α-helices [272], elastin–*b*–collagen-like peptide bioconjugates [273] and β-hairpin peptide amphiphile assemblies [91] were also analysed by using CD spectroscopy. In addition, quantitative analysis of secondary structures within the peptide nanostructures is possible via exploration of the CD spectra using computational methods [274]. Previously, the random coil, β-turns, ordered and disordered α-helix and β-sheets amounts within the solution were calculated using the CD spectra collected via synchrotron radiation, and the comparison based on the differences of secondary structure organizations were reported [275]. In addition to secondary structure analysis, it is also possible to monitor π–π interactions between aromatic peptide assemblies [100, 276], and the intensity of the β-sheet signal at 200 nm is especially useful for monitoring the self-assembly process [98].

Dynamic light scattering (DLS) is another method that relies on fluctuations in the scattered light due to the internal mobility of the structures within the 1–1000 nm size range in the solution [277, 278]. This technique enables examination of noncovalent interactions between small molecules and self-assembling peptides [279]. It can also be used to gain greater insight in assembly mechanisms [280–282] and to determine the physical properties of peptide nanostructures in solution [283]. Various supramolecular peptide nanostructures and peptide–polymer conjugates [273, 284, 285] have been analysed via DLS, and the size distribution, hydrodynamic radii [286, 287], polydispersity index and zeta potential [54] of the assemblies were reported in conjunction with other characterization techniques. The pH dependent size and zeta potential change of the tailorable cyclic peptide nanostructures were studied by using this technique [92]. In addition to the structural characterizations, the aggregation mechanism of collagen-based peptides upon addition of different metal ions was also studied [58].

In addition, fluorescence emission spectroscopy measures the changes in the wavelength of light that result from the intramolecular resonance transfer between donor and acceptor units, and can be used to investigate the aggregation kinetics and self-assembly mechanisms of chromophore-conjugated peptides. The time resolved self-assembly properties of chromophore-conjugated peptides were shown by using this technique [288]. It was also used to show assembly characteristics of aromatic peptides [289, 290] and β-sheet peptide fibrils [291] monitoring the signal of π–π stacking on the fluorescence emission spectra. The fluorescence resonance energy transfer (FRET) process can also be used to investigate peptide self-assembly mechanisms through the use of fluorescence probe-conjugated peptide molecules, as the distance between individual peptide units decreases during self-assembly, and the resulting quenching effect can be quantified by fluorescence spectroscopy [292, 293].

In addition to the conventional techniques, several spectroscopic characterizations have been improved for the specific requirements of sample analysis. For example, the analysis of peptide assemblies at the interface is quite challenging using conventional methods, but the sum frequency generation (SFG) spectroscopy technique provides a new opportunity for analysing the secondary structure and the molecular organization of the peptide assemblies at the lipid–water and solid–air interfaces [294, 295]. The structural dynamics of surface-bonded peptide monolayers has been studied using a 2D SFG approach, and IR spectra were used to demonstrate that the helical structure of the soluble peptide is retained following its incorporation onto a gold surface [296]. In addition, internal dynamics and fluctuations of supramolecular PA nanostructures have been studied with the help of quantitative electron paramagnetic resonance spectroscopy, where local molecular motion within the assemblies can be tracked via site specific spin-label probes located in the PA molecules [297]. This technique also enables the investigation of the relationship between hydrogen bonding density within the β-sheet internal organization and the supramolecular cohesion of self-assembled PA nanostructures [298].

Computer simulation studies also aim to predict the molecular organization of peptide molecules and can be used for the optimization of peptide design in conjunction with experimental findings [299–303]. Incorporation of the experimental results and the simulation outputs developed using different molecular dynamics (MD) simulation programs improves the information on the structural properties of the peptide assemblies [93, 228, 304–307]. Previously, successful candidates were determined among 8000 different peptide molecules using computational approaches. They were synthesized and their supramolecular assemblies were characterized using spectroscopic techniques including NMR, FTIR and DLS [308]. The assembly characteristics of synthetic amyloid peptide fragment at different conditions were characterized via detailed 2D NMR spectroscopy and the structural model was developed in the light of both experimental methods and the molecular dynamics simulations [309]. In addition, the spectral simulations of IR, vibrational CD, and Raman techniques were conducted for the conformational study of the various peptide assemblies to highlight aggregation and fibril formation behaviours [310, 311].

5.2. X-ray techniques

X-rays are high energy electromagnetic waves and their interactions (reflection, diffraction or scattering) with the self-assembled peptide nanostructures provide valuable

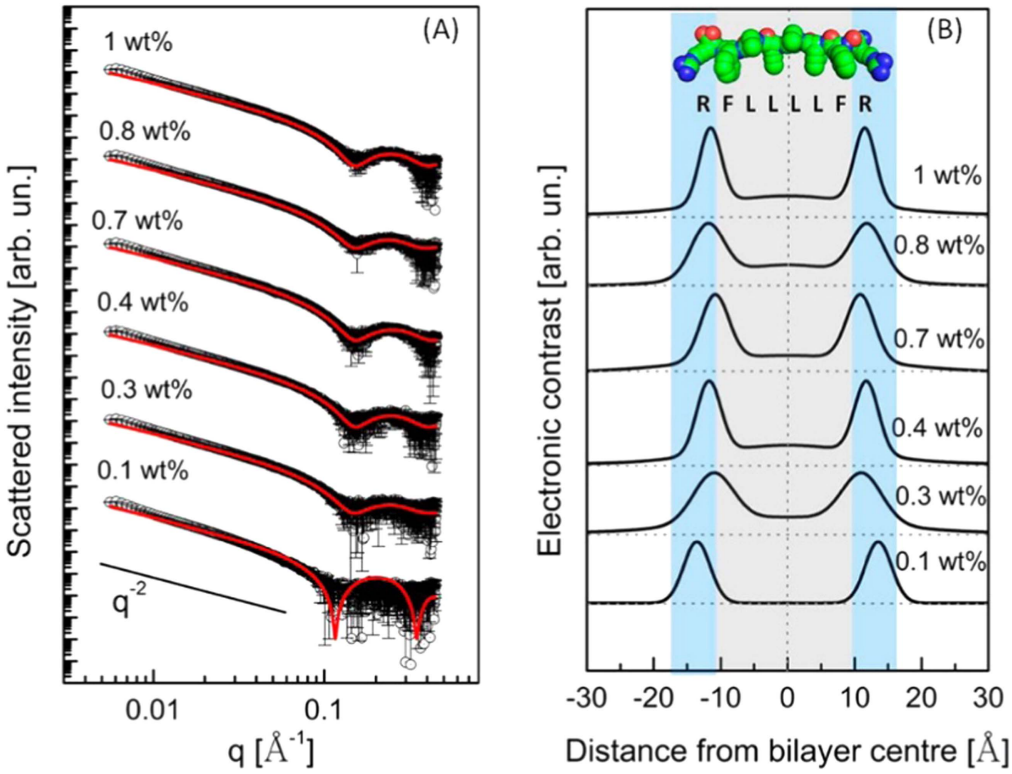

Figure 5. The scattering (a) and electron density (b) profiles of the self-assembled arginine-capped peptide bolaamphiphile solutions prepared at different concentrations, and the fitting lines of the model according to a bilayer form factor. Adapted with permission from reference [98].

information for the determination of size, shape and structural orientation. X-ray diffraction (XRD) patterns of self-assembled peptide nanostructures were used to determine packing parameters and molecular organization focusing on the non-covalent interactions between the building blocks [67, 169, 312]. The peaks associated with the hydrogen bonding, π–π stacking and β-sheet secondary structure organization were reported and the spacing between peptide molecules were estimated using Bragg's law [132, 313]. The crystalline organization and unit cell parameters of the self-assembled arginine-capped peptide bolaamphiphile nanosheets were revealed via XRD measurements in addition to the other characterization techniques [98]. On the other hand, the estimated structural parameters for the secondary structure could slightly change depending on the ordered and disordered degree of the peptide organization consisting of amino acid sequences to direct self-assembly. In addition to the powder diffraction examples, the oriented nanofiber wide angle x-ray scattering of isomeric tetrapeptide amphiphiles was performed with the peptide solutions by loading into quartz capillaries [133]. In another study, molecular organization of dipeptide assemblies and interatomic distances at the gel state were determined using the x-ray fibre diffraction technique [314].

Small-angle x-ray scattering (SAXS) eliminates the drawbacks of powder diffraction and enables the analysis of disordered peptide assemblies in their native conditions without time consuming sample preparation steps. SAXS is performed using lower angle x-ray scatterings at a range of 1° to 10° [315, 316]. The SAXS analysis of arginine-capped peptide bolaamphiphile structures at liquid conditions revealed the nanosheet assembly with bilayer organization complementary to the other structural characterizations (figure 5) [98]. SAXS profiles of the oppositely charged PA mixtures prepared at different ratios underlined the formation of bilayers after the thermal treatment process [152]. The self-assembly of the maspin-mimetic PA into a mixture of cylindrical and ribbon-like shapes was characterized based on the analysis of the scattering data in the Guinier region [317].

Although x-ray applications are known as nondestructive ways to analyse the biological samples, the effect of the x-ray radiation on the structural organization of the self-assembled peptide nanostructures were shown in the literature [318]. Hence, radiation time and optimization experiments should be conducted carefully to eliminate the outcomes of the measurements on the structural parameters.

5.3. Imaging techniques

With the invention of transmission electron microscopy (TEM) in the 1930s, microscopic approaches became a fundamental way of understanding the structural and material properties of materials at the nanoscale. Advances in microscopic tools enhanced the visualization of the peptide-based nanostructures using different imaging techniques including TEM, atomic force microscopy (AFM), scanning electron microscopy (SEM), fluorescence and other microscopies at high resolutions. Conventional TEM imaging of the peptide

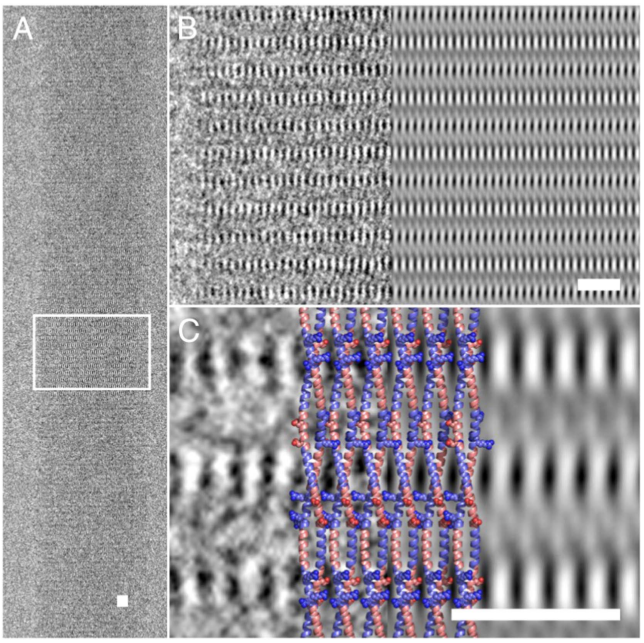

Figure 6. Direct visualization of the self-assembled dimeric α-helical coiled coils within peptide assemblies (a), and (b, c) the regular lattice of high-contrast striations within the magnified region before (left) and after (right) image processing. Adapted with permission from reference [325].

nanostructures requires special sample preparation procedures, including staining via heavy metal salts such as uranyl acetate and drying of the sample before imaging [319]. A variety of TEM images of the self-assembled peptide aggregates including nanofibers, nanospheres, nanobundles, nanotubes, helices, etc have been reported and the details of the sample preparation procedures shown [140, 154, 320, 321]. Although TEM imaging is a crucial way for showing the structural properties of the peptide nanostructures, the effect of drying and staining on the peptide organization could be important. On the other hand, cryogenic TEM (cryo-TEM), in which the sample is vitrified using special tools, overcomes the sample preparation limits and enables the imaging of peptide nanostructures in their native conditions [322–324]. The direct structural analysis of the dimeric α-helical coiled coils within the *de novo* designed self-assembled nanofiber system was performed via incorporation of cryo-TEM imaging with image processing (figure 6) [325]. In another study, the effect of salt concentration on the morphology of self-assembled amyloid peptide assemblies was shown via cryo-TEM, and the results suggested that the formation of flat ribbons and a decrease in twisted fibrils occurs due to the salt screening of electrostatic interactions between the peptide molecules [326].

AFM facilitates *in situ* visualization of the self-assembly process of the variety of peptide building blocks into supramolecular nanostructures with nanoscale resolutions at liquid conditions [327]. Monitoring structural changes associated with the environmental factors including pH, ion effect, temperature, concentration, etc is also possible via time-lapse AFM procedures. AFM imaging has also been performed to monitor time dependent changes of the resilin-elastin-collagen-like chimeric polypeptide assemblies incubated in water at 50 °C [328]. AFM imaging has also been used to observe the formation of right-twisted helical ribbons and their conversion to micro-crystals in an amyloid derived peptide fragment, ILQINS hexapeptide, which is normally found as left-handed helical ribbons and is organized into nanotubes in lysozyme [329].

Direct observation of peptide self-assembly is also possible via covalent conjugation of fluorescence probes to the peptides using fluorescence imaging techniques [330]. Stochastic imaging and deconvolution methods were also used to decrease resolution limits and monitor the supramolecular peptide organization at nanoscale. In addition, the intrinsic fluorescence properties of the peptide nanostructures were used for imaging of the assemblies via confocal microscopy without any probe conjugation [331, 332]. Without any staining or probe conjugation, chemical and spatial information collected via Raman spectroscopy enhanced the stochastic imaging of biological samples [333, 334]. Self-assembled amyloid inspired peptide nanofibres were imaged using the SERS blinking effect during *in situ* Raman spectrum measurements [259]. In addition, the tip-enhanced Raman imaging technique, which is the incorporation of scanning probe microscopy with Raman spectroscopy [335], enabled the imaging of self-assembled peptide nanotapes with additional chemical information [261].

5.4. Electrical characterization techniques

Electrical properties of the peptide nanostructures, including conductivity, resistivity and charge mobility, are determined based on current (I)–voltage (V) measurements using the probe stations connected to the electrodes [331, 336, 337]. The linear fitting of I–V data of amyloid-based peptide fibrils obtained via a probe station was processed to understand resistance characteristics of the self-assembled nanostructures depending on the nonnatural heterocyclic side chain differences [338]. Recently, the effect of relative humidity on the electron and proton transfer mechanisms of amyloid derived peptide filaments were discussed in the light of I–V measurements [199].

In addition to the probe stations, AFM-based approaches including conductive probe AFM (CP-AFM) is commonly used for I–V measurements of peptide nanostructures. The charge transfer characteristics of self-assembled peptide nanotubes have been determined using CP-AFM [339], which combines force and current measurements using - mechanically oscillating conductive probes [340, 341]. The most important advantage of CP-AFM compared to scanning tunnelling microscopy is the independent optical feed-back mechanism that controls the exact position of the probe in contact with the sample [342, 343]. The applied force dependent electronic characteristics of coil-coiled architectures [344] and α-helical peptide monolayers [345] immobilized on the gold surfaces, and the conductive properties of tryptophan containing peptide assemblies [346] have also been characterized using CP-AFM.

Electrostatic force microscopy (EFM) is another nanoscale electrical characterization technique based on the resonance frequency shift of the mechanically oscillating cantilever due to the electrostatic interactions between the tip and the surface during noncontact AFM operation [347]. The technique assists the structural imaging of the peptide nanostructures before the electrical phase measurement, which is also called the lift-off mode [348]. EFM analysis of the self-assembled dipeptide nanotubes was conducted to analyse the electrochemical differences between the designed nanostructures [349]. Surface potential mapping of the surfaces functionalized with synthetic peptide assemblies were obtained using the EFM technique to distinguish purple membrane–peptide interactions at the interfaces [350]. EFM measurements were also performed to study the electronic behaviour of the polymerizable unit conjugated peptide assemblies [43] and peptide–carbon nanotube hybrid architectures [351]. Within AFM-based approaches, Kelvin probe force microscopy (KPFM) [352] is used for the characterization of peptide assemblies to determine contact potential differences (CPD), which is related to the work function of the samples. In the literature, synthetic coil-coiled structures absorbed on gold surfaces were characterized using this technique [353]. KPFM images of the short peptide nanostructures, which revealed both CPD parameters and the structural properties of the assemblies have been also reported [354].

Impedance spectroscopy (IS) enables the analysis of the electrochemical properties of peptide functionalized surfaces [355, 356] and the interactions of peptide nanostructures with other components [357]. IS functions by applying a periodic AC bias to the sample while collecting signals related to its complex impedance behaviour. The conductive properties of the dried peptide nanostructure obtained via enzyme-triggered self-assembly of aromatic PAs were studied using complex impedance spectroscopy that determined the sheet resistivity of the nanotubular architectures [358]. The electrochemical behaviour of the self-assembled peptide nanofibre functionalized gold surfaces developed as a metal ion biosensor was also evaluated using this technique [359].

5.5. Mechanical characterization techniques

Development of nanomechanical characterization techniques for peptide nanostructures is a requirement since the traditional mechanical characterization methods are incapable of operating at biologically relevant length and force scales with applicable time periods. The nanoscale AFM probes facilitate the implementation of traditional approaches including adhesion, tensile, compression or bending tests to analyse the nanomechanics of self-assembled peptide nanostructures at miniaturized experimental conditions.

AFM-based nanoindentation is a widely used approach to determine the mechanical properties of peptide nanostructures (e.g. their hardness, stiffness and elasticity) based on the load–distance curves collected during analysis [360, 361]. Interactions between the tip and nanostructures are modelled based on different approaches to estimate their nanomechanical characteristics [362–364]. The elastic modulus values of the self-assembled PA nanofibers formed via Ca^{2+} crosslinking or pH change were estimated using the force–distance data obtained via AFM nanoindentation [365]. AFM nanoindentation experiments were conducted to show the nanomechanical differences of azide containing spherical peptide assemblies before and after UV irradiation [366]. In another study, the effect of the structural transition of chemically modified self-assembled diphenyl nanostructures on their mechanical properties were analysed via AFM-based nanomechanical measurements [195]. Moreover, double pass-force–distance mapping is able to combine topography imaging with the mechanical characterization of the imaged area, and uses tapping mode AFM in conjunction with the acquisition of force–distance curves associated with tip-oscillating sample interactions [367]. The technique increased the speed of nanomechanical characterization of the nanostructures and enhanced the high resolution force mapping of the amyloid inspired peptide assemblies using AFM [87].

The unique mechanical behaviour of the amyloid like peptide assemblies contributed to the design of functional materials including conductive fibres, energy harvesting systems or tissue scaffolds [368–372]. Cross-β sheet organization, excess hydrogen bonding and aromatic interactions between the amyloid-based peptides are the inherent sources of the mechanical stability and rigidity of the amyloid derived peptide assemblies [373]. Several studies were conducted to determine the nanomechanical properties of the amyloid-based assemblies using the AFM nanoindentation technique. Recently, the nanomechanics of amyloid like fibrils assembled at different pH were revealed by peak-force quantitative nanomechanical property mapping (PF-QNM) [374]. In another study, the mechanical reinforcement of electrospun polymer fibres incorporated into peptide assemblies was demonstrated via AFM-based nanoindentation experiments with a spherical colloidal tip [375].

In addition to AFM-based nanoindentation, different characterization approaches have been developed to determine the mechanical characteristics of the self-assembled peptide nanostructures and their three-dimensional supramolecular networks [376]. Similar to amyloid peptide assemblies, cyclic peptide architectures reveal intriguing hierarchical organizations with tunable mechanical properties and rigid geometries [15]. The nanomechanical properties of these architectures including elastic modulus, hardness, strength and Young's modulus were determined by using AFM nanoindentation; self-assembled cyclic QL4 fibres exhibited the stiffest material characteristics within the known proteinaceous micro- and nanofibres (figure 7) [93].

The viscoelastic behaviour of different peptide assemblies were also determined using oscillatory rheology or microrheology techniques, which highlight the sol–gel transition of the peptide architectures due to the external or internal stimulus [377–381]. In addition, a microfluidic-based microcantilever system was developed to determine the forces produced by amyloid peptide polymerization, by monitoring microcantilever deflections that are correlated with the mechanical changes that occur during the process [382].

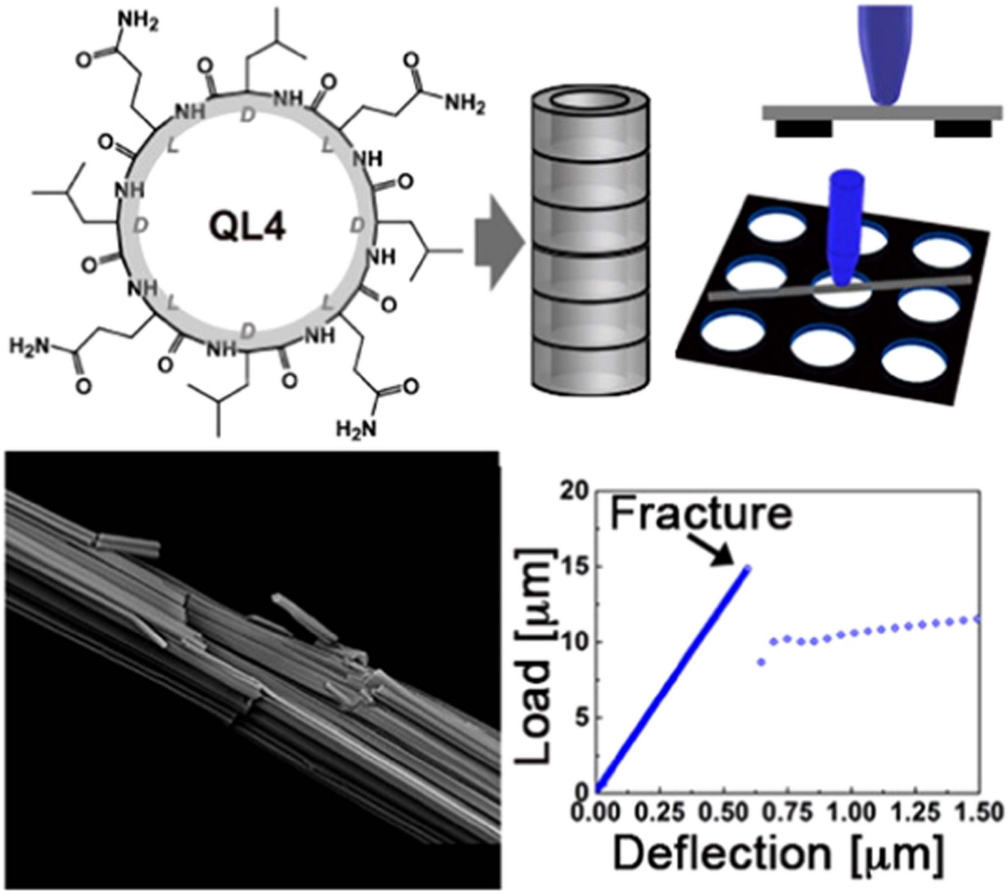

Figure 7. Nanomechanical properties of the D, L cyclic peptide assemblies were determined via depth sensing-based bending system (top) and the fractures formed on the nanostructures during the measurement were imaging using electron microscopy (bottom). Adapted with permission from [93]. Copyright 2015 American Chemical Society.

6. Functional self-assembled peptide nanostructures

Supramolecular chemistry is a powerful tool for fabricating innovative materials for the next generation devices and applications. Peptide self-assembly has been extensively utilized to produce functional nanomaterials. In this section, we review recent functional materials applications of self-assembled peptide nanostructures.

6.1. Supramolecular self-assembled peptide catalysts

Extraordinary catalytic performance and superior selectivity of enzymes in organic transformations under physiological conditions have always been a source of inspiration for scientists. The complex structure and function of biocatalysts have forced scientists to develop minimalistic approaches and mimic fragments of multifaceted biocatalysts such as active site, hydrophobic pocket or structure [383]. Supramolecular self-assembled peptide nanostructures have been utilized to build essential functional groups within a nanoenviroment to catalyse the desired organic transformations in an efficient manner. The Stupp group demonstrated self-assembled peptide amphiphile nanostructures, which are well-defined catalytic nanostructures in aqueous media [384]. Four different peptide sequences containing histidine residues as reactive sites were designed and synthesized (figures 8(A) and (B)). The peptide **1** having alanine and valine residues promoted formation of β-sheets and palmitoyl tail assisted hydrophobic collapse of the peptide molecules into high aspect ratio 1D nanofibers, as shown in figure 8(C).

The same peptide sequence without palmitoyl tail (**3**) formed nanospheres is shown in figure 8(D), meanwhile the peptide sequences having proline residues (**2** and **4**) also formed polydisperse nanospheres. Hydrolysis of 2, 4-dinitrophenyl acetate (DNPA) by these nanostructures has shown that 1D nanofibers promoted the highest hydrolysis rate when compared to nanospheres or soluble histidine residues. Interestingly, 1D nanofibres showed a Michaelis–Menten enzyme-like behaviour, whereas the other peptide sequences (**2**–**4**) demonstrated a linear rate increase with substrate concentration increase. This study showed that assembling reactive sites within a nanoenviroment could afford a synergistic effect that enhances the rate of hydrolysis of DNPA. This study was one of the first examples of a supramolecular self-assembled peptide catalyst, which inspired many research groups to develop new catalytic supramolecular peptide nanostructures. The Escuder and Miravet research groups have extensively studied the structure and catalytic activity of proline-based supramolecular gelators

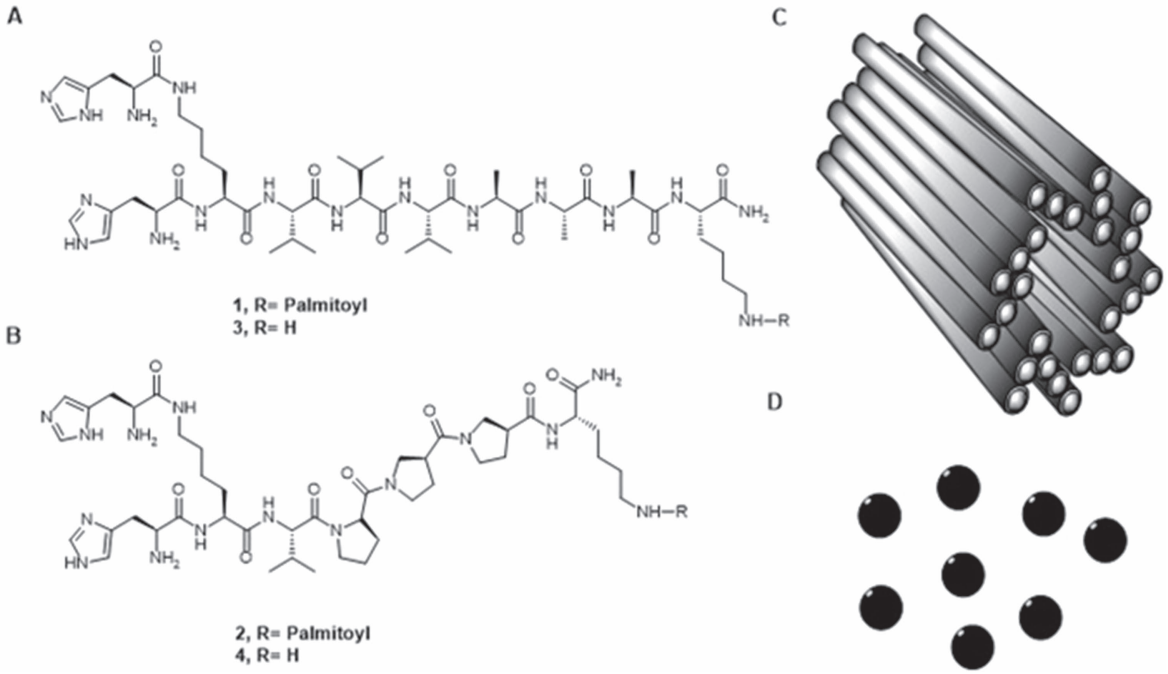

Figure 8. Chemical structures of peptide molecules (A) and (B), schematic representation of self-assembled nanofibres (C) and spherical aggregates (D).

[385]. L-proline is a well-known stereoselective organocatalyst for catalysing C–C bond formation reactions, such as aldol and Michael addition reactions [386]. A series of bolaamphiphilic molecules containing two L-prolines have been designed and used in aldol reactions [387]. Due to the presence of hydrogen-bond promoting valine residues in the structure of bolaamphiphilic peptide molecules, they could encapsulate a large amount of organic solvents (acetonitrile and ethyl acetate) to form gels. These peptide molecules catalysed the aldol reaction in solution state while racemization of the products was observed in the gel state where the reactions were left for several days. The reason for racemization was explained by the increase of basicity of the solution due to the close assembly of prolines in the gel state. The authors exploited the emergence of a new property (increased basicity) caused by cooperativity of neighbouring prolines in the gel state [388]. They performed the Henry nitroaldol reaction, which requires a basic catalyst for deprotonation of nitroalkane and then addition to carbonyl functional group to form new C–C bonds. A bolaamphiphile peptide molecule was used to form a gel in nitromethane and nitroethane. This basic catalytic gel promoted the addition of nitroalkane to 4-nitrobenzylaldehyde. The assembled bolaamphiphile peptide molecules into fibrous networks showed excellent catalytic activity while dispersed peptide molecules showed poor catalytic activity. Performing organic reactions in aqueous media motivated the researchers to synthesize a new proline conjugated amphiphilic peptide molecule, which formed hydrogels [389]. This catalytic hydrogel assisted the direct aldol reaction between cyclohexanone and 4-nitrobenzaldehyde. The reactants dissolved in toluene were gently dropped on a pre-formed peptide hydrogel and showed high stereoselectivity (anti: syn 92:8, 88% ee). The catalytic nanostructure was recycled three times without loss of efficiency and stereoselectivity.

In addition to L-proline-based supramolecular catalysts, the researchers have also developed different novel approaches to mimic active sites of enzymes. Liu *et al* demonstrated that co-assembly of two different amino acid residues could enhance the rate of hydrolysis [390]. They synthesized two short amphiphilic peptide sequences, one bearing histidine (Fmoc-FFH-Am) and other bearing arginine residues (Fmoc-FFR-Am). The Fmoc-FFH-Am molecule self-assembled into nanotubes in aqueous medium can catalyse *p*-nitrophenyl acetate efficiently. Upon co-assembly of both peptides into nanotubes, the catalytic activity was further enhanced. A similar study was conducted by the Liang group [391]. Co-assembly of histidine and arginine bearing self-assembled peptide nanofibres can enhance the hydrolysis of *p*-nitrophenyl acetate. These two studies underlined the importance of arginine residues, which stabilized the transition state of the hydrolytic reaction.

Metal ions play an important role as cofactors in metalloenzymes. Metal ion-based cofactors are present in the active site of enzymes, which aid the chemical reactions in proceeding [392]. Self-assembled supramolecular peptide nanostructures can be used to emulate part of the metalloenzyme and replicate the function of the whole enzyme. Liu *et al* designed and synthesized glutamic acid bearing bolaamphiphile nanotubes that are able to bind copper (II) ions through electrostatic interactions. The nanotubes induced chirality to copper (II) ions and catalysed the Diels–Alder reaction between cyclopentadiene and an aza-chalcone [393]. The Korendovych group studied short metallopeptides for

mimicking metalloenzymes. A series of short amyloid like peptides, which have binding affinity towards Zn (II) ions were designed and synthesized [394]. A β-sheet forminga heptapeptide sequence (LKLKLKL) was modified at positions 2, 4 and 6 by different amino acids. Hydrophobic leucine (L) required for self-assembly was kept unchanged while lysine (K) residues at positions 2 and 4 were replaced by Zn^{+2} binding histidine residues. Lysine at position 6 was replaced by either acidic (Asp, Glu), neutral (Gln, Tyr) or basic (His, Lys, Arg) residues with various pKa values. The peptide sequence Ac-LHLHLRL-Am in the presence of $ZnCl_2$ showed Michaelis–Menten behaviour with catalytic efficiency of $k_{cat}/K_M = 18 \pm 4\,M^{-1}\,s^{-1}$. When the R residue was replaced by Q residue (Ac-LHLHLQL-$CONH_2$), the catalytic efficiency was further increased to $k_{cat}/K_M = 30 \pm 3\,M^{-1}\,s^{-1}$. Peptides with Asp, Glu or His residues at position 6 had little catalytic activity. However, catalytic activity was drastically enhanced ($k_{cat}/K_M = 62 \pm 2\,M^{-1}\,s^{-1}$) when the hydrophobic L was replaced by the isoleucine (I) in the heptapeptide sequence, while keeping Gln at the 6th position (Ac-IHIHIQI-Am).

We also recently developed a β-sheet forming peptide amphiphile, which had high binding affinity towards copper ions. This short peptide sequence assembled into nanofibres having histidine residues over the surface. The copper ions bound on pre-assembled peptide nanofibres could catalyse click alkyne–azide cycloaddition in aqueous media [395]. The conversion of the reactants into product was almost quantitative (95%) using our supramolecular nanocatalyst, while soluble histidine-Cu complexes showed a moderate efficiency of 65%. Active sites demonstrated positive cooperativity when assembled within a confined environment on the peptide nanofibres. The supramolecular nanocatalyst did not only show superior catalytic activity but also lowered the cytotoxicity of the copper ion. Therefore, we utilized the metallopeptide to label alkyne decorated live cells by click alkyne–azide cycloaddition.

6.2. Supramolecular semiconductor peptide nanostructures

Organic electronics can be divided into three major fields: supramolecular, plastic and molecular electronics [396]. The latter two fields have been studied in detail and a Nobel Prize in chemistry was awarded for the discovery of electrically conductive polymers (plastic electronics) in 2000. Although supramolecular electronics is a relatively obscure research field, it has nonetheless achieved considerable progress in the last decade. Supramolecular chemistry is a powerful tool for designing and constructing well-defined nanowires for nanosized optoelectronic devices using noncovalent interactions [396]. The rich chemistry of 20 natural amino acids makes them an eye-catching tool for building novel supramolecular soft semiconducting materials that could be employed for bioelectronics [204], light harvesting systems [397], OFETS, nanoscale devices and nanosensors [398].

The main strategy for fabricating a nanosized semiconducting wire is to conjugate hydrophobic, π-conjugated p-n-type semiconductor molecules to hydrophilic or charged self-assembling peptide sequences. Upon hydrophobic collapse in aqueous media, the semiconductor conjugated peptide molecules can form variety of nanostructures. This strategy also allows working with highly hydrophobic molecules in aqueous media. Parquette *et al* conjugated an n-type semiconducting molecule (1,4,5,8-naphthalenetetracarboxylic acid diimide, NDI) to a series of dipeptides (Ac-KK-Am) and studied their self-assembly in aqueous medium and trifluoroethanol (TFE) [399]. The NDI semiconductor peptide conjugate assembly was studied by UV and CD spectroscopies. The NDI-peptide molecule dissolved in TFE showed absorption peaks at 240 nm (band II) and in the range of 300–400 nm (band I), which are characteristic absorption peaks of molecular NDI molecules. When TFE was exchanged with water, there was a decrease in absorption intensities followed by large red shift in the absorption bands of NDI. This change showed formation of j-aggregates in water. The IR bands at 1612 and 1608 cm^{-1}, and XRD analysis proved the presence of a β-sheet in Ac-KK (NDI)-Am and in Ac-K (NDI)-K-Am peptides. TEM and AFM images of Ac-KK (NDI)-Am peptide molecules showed helical nanofibres while Ac-K(NDI)-K-Am peptides showed flattened, twisted nanoribbon morphology. They also conducted a similar study by conjugating two lysine moieties to the two arms of NDI forming n-type bolaamphiphiles [400]. Bolaamphiphile molecules formed hydrogel when dissolved 1% (w/w). The designed molecule formed nanotubes as imaged by TEM and AFM. UV–vis absorption spectroscopy demonstrated a red shift in the absorption bands showing the formation of NDI *j*-aggregates in assembled state. CD spectra revealed additional peaks at the absorption bands of the NDI molecule demonstrating that induced chirality is due to supramolecular organization of NDI molecules within the assembled nanotubes. The fluorescence decay of nanotubes excited at 350 nm was monitored by time-correlated single photon counting at 410 and 505 nm. The lifetime (64 ps) of excited NDI nanotubes was slightly longer than that of molecular NDI. The excimer emission at 505 nm showed much longer decay lifetime (197 ps (86%) and 950 ps (14%)), which is due to closely stacked and packed NDI molecules in the nanotubes.

Tovar [43, 173, 401–404] and others [200, 405, 406] have developed semiconducting oligomers conjugated to peptides (figure 9) assembled into well-defined nanostructures in aqueous media. In this design, oligomers were located at middle and peptide sequences were conjugated at two sides. This strategy facilitated face to face aggregation of the semiconducting molecules, which may increase their conductivity by enhancing their hole or electron transporting properties. The Tovar group also developed a straightforward method for conjugating oligomer molecules on solid phase resin. On resin synthesis avoids multiple synthetic routes and complex purification techniques. Charge transport properties of self-assembled soft fibrous nanonetworks were measured by constructing a field-effect transistor [401]. The peptide conjugated quaterthiophene was used as a semiconductor layer and mobilities of 10^{-3}–$10^{-5}\,cm^2\,V^{-1}\,s^{-1}$ were measured. When the nanowires were aligned via shear-assembly, the mobilities were increased to $0.03\,cm^2\,V^{-1}\,s^{-1}$.

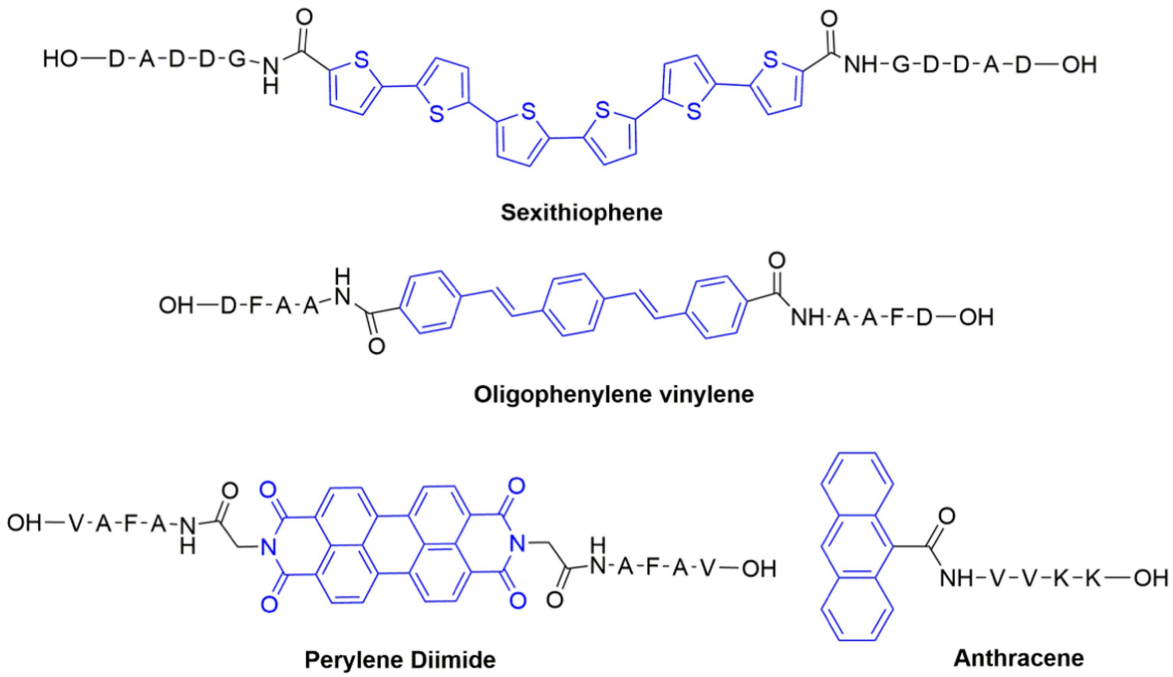

Figure 9. Semiconducting oligomers conjugated to peptide molecules.

The Ashkenasy group conducted a detailed study on the conductivity of self-assembled semiconducting peptide nanostructures [199, 337]. A well-known amyloid β-peptide (AAKLVFF) was studied by incorporating 2-thienylalanine and 3-thienylalanine moieties instead of FF. They investigated the self-assembly of these molecules in different solvents and demonstrated that the solvent type had a considerable effect on nanostructure morphology. They also observed that the peptide molecule forming long range and straight nanofibers showed highest conductivity. In another research work [405], they demonstrated that both protons and electrons are responsible for the charge transport process in self-assembled nanostructures. In a highly humid environment, proton conductivity dominated electron conductivity. Hodgkiss *et al* have recently constructed a water-processed bio-organic field-effect transistor (biOFET) based on bioinspired assembled peptide–perylene conjugates [407]. The peptide sequence of IKHLSVN, which is responsible for the homo dimerization of peroxiredoxin protein was modified as IRHLSVN. Three glumatic acid residues were conjugated to IRHLSVN to enhance the solubility of IRHLSVN–perylene molecules in water. The self-assembly of these bioinspired molecules was studied by CD and UV–vis spectroscopy to see whether the β-sheet forming characteristic of the native IKHLSVN sequence was affected by the modifications and perylene conjugation. Long nanofibers of assembled IRHLSVN–perylene were imaged by TEM and AFM. Interestingly, the semiconducting nanofibers showed p-type behaviour, responding to an increasing positive gate bias with a decreasing current.

One component semiconductor peptide self-assembly was further extended to two components including co-assembly of p-n-type semiconductors to achieve charge transfer or photoconductive supramolecular nanomaterials. The Ulijn group [408–410] conducted a series of research on biocatalytic self-assembly of n-type semiconductor conjugated peptides that could form charge transfer supramolecular nanostructures with variety of p-type semiconductors (figure 10). NDI-functionalized tyrosine (NDI-Y) was conjugated to phenylalanine-amide (F-NH_2) by the addition of thermolysin to trigger self-assembly and formation of thermodynamic nanostructures. In the presence of p-type dihydroxy/alkoxy naphthalene donors, NDI-Y formed polydisperse spherical nanostructures when thermolysin was absent, as imaged by TEM and AFM. Upon addition of a biocatalyst to a solution of NDI-Y and naphthalene donors, a yellowish gel was formed and spherical nanostructures were converted to highly-ordered long nanofibers. The change in the colour of the solution was followed by donor emission quenching and the appearance of a new absorption band at 550 nm, which was attributed to the successful formation of a charge transfer complex. The same group conjugated a well-known p-type tetrathiafulvalene (TTF) to a self-assembling peptide sequence (-FF-Am). TTF-FF-Am molecules formed self-standing gel in chloroform and dried gels showed conductivity of 1.9×10^{-10} s cm^{-1}. When the organogel was doped by an acceptor molecule (TCNQ) the conductivity was increased to 3.6×10^{-4} s cm^{-1}. However, iodine vapour doping did not enhance the conductivity to a great extent as in the case of acceptor doping [411]. There are also some studies showing energy transfer within self-assembled peptide nanostructures through donor–acceptor interactions [412, 413].

Recently, the Martín research group exploited electrostatic interactions to assemble donor–acceptor molecules in a highly organized manner within a peptide nanofiber [414].

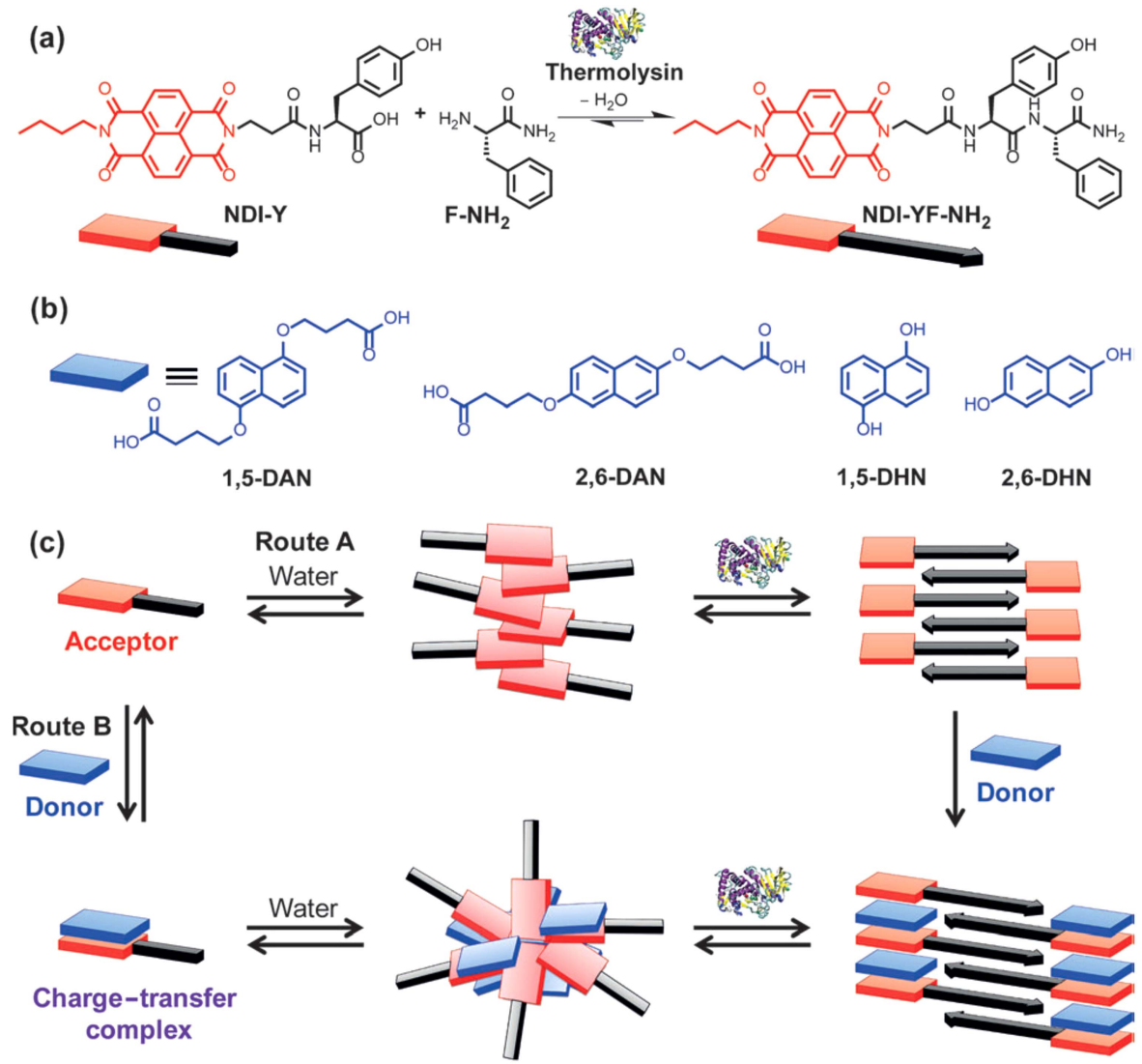

Figure 10. Biocatalytic self-assembly of acceptor-appended peptides to form charge transfer nanostructures. Adapted with permission from [409]. Copyright 2014, Wiley-VCH.

Electron donor tetrathiafulvalene was conjugated to an anionic peptide sequence bearing glutamic acid while electron–acceptor perylene-bisimide was conjugated to a cationic peptide sequence bearing residue. These two complimentary p-n nanofibers could co-assemble into highly alternating p-n stacks in the single nanofiber. The co-assembled p-n nanofibers showed photoconductivity of $0.8\,cm^2\,V^{-1}\,s^{-1}$. These types of novel and straightforward methodologies are promising for design and fabrication of next generation nanodevices.

6.3. Self-assembled peptide nanostructure templated synthesis of inorganic nanomaterials

Synthesis of inorganic nanomaterials with precise shape, size and composition has potential industrial applications. Biomolecules having well-defined shapes and sizes are remarkable platforms for the synthesis of inorganic functional nanomaterials [415]. Cutting-edge developments have been achieved by utilizing biotemplates such as viruses [416–418], bacteria [419, 420], nucleic acids (DNA or RNA) [421] and proteins [422, 423] for the mineralization process, resulting in the fabrication of well-ordered functional nanomaterials for catalysis, sensing, imaging, therapy, energy storage/conversion, and electronic and piezoelectric devices. Self-assembling peptide-templated synthesis of functional nanostructures is another emerging area, which has been extensively studied.

Matsui *et al* designed a bolaamphiphile peptide molecule (bis (*N*-R-amido-glycylglycine)-1,7-heptane dicarboxylate), which assembled into nanotubes at pH 6 citric acid/NaOH solution. The amide groups on pre-assembled nanotubes could coordinate with metal ions (Cu and Ni) which served as nucleation sites. Nanotube coated ions were further reduced by reducing agents to get metalized nanotubes [424]. In another study conducted by Matsui, the same bolaamphiphile peptide nanotube was further modified by a histidine-rich peptide sequence (AHHAHHAAD). Histidine modified nanotubes were treated with gold ions followed by $NaBH_4$

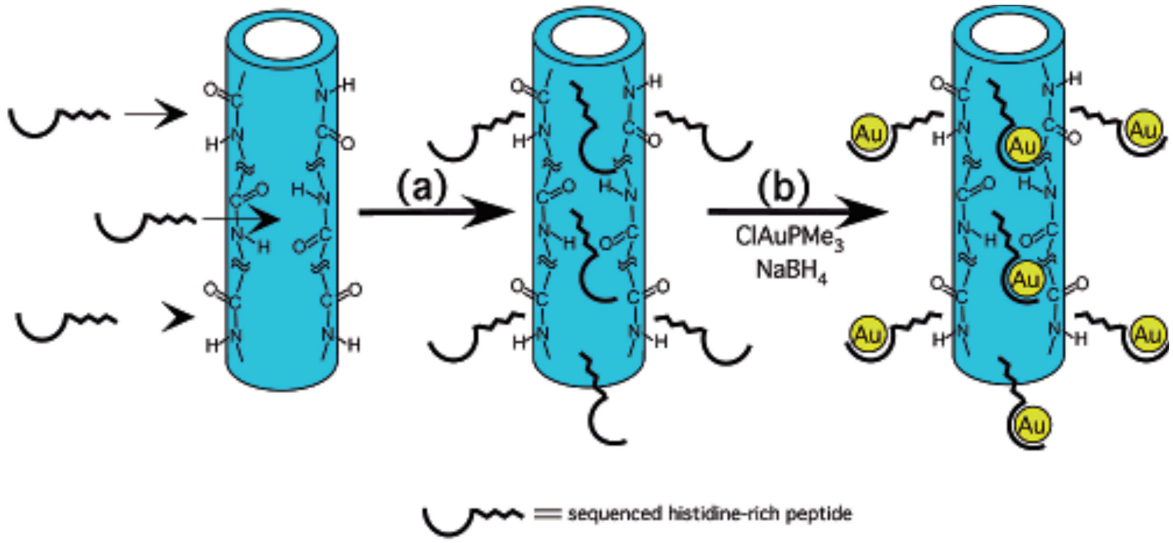

Figure 11. Schematice diagram of Au nanowire fabrication. (a) Modification of pre-assembled nanofibres by histidine-rich peptide. (b) Formation of gold nanoparticles at the histidine sites of the nanofibres. Adapted with permission from [425]. Copyright 2002 American Chemical Society.

reduction to form gold nanoparticles (figure 11). Metal-binding histidine residues directed the formation of gold nanoparticles over nanotubes homogenously. The crystal lattice of gold nanoparticles was calculated as (111) and (220) from electron diffraction patterns [425].

The Stupp group developed unasymmetric bolaamphiphile peptide molecules such as (L-glutamyl)$_3$ glycine-terminated bolaamphiphile (**1**) and (L-lysine)$_3$-terminated bolaamphiphile. This molecule formed a self-standing hydrogel in the presence of ammonia vapour. When the secondary structure of these molecules were studied by CD, they showed random coil structure in their soluble form while β-sheets were observed upon gelation. These 1D nanofibrous networks were utilized to mineralize CdS nanostructures. Peptide nanostructures were treated with a dilute solution of $Cd(NO_3)_2$ followed by exposure to H_2S vapour. Peptide nanostructure templated CdS nanostructures had wurtzite and zinc blende polymorph crystal structures [426].

In another study, the Stupp group demonstrated the metal ion-binding capacity of a self-assembling peptide amphiphile containing three histidine residues [427]. The peptide amphiphile molecule dissolved in water formed a gel upon increasing the pH above 6. The gel consisted of peptide nanofibers with 8–10 nm diameters and microns in length as imaged by TEM. This nanofibrous network was used to template magnetite mineralization. A black precipitate was formed upon mixing of 1:2 ratio of $FeCl_2$:$FeCl_3$ solutions with peptide nanofibres followed by exposure to ammonia vapour. This black precipitate was responsive to magnetic fields, suggesting that it contained magnetite (Fe_3O_4) nanostructures embedded in the peptide matrix. Raman spectroscopy showed a peak at 674 cm^{-1}, which further confirmed the presence of Fe_3O_4 mineralized on peptide nanofibres.

Our group also developed various self-assembled peptide templates to synthesize Pd, Au, SiO_2, TiO_2 and ZnO nanostructures. An amyloid inspired short peptide sequence (Ac-KFFAAK-Am) was designed and synthesized which formed 1D nanofibres. This fibrous nanonetwork was used as a template to mineralize SiO_2 and TiO_2. After calcination of the organic part, micron-long nanotubes of SiO_2 and TiO_2 were formed [428]. Amyloid inspired templated porous silica nanotubes were used as a high surface area explosive detector. The surface of the silica nanotubes was modified using a fluorescent probe by physical adsorption. These fluorescent silica nanotubes demonstrated fast, sensitive and highly selective fluorescence quenching towards nitro-explosive vapours [429]. We further utilized amyloid inspired templated porous titania nanotubes as dye sensitized solar cell anodic materials. In this study, we showed that porous, high surface area (150 $m^2 g^{-1}$) titania nanotubes could adsorb more dye than the nontemplated titania. As a result, dye sensitized solar cell constructed from porous titania nanotubes showed an efficiency of 0.83%, which is three-fold better than non-templated titania [430].

Amyloid inspired peptide nanofibres were further exploited to template gold nanostructure synthesis. Amine decorated peptide nanofibres interacted with gold ions and gold nanostructures were grown upon reduction by ascorbic acid. AFM was used to investigate the nanoscale electrical properties of the gold decorated peptide nanofibres. Bias dependent current (I–V) measurements on gold nanofibers demonstrated tunnelling dominated transport and resistive switching [336].

In addition to amyloid inspired peptide templates, our group also designed self-assembling peptide amphiphiles, which could template palladium nanoparticle synthesis. A histidine-rich peptide amphiphile nanofibre was designed to synthesize Pd nanoparticles, which could be utilized as a nanocatalyst for Suzuki coupling reactions. Our designed Pd nanocatalyst showed high catalytic activities under environmentally friendly conditions. Reaction products were obtained almost quantitatively in the presence of our catalyst

in addition to the ease of recycling [431]. In another study, we utilized critically-dried 3D peptide nanonetworks as a scaffold for atomic layer deposition, using the porosity and high surface area of the peptide material to produce highly conformal and uniform titania and silica nanotubes. These highly precise nanostructures showed high photocatalytic activities towards methylene blue degradation. The photocatalytic activity was exclusively dependent on wall thickness and surface area per unit mass of titania and silica nanotubes [432].

Others have also exploited various self-assembled peptide templates such as I_3K, phage-displayed P7A peptides [433] and aniline–GGAAKLVFF [434] to synthesize Pt nanoparticles for different applications. I_3K assembled nanofibres have been used to template Pt nanoparticles while phage-displayed P7A peptides were utilized to tune morphologies of Pt nanoparticles. I_3K assembled nanofibre decorated Pt nanostructures were used for electrochemical oxidation of hydrogen and methanol while aniline–GGAAKLVFF supported Pt nanoparticles were used as an electrocatalyst to improve oxygen-reduction reaction [434].

Tuning the spatial arrangement of metallic nanostructures via peptide morphology to induce new properties is another exciting field. A peptide amphiphile (lauryl-FPPMPPAGAYSS), which formed double helices, directed the formation of left-handed gold nanoparticles [435]. The -Liu research group produced chiral silica nanotubes via helical bolaamphiphilic peptide templates. Chiral silica nanotubes modified by photoactive azobenzene moieties can recognize a chiroptical switch [436].

7. Conclusion and future perspective

One of the reasons behind the rapid growth of self-assembly is that it allows the synthesis of larger structures that are not feasible with covalent bonds due to poor stability. Accordingly, peptide constructs with well-defined characteristics can be created through a self-assembly process, and the morphology and function of the resulting structures can be manipulated at the molecular level by altering the number, type and sequence of amino acids, or exposing the system to external stimuli such as pH, temperature, electric or magnetic fields, light and sound. The systematic investigation of the structure-function relation of the self-assembled peptide nanostructures using variety of advanced characterization techniques at nanometre scale will accelerate the progress on developments of functional peptide-based architectures. Although different characterization tools and methods have been developed for self-assembled peptide-based functional nanostructures, most of the techniques still require advanced sample preparation and sophisticated analysis tools to reveal deep knowledge on the intriguing properties and energy landscapes of self-assembly. On the other hand, we believe that advancements on these techniques can be pursued via incorporation of the different scientific disciplines, including chemistry, biology, material science and engineering, since the problems in the technical advances require an interdisciplinary research environment. Constructing novel nanomaterials with new properties using supramolecular interactions is an exciting research field. A vast number of cutting-edge applications of supramolecular materials have been demonstrated so far. Designing controllable materials with precise length, composition and complex shapes will be the challenge of next generation supramolecular materials.

Acknowledgments

MSE, GC and MAK are supported by a TUBITAK BIDEB PhD fellowship. This work is partially supported by TUBITAK 114Z753.

References

[1] Stephanopoulos N, Ortony J H and Stupp S I 2013 Self-assembly for the synthesis of functional biomaterials *Acta Mater.* **61** 912–30
[2] Ozin G A, Hou K, Lotsch B V, Cademartiri L, Puzzo D P, Scotognella F, Ghadimi A and Thomson J 2009 Nanofabrication by self-assembly *Mater. Today* **12** 12–23
[3] Arslan E, Garip I C, Gulseren G, Tekinay A B and Guler M O 2014 Bioactive supramolecular peptide nanofibers for regenerative medicine *Adv. Healthcare Mater.* **3** 1357–76
[4] Hosseinkhani H, Hong P D and Yu D S 2013 Self-assembled proteins and peptides for regenerative medicine *Chem. Rev.* **113** 4837–61
[5] Panda J J and Chauhan V S 2014 Short peptide based self-assembled nanostructures: implications in drug delivery and tissue engineering *Polym. Chem.* **5** 4418–36
[6] Ravichandran R, Griffith M and Phopase J 2014 Applications of self-assembling peptide scaffolds in regenerative medicine: the way to the clinic *J. Mater. Chem.* B **2** 8466–78
[7] Klok H A 2002 Protein-inspired materials: synthetic concepts and potential applications *Angew. Chem. Int. Ed.* **41** 1509–13
[8] Cavalli S, Albericio F and Kros A 2010 Amphiphilic peptides and their cross-disciplinary role as building blocks for nanoscience *Chem. Soc. Rev.* **39** 241–63
[9] Merrifield R B 1963 Solid phase peptide synthesis: I. The synthesis of a tetrapeptide *J. Am. Chem. Soc.* **85** 2149–54
[10] Isidro-Llobet A, Alvarez M and Albericio F 2009 Amino acid-protecting groups *Chem. Rev.* **109** 2455–504
[11] El-Faham A and Albericio F 2011 Peptide coupling reagents, more than a letter soup *Chem. Rev.* **111** 6557–602
[12] Pedersen S L, Tofteng A P, Malik L and Jensen K J 2012 Microwave heating in solid-phase peptide synthesis *Chem. Soc. Rev.* **41** 1826–44
[13] Maude S, Tai L, Davies R, Liu B, Harris S, Kocienski P and Aggeli A 2012 *Peptide-Based Materials* (Heidelberg: Springer) pp 27–69
[14] Hamley I 2011 Self-assembly of amphiphilic peptides *Soft Matter* **7** 4122–38
[15] Chapman R, Danial M, Koh M L, Jolliffe K A and Perrier S 2012 Design and properties of functional nanotubes from the self-assembly of cyclic peptide templates *Chem. Soc. Rev.* **41** 6023–41
[16] Ramakers B, van Hest J and Löwik D 2014 Molecular tools for the construction of peptide-based materials *Chem. Soc. Rev.* **43** 2743–56

[17] Garanger E and Lecommandoux S 2012 Towards bioactive nanovehicles based on protein polymers *Angew. Chem. Int. Ed.* **51** 3060–2

[18] ávan Hest J C 2001 Protein-based materials, toward a new level of structural control *Chem. Commun.* **19** 1897–904

[19] Dougherty D A 2000 Unnatural amino acids as probes of protein structure and function *Curr. Opin. Chem. Biol.* **4** 645–52

[20] Cheng J and Deming T J 2012 *Peptide-Based Materials* (Heidelberg: Springer) pp 1–26

[21] Hadjichristidis N, Iatrou H, Pitsikalis M and Sakellariou G 2009 Synthesis of well-defined polypeptide-based materials via the ring-opening polymerization of α-amino acid N-carboxyanhydrides *Chem. Rev.* **109** 5528–78

[22] Huang J and Heise A 2013 Stimuli responsive synthetic polypeptides derived from N-carboxyanhydride (NCA) polymerisation *Chem. Soc. Rev.* **42** 7373–90

[23] Pattabiraman V R and Bode J W 2011 Rethinking amide bond synthesis *Nature* **480** 471–9

[24] Tam J P, Xu J and Eom K D 2001 Methods and strategies of peptide ligation* *Pept. Sci.* **60** 194–205

[25] Fairman R and Åkerfeldt K S 2005 Peptides as novel smart materials *Curr. Opin. Struct. Biol.* **15** 453–63

[26] Zhao X, Pan F, Xu H, Yaseen M, Shan H, Hauser C A, Zhang S and Lu J R 2010 Molecular self-assembly and applications of designer peptide amphiphiles *Chem. Soc. Rev.* **39** 3480–98

[27] Toksoz S, Acar H and Guler M O 2010 Self-assembled one-dimensional soft nanostructures *Soft Matter* **6** 5839–49

[28] Steed J W and Atwood J L 2013 *Supramolecular Chemistry* (Chichester: John Wiley & Sons)

[29] Moreira Leite D, Barbu E, Pilkington G J and Lalatsa A 2015 Peptide self-assemblies in drug delivery *Curr. Top. Med. Chem.* **15** 2277–89

[30] Castillo J, Sasso L and Svendsen W E 2012 *Self-Assembled Peptide Nanostructures: Advances and Applications in Nanobiotechnology* (Boca Raton, FL: Pan Stanford Publishing) pp 67–85

[31] Brack A and Orgel L E 1975 β structures of alternating polypeptides and their possible prebiotic significance *Nature* **256** 383–7

[32] Berg J M, Tymoczko J L and Stryer L 2002 Secondary structure: Polypeptide chains can fold into regular structures such as the alpha helix, the beta sheet, and turns and loops *Biochemistry* 5th edn (New York: W H Freeman) ch 3

[33] Apostolovic B, Danial M and Klok H-A 2010 Coiled coils: attractive protein folding motifs for the fabrication of self-assembled, responsive and bioactive materials *Chem. Soc. Rev.* **39** 3541–75

[34] Löwik D W, Leunissen E, Van den Heuvel M, Hansen M and van Hest J C 2010 Stimulus responsive peptide based materials *Chem. Soc. Rev.* **39** 3394–412

[35] Dehsorkhi A, Castelletto V, Hamley I W, Adamcik J and Mezzenga R 2013 The effect of pH on the self-assembly of a collagen derived peptide amphiphile *Soft Matter* **9** 6033–6

[36] Hartgerink J D, Beniash E and Stupp S I 2002 Peptide-amphiphile nanofibers: a versatile scaffold for the preparation of self-assembling materials *Proc. Natl. Acad. Sci. USA* **99** 5133–8

[37] Lin B F, Megley K A, Viswanathan N, Krogstad D V, Drews L B, Kade M J, Qian Y and Tirrell M V 2012 pH-responsive branched peptide amphiphile hydrogel designed for applications in regenerative medicine with potential as injectable tissue scaffolds *J. Mater. Chem.* **22** 19447–54

[38] Tang C, Smith A M, Collins R F, Ulijn R V and Saiani A 2009 Fmoc-diphenylalanine self-assembly mechanism induces apparent pK_a shifts *Langmuir* **25** 9447–53

[39] Moyer T J, Finbloom J A, Chen F, Toft D J, Cryns V L and Stupp S I 2014 pH and amphiphilic structure direct supramolecular behavior in biofunctional assemblies *J. Am. Chem. Soc.* **136** 14746–52

[40] Lowik D, Meijer J T, Minten I J, Van Kalkeren H, Heckenmuller L, Schulten I, Sliepen K, Smittenaar P and van Hest J 2008 Controlled disassembly of peptide amphiphile fibres *J. Pept. Sci.* **14** 127–33

[41] Muraoka T, Cui H and Stupp S I 2008 Quadruple helix formation of a photoresponsive peptide amphiphile and its light-triggered dissociation into single fibers *J. Am. Chem. Soc.* **130** 2946–7

[42] Muraoka T, Koh C Y, Cui H and Stupp S I 2009 Light-triggered bioactivity in three dimensions *Angew. Chem. Int. Ed.* **121** 6060–3

[43] Diegelmann S R, Hartman N, Markovic N and Tovar J D 2012 Synthesis and alignment of discrete polydiacetylene-peptide nanostructures *J. Am. Chem. Soc.* **134** 2028–31

[44] Altman M, Lee P, Rich A and Zhang S 2000 Conformational behavior of ionic self-complementary peptides *Protein Sci.* **9** 1095–105

[45] Hamley I W, Dehsorkhi A, Castelletto V, Furzeland S, Atkins D, Seitsonen J and Ruokolainen J 2013 Reversible helical unwinding transition of a self-assembling peptide amphiphile *Soft Matter* **9** 9290–3

[46] Miravet J F, Escuder B, Segarra-Maset M D, Tena-Solsona M, Hamley I W, Dehsorkhi A and Castelletto V 2013 Self-assembly of a peptide amphiphile: transition from nanotape fibrils to micelles *Soft Matter* **9** 3558–64

[47] Pochan D J, Schneider J P, Kretsinger J, Ozbas B, Rajagopal K and Haines L 2003 Thermally reversible hydrogels via intramolecular folding and consequent self-assembly of a *de novo* designed peptide *J. Am. Chem. Soc.* **125** 11802–3

[48] Nuhn H and Klok H-A 2008 Secondary structure formation and LCST behavior of short elastin-like peptides *Biomacromolecules* **9** 2755–63

[49] Lock L L, Reyes C, Zhang P and Cui H 2016 Tuning cellular uptake of molecular probes by rational design of their assembly into supramolecular nanoprobes *J. Am. Chem. Soc.* **138** 3533–40

[50] Pim W 2015 Transient supramolecular reconfiguration of peptide nanostructures using ultrasound *Mater. Horiz.* **2** 198–202

[51] Hong Y, Pritzker M D, Legge R L and Chen P 2005 Effect of NaCl and peptide concentration on the self-assembly of an ionic-complementary peptide EAK16-II *Colloids Surf.* B **46** 152–61

[52] Ozbas B, Kretsinger J, Rajagopal K, Schneider J P and Pochan D J 2004 Salt-triggered peptide folding and consequent self-assembly into hydrogels with tunable modulus *Macromolecules* **37** 7331–7

[53] Mishra A, Chan K-H, Reithofer M R and Hauser C A 2013 Influence of metal salts on the hydrogelation properties of ultrashort aliphatic peptides *RSC Adv.* **3** 9985–93

[54] Toksoz S, Mammadov R, Tekinay A B and Guler M O 2011 Electrostatic effects on nanofiber formation of self-assembling peptide amphiphiles *J. Colloid Interface Sci.* **356** 131–7

[55] Stendahl J C, Rao M S, Guler M O and Stupp S I 2006 Intermolecular forces in the self-assembly of peptide amphiphile nanofibers *Adv. Funct. Mater.* **16** 499–508

[56] Beyer R L, Hoang H N, Appleton T G and Fairlie D P 2004 Metal clips induce folding of a short unstructured peptide into an α-helix via turn conformations in water. Kinetic versus thermodynamic products *J. Am. Chem. Soc.* **126** 15096–105

[57] Dublin S N and Conticello V P 2008 Design of a selective metal ion switch for self-assembly of peptide-based fibrils *J. Am. Chem. Soc.* **130** 49–51

[58] Pires M M and Chmielewski J 2009 Self-assembly of collagen peptides into microflorettes via metal coordination *J. Am. Chem. Soc.* **131** 2706–12

[59] Pagel K, Seri T, von Berlepsch H, Griebel J, Kirmse R, Böttcher C and Koksch B 2008 How metal ions affect amyloid formation: Cu^{2+}-and Zn^{2+}-sensitive peptides *Chem. Bio. Chem.* **9** 531–6

[60] Kar T, Mandal S K and Das P K 2011 Organogel–hydrogel transformation by simple removal or inclusion of N-Boc-protection *Chem. Eur. J.* **17** 14952–61

[61] Koley P, Gayen A, Drew M G, Mukhopadhyay C and Pramanik A 2012 Design and self-assembly of a leucine-enkephalin analogue in different nanostructures: application of nanovesicles *Small* **8** 984–90

[62] Zhao Y, Deng L, Wang J, Xu H and Lu J R 2015 Solvent controlled structural transition of KI4K self-assemblies: from nanotubes to nanofibrils *Langmuir* **31** 12975–83

[63] Madine J, Davies H A, Shaw C, Hamley I W and Middleton D A 2012 Fibrils and nanotubes assembled from a modified amyloid-β peptide fragment differ in the packing of the same β-sheet building blocks *Chem. Commun.* **48** 2976–8

[64] Webber M J, Newcomb C J, Bitton R and Stupp S I 2011 Switching of self-assembly in a peptide nanostructure with a specific enzyme *Soft Matter* **7** 9665–72

[65] Castelletto V, McKendrick J, Hamley I, Olsson U and Cenker C 2010 PEGylated amyloid peptide nanocontainer delivery and release system *Langmuir* **26** 11624–7

[66] Hirst A R, Roy S, Arora M, Das A K, Hodson N, Murray P, Marshall S, Javid N, Sefcik J and Boekhoven J 2010 Biocatalytic induction of supramolecular order *Nat. Chem.* **2** 1089–94

[67] Hughes M, Birchall L S, Zuberi K, Aitken L A, Debnath S, Javid N and Ulijn R V 2012 Differential supramolecular organisation of Fmoc-dipeptides with hydrophilic terminal amino acid residues by biocatalytic self-assembly *Soft Matter* **8** 11565–74

[68] Dehsorkhi A, Hamley I W, Seitsonen J and Ruokolainen J 2013 Tuning self-assembled nanostructures through enzymatic degradation of a peptide amphiphile *Langmuir* **29** 6665–72

[69] Li S-C and Deber C M 1992 Glycine and β-branched residues support and modulate peptide helicity in membrane environments *FEBS Lett.* **311** 217–20

[70] Ulijn R V and Smith A M 2008 Designing peptide based nanomaterials *Chem. Soc. Rev.* **37** 664–75

[71] Ackbarow T and Buehler M J 2009 Alpha-helical protein domains unify strength and robustness through hierarchical nanostructures *Nanotechnology* **20** 075103

[72] Smeenk J M, Otten M B, Thies J, Tirrell D A, Stunnenberg H G and van Hest J 2005 Controlled assembly of macromolecular β-sheet fibrils *Angew. Chem. Int. Ed.* **44** 1968–71

[73] Alemán C, Bianco A and Venanzi M 2013 *Peptide Materials: From Nanostuctures to Applications* (Chichester: John Wiley & Sons)

[74] Guler M O, Claussen R C and Stupp S I 2005 Encapsulation of pyrene within self-assembled peptide amphiphile nanofibers *J. Mater. Chem.* **15** 4507–12

[75] Vauthey S, Santoso S, Gong H, Watson N and Zhang S 2002 Molecular self-assembly of surfactant-like peptides to form nanotubes and nanovesicles *Proc. Natl. Acad. Sci. USA* **99** 5355–60

[76] Xu H, Wang J, Han S, Wang J, Yu D, Zhang H, Xia D, Zhao X, Waigh T A and Lu J R 2008 Hydrophobic-region-induced transitions in self-assembled peptide nanostructures *Langmuir* **25** 4115–23

[77] Han S, Cao S, Wang Y, Wang J, Xia D, Xu H, Zhao X and Lu J R 2011 Self-assembly of short peptide amphiphiles: the cooperative effect of hydrophobic interaction and hydrogen bonding *Chem. Eur. J.* **17** 13095–102

[78] Baumann M K, Textor M and Reimhult E 2008 Understanding self-assembled amphiphilic peptide supramolecular structures from primary structure helix propensity *Langmuir* **24** 7645–7

[79] Khoe U, Yang Y and Zhang S 2008 Self-assembly of nanodonut structure from a cone-shaped designer lipid-like peptide surfactant *Langmuir* **25** 4111–4

[80] Hamley I W, Dehsorkhi A, Castelletto V, Seitsonen J, Ruokolainen J and Iatrou H 2013 Self-assembly of a model amphiphilic oligopeptide incorporating an arginine headgroup *Soft Matter* **9** 4794–801

[81] Yoon Y-R, Lim Y-B, Lee E and Lee M 2008 Self-assembly of a peptide rod–coil: a polyproline rod and a cell-penetrating peptide Tat coil *Chem. Commun.* **16** 1892–4

[82] Ruan L, Zhang H, Luo H, Liu J, Tang F, Shi Y-K and Zhao X 2009 Designed amphiphilic peptide forms stable nanoweb, slowly releases encapsulated hydrophobic drug, and accelerates animal hemostasis *Proc. Natl. Acad. Sci. USA* **106** 5105–10

[83] Castelletto V, Hamley I, Segarra-Maset M, Gumbau C B, Miravet J, Escuder B, Seitsonen J and Ruokolainen J 2014 Tuning chelation by the surfactant-like peptide A6H using predetermined pH values *Biomacromolecules* **15** 591–8

[84] Meng Q, Kou Y, Ma X, Liang Y, Guo L, Ni C and Liu K 2012 Tunable self-assembled peptide amphiphile nanostructures *Langmuir* **28** 5017–22

[85] van Hell A J, Costa C I, Flesch F M, Sutter M, Jiskoot W, Crommelin D J, Hennink W E and Mastrobattista E 2007 Self-assembly of recombinant amphiphilic oligopeptides into vesicles *Biomacromolecules* **8** 2753–61

[86] da Silva E R, Alves W A, Castelletto V, Reza M, Ruokolainen J, Hussain R and Hamley I W 2015 Self-assembly pathway of Peptide nanotubes formed by a glutamatic acid-based bolaamphiphile *Chem. Commun.* **51** 11634–7

[87] Cinar G, Ceylan H, Urel M, Erkal T S, Deniz Tekin E, Tekinay A B, Dâna A and Guler M O 2012 Amyloid inspired self-assembled peptide nanofibers *Biomacromolecules* **13** 3377–87

[88] Cao M, Cao C, Zhou P, Wang N, Wang D, Wang J, Xia D and Xu H 2015 Self-assembly of amphiphilic peptides: effects of the single-chain-to-gemini structural transition and the side chain groups *Colloids Surf.* A **469** 263–70

[89] Holmes T C, de Lacalle S, Su X, Liu G, Rich A and Zhang S 2000 Extensive neurite outgrowth and active synapse formation on self-assembling peptide scaffolds *Proc. Natl. Acad. Sci. USA* **97** 6728–33

[90] Lee N R, Bowerman C J and Nilsson B L 2013 Effects of varied sequence pattern on the self-assembly of amphipathic peptides *Biomacromolecules* **14** 3267–77

[91] Micklitsch C M, Medina S H, Yucel T, Nagy-Smith K J, Pochan D J and Schneider J P 2015 Influence of hydrophobic face amino acids on the hydrogelation of β-hairpin peptide amphiphiles *Macromolecules* **48** 1281–8

[92] Sun L, Fan Z, Wang Y, Huang Y, Schmidt M and Zhang M 2015 Tunable synthesis of self-assembled cyclic peptide nanotubes and nanoparticles *Soft Matter* **11** 3822–32

[93] Rubin D J, Amini S, Zhou F, Su H, Miserez A and Joshi N S 2015 Structural, nanomechanical, and computational characterization of d, l-cyclic peptide assemblies *ACS Nano* **9** 3360–8

[94] Mandal D, Tiwari R K, Shirazi A N, Oh D, Ye G, Banerjee A, Yadav A and Parang K 2013 Self-assembled surfactant cyclic peptide nanostructures as stabilizing agents *Soft Matter* **9** 9465–75

[95] Bakota E L, Sensoy O, Ozgur B, Sayar M and Hartgerink J D 2013 Self-assembling multidomain peptide fibers with aromatic cores *Biomacromolecules* **14** 1370–8

[96] von Maltzahn G, Vauthey S, Santoso S and Zhang S 2003 Positively charged surfactant-like peptides self-assemble into nanostructures *Langmuir* **19** 4332–7

[97] Qiu F, Chen Y, Tang C, Zhou Q, Wang C, Shi Y K and Zhao X 2008 *De novo* design of a bolaamphiphilic peptide with only natural amino acids *Macromol. Biosci.* **8** 1053–9

[98] da Silva E R, Walter M N M, Reza M, Castelletto V, Ruokolainen J, Connon C J, Alves W A and Hamley I W 2015 Self-assembled arginine-capped peptide bolaamphiphile nanosheets for cell culture and controlled wettability surfaces *Biomacromolecules* **16** 3180–90

[99] Chen Y, Qiu F, Lu Y, Shi Y-K and Zhao X 2009 Geometrical shape of hydrophobic section determines the self-assembling structure of peptide detergents and bolaamphiphilic peptides *Curr. Nanosci.* **5** 69–74

[100] Hu Y, Lin R, Zhang P, Fern J, Cheetham A G, Patel K, Schulman R, Kan C and Cui H 2015 Electrostatic-driven lamination and untwisting of β-sheet assemblies *ACS Nano* **10** 880–8

[101] Mishra A, Loo Y, Deng R, Chuah Y J, Hee H T, Ying J Y and Hauser C A 2011 Ultrasmall natural peptides self-assemble to strong temperature-resistant helical fibers in scaffolds suitable for tissue engineering *Nano Today* **6** 232–9

[102] Hauser C A, Deng R, Mishra A, Loo Y, Khoe U, Zhuang F, Cheong D W, Accardo A, Sullivan M B and Riekel C 2011 Natural tri-to hexapeptides self-assemble in water to amyloid β-type fiber aggregates by unexpected α-helical intermediate structures *Proc. Natl. Acad. Sci. USA* **108** 1361–6

[103] Seow W Y and Hauser C A 2013 Tunable mechanical properties of ultrasmall peptide hydrogels by crosslinking and functionalization to achieve the 3D distribution of cells *Adv. Healthcare Mater.* **2** 1219–23

[104] Zhang S, Holmes T, Lockshin C and Rich A 1993 Spontaneous assembly of a self-complementary oligopeptide to form a stable macroscopic membrane *Proc. Natl. Acad. Sci. USA* **90** 3334–8

[105] Zhang S, Holmes T C, DiPersio C M, Hynes R O, Su X and Rich A 1995 Self-complementary oligopeptide matrices support mammalian cell attachment *Biomaterials* **16** 1385–93

[106] Bowerman C J and Nilsson B L 2012 Review self-assembly of amphipathic β-sheet peptides: insights and applications *Biopolymers* **98** 169–84

[107] Mart R J, Osborne R D, Stevens M M and Ulijn R V 2006 Peptide-based stimuli-responsive biomaterials *Soft Matter* **2** 822–35

[108] Ramachandran S, Tseng Y and Yu Y B 2005 Repeated rapid shear-responsiveness of peptide hydrogels with tunable shear modulus *Biomacromolecules* **6** 1316–21

[109] Schneider J P, Pochan D J, Ozbas B, Rajagopal K, Pakstis L and Kretsinger J 2002 Responsive hydrogels from the intramolecular folding and self-assembly of a designed peptide *J. Am. Chem. Soc.* **124** 15030–7

[110] Haines L A, Rajagopal K, Ozbas B, Salick D A, Pochan D J and Schneider J P 2005 Light-activated hydrogel formation via the triggered folding and self-assembly of a designed peptide *J. Am. Chem. Soc.* **127** 17025–9

[111] De Santis P, Morosetti S and Rizzo R 1974 Conformational analysis of regular enantiomeric sequences *Macromolecules* **7** 52–8

[112] Ghadiri M R, Granja J R, Milligan R A, McRee D E and Khazanovich N 1993 Self-assembling organic nanotubes based on a cyclic peptide architecture *Nature* **366** 324–7

[113] Hamley I W 2014 Peptide nanotubes *Angew. Chem. Int. Ed.* **53** 6866–81

[114] Rodriguez-Vazquez N, Lionel Ozores H, Guerra A, Gonzalez-Freire E, Fuertes A, Panciera M, Outeiral J, Montenegro J and Garcia-Fandino R 2014 Membrane-targeted self-assembling cyclic peptide nanotubes *Curr. Top. Med. Chem.* **14** 2647–61

[115] Dong H, Paramonov S E, Aulisa L, Bakota E L and Hartgerink J D 2007 Self-assembly of multidomain peptides: balancing molecular frustration controls conformation and nanostructure *J. Am. Chem. Soc.* **129** 12468–72

[116] Aulisa L, Dong H and Hartgerink J D 2009 Self-assembly of multidomain peptides: sequence variation allows control over cross-linking and viscoelasticity *Biomacromolecules* **10** 2694–8

[117] Hinterding K, Alonso-Díaz D and Waldmann H 1998 Organic synthesis and biological signal transduction *Angew. Chem. Int. Ed.* **37** 688–749

[118] Löwik D W and van Hest J C 2004 Peptide based amphiphiles *Chem. Soc. Rev.* **33** 234–45

[119] Hamley I W, Dehsorkhi A, Jauregi P, Seitsonen J, Ruokolainen J, Coutte F, Chataigné G and Jacques P 2013 Self-assembly of three bacterially-derived bioactive lipopeptides *Soft Matter* **9** 9572–8

[120] Israelachvili J N 2011 *Intermolecular and Surface Forces: Revised* 3rd edn (Amsterdam: Elsevier)

[121] Lalatsa A, Schätzlein A G, Mazza M, Le T B H and Uchegbu I F 2012 Amphiphilic poly (l-amino acids)—new materials for drug delivery *J. Control. Release* **161** 523–36

[122] Shrestha L K, Strzelczyk K M, Shrestha R G, Ichikawa K, Aramaki K, Hill J P and Ariga K 2015 Nonionic amphiphile nanoarchitectonics: self-assembly into micelles and lyotropic liquid crystals *Nanotechnology* **26** 204002

[123] M Leite D, Barbu E, J Pilkington G and Lalatsa A 2015 Peptide self-assemblies for drug delivery *Curr. Top. Med. Chem.* **15** 2277–89

[124] Velichko Y S, Stupp S I and de la Cruz M O 2008 Molecular simulation study of peptide amphiphile self-assembly *J. Phys. Chem.* B **112** 2326–34

[125] Paramonov S E, Jun H-W and Hartgerink J D 2006 Self-assembly of peptide-amphiphile nanofibers: the roles of hydrogen bonding and amphiphilic packing *J. Am. Chem. Soc.* **128** 7291–8

[126] Cui H, Webber M J and Stupp S I 2010 Self-assembly of peptide amphiphiles: From molecules to nanostructures to biomaterials *Biopolymers* **94** 1–18

[127] Tsonchev S, Schatz G C and Ratner M A 2004 Electrostatically-directed self-assembly of cylindrical peptide amphiphile nanostructures *J. Phys. Chem.* B **108** 8817–22

[128] Lee O-S, Stupp S I and Schatz G C 2011 Atomistic molecular dynamics simulations of peptide amphiphile self-assembly into cylindrical nanofibers *J. Am. Chem. Soc.* **133** 3677–83

[129] Fu I W, Markegard C B, Chu B K and Nguyen H D 2013 The role of electrostatics and temperature on morphological transitions of hydrogel nanostructures self-assembled by peptide amphiphiles via molecular dynamics simulations *Adv. Healthcare Mater.* **2** 1388–400

[130] Greenfield M A, Hoffman J R, Olvera de la Cruz M and Stupp S I 2009 Tunable mechanics of peptide nanofiber gels *Langmuir* **26** 3641–7

[131] Zhang S, Greenfield M A, Mata A, Palmer L C, Bitton R, Mantei J R, Aparicio C, de La Cruz M O and Stupp S I 2010 A self-assembly pathway to aligned monodomain gels *Nat. Mater.* **9** 594–601

[132] Pashuck E T and Stupp S I 2010 Direct observation of morphological tranformation from twisted ribbons into helical ribbons *J. Am. Chem. Soc.* **132** 8819–21

[133] Cui H, Cheetham A G, Pashuck E T and Stupp S I 2014 Amino acid sequence in constitutionally isomeric

tetrapeptide amphiphiles dictates architecture of one-dimensional nanostructures *J. Am. Chem. Soc.* **136** 12461–8
[134] Moyer T J, Cui H and Stupp S I 2012 Tuning nanostructure dimensions with supramolecular twisting *J. Phys. Chem.* B **117** 4604–10
[135] Shimada T, Lee S, Bates F S, Hotta A and Tirrell M 2009 Wormlike micelle formation in peptide-lipid conjugates driven by secondary structure transformation of the headgroups *J. Phys. Chem.* B **113** 13711–4
[136] Missirlis D, Chworos A, Fu C J, Khant H A, Krogstad D V and Tirrell M 2011 Effect of the peptide secondary structure on the peptide amphiphile supramolecular structure and interactions *Langmuir* **27** 6163–70
[137] Zhang J, Hao R, Huang L, Yao J, Chen X and Shao Z 2011 Self-assembly of a peptide amphiphile based on hydrolysed Bombyx mori silk fibroin *Chem. Commun.* **47** 10296–8
[138] Ghosh A, Dobson E T, Buettner C J, Nicholl M J and Goldberger J E 2014 Programming pH-triggered self-assembly transitions via isomerization of peptide sequence *Langmuir* **30** 15383–7
[139] Sever M, Mammadov B, Guler M O and Tekinay A B 2014 Tenascin-C mimetic peptide nanofibers direct stem cell differentiation to osteogenic lineage *Biomacromolecules* **15** 4480–7
[140] Mumcuoglu D, Sardan M, Tekinay T, Guler M O and Tekinay A B 2015 Oligonucleotide delivery with cell surface binding and cell penetrating peptide amphiphile nanospheres *Mol. Pharm.* **12** 1584–91
[141] Moyer T J, Kassam H A, Bahnson E S, Morgan C E, Tantakitti F, Chew T L, Kibbe M R and Stupp S I 2015 Shape-dependent targeting of injured blood vessels by peptide amphiphile supramolecular nanostructures *Small* **11** 2750–5
[142] Xu X-D, Jin Y, Liu Y, Zhang X-Z and Zhuo R-X 2010 Self-assembly behavior of peptide amphiphiles (PAs) with different length of hydrophobic alkyl tails *Colloids Surf.* B **81** 329–35
[143] van den Heuvel M, Löwik D W and van Hest J C 2010 Effect of the diacetylene position on the chromatic properties of polydiacetylenes from self-assembled peptide amphiphiles *Biomacromolecules* **11** 1676–83
[144] Black M, Trent A, Kostenko Y, Lee J S, Olive C and Tirrell M 2012 Self-assembled peptide amphiphile micelles containing a cytotoxic T-cell epitope promote a protective immune response *in vivo Adv. Mater.* **24** 3845–9
[145] Zhang P, Cheetham A G, Lin Y-a and Cui H 2013 Self-assembled Tat nanofibers as effective drug carrier and transporter *ACS Nano* **7** 5965–77
[146] Cui H, Muraoka T, Cheetham A G and Stupp S I 2009 Self-assembly of giant peptide nanobelts *Nano Lett.* **9** 945–51
[147] Castelletto V, Hamley I W, Perez J, Abezgauz L and Danino D 2010 Fibrillar superstructure from extended nanotapes formed by a collagen-stimulating peptide *Chem. Commun.* **46** 9185–7
[148] Niece K L, Hartgerink J D, Donners J J and Stupp S I 2003 Self-assembly combining two bioactive peptide-amphiphile molecules into nanofibers by electrostatic attraction *J. Am. Chem. Soc.* **125** 7146–7
[149] Behanna H A, Donners J J, Gordon A C and Stupp S I 2005 Coassembly of amphiphiles with opposite peptide polarities into nanofibers *J. Am. Chem. Soc.* **127** 1193–200
[150] Mammadov B, Mammadov R, Guler M O and Tekinay A B 2012 Cooperative effect of heparan sulfate and laminin mimetic peptide nanofibers on the promotion of neurite outgrowth *Acta Biomater.* **8** 2077–86
[151] Ceylan H, Kocabey S, Tekinay A B and Guler M O 2012 Surface-adhesive and osteogenic self-assembled peptide nanofibers for bioinspired functionalization of titanium surfaces *Soft Matter* **8** 3929–37
[152] Hamley I, Dehsorkhi A and Castelletto V 2013 Coassembly in binary mixtures of peptide amphiphiles containing oppositely charged residues *Langmuir* **29** 5050–9
[153] Mumcuoglu D, Sardan Ekiz M, Gunay G, Tekinay T, Tekinay A B and Guler M O 2016 Cellular internalization of therapeutic oligonucleotides by peptide amphiphile nanofibers and nanospheres *ACS Appl. Mater. Interfaces* **8** 11280–7
[154] Mammadov R *et al* 2015 Virus-like nanostructures for tuning immune response *Sci. Rep.* **5** 16728
[155] Löwik D W, Garcia-Hartjes J, Meijer J T and van Hest J C 2005 Tuning secondary structure and self-assembly of amphiphilic peptides *Langmuir* **21** 524–6
[156] Meijer J T, Roeters M, Viola V, Löwik D W, Vriend G and van Hest J C 2007 Stabilization of peptide fibrils by hydrophobic interaction *Langmuir* **23** 2058–63
[157] He C, Han Y, Fan Y, Deng M and Wang Y 2012 Self-assembly of Aβ-based peptide amphiphiles with double hydrophobic chains *Langmuir* **28** 3391–6
[158] Berndt P, Fields G B and Tirrell M 1995 Synthetic lipidation of peptides and amino acids: monolayer structure and properties *J. Am. Chem. Soc.* **117** 9515–22
[159] Yu Y-C, Berndt P, Tirrell M and Fields G B 1996 Self-assembling amphiphiles for construction of protein molecular architecture *J. Am. Chem. Soc.* **118** 12515–20
[160] Gore T, Dori Y, Talmon Y, Tirrell M and Bianco-Peled H 2001 Self-assembly of model collagen peptide amphiphiles *Langmuir* **17** 5352–60
[161] Adler-Abramovich L and Gazit E 2014 The physical properties of supramolecular peptide assemblies: from building block association to technological applications *Chem. Soc. Rev.* **43** 6881–93
[162] Fichman G and Gazit E 2014 Self-assembly of short peptides to form hydrogels: design of building blocks, physical properties and technological applications *Acta Biomater.* **10** 1671–82
[163] Fleming S and Ulijn R V 2014 Design of nanostructures based on aromatic peptide amphiphiles *Chem. Soc. Rev.* **43** 8150–77
[164] Tang C, Ulijn R V and Saiani A 2011 Effect of glycine substitution on Fmoc–diphenylalanine self-assembly and gelation properties *Langmuir* **27** 14438–49
[165] Ryan D M, Anderson S B and Nilsson B L 2010 The influence of side-chain halogenation on the self-assembly and hydrogelation of Fmoc-phenylalanine derivatives *Soft Matter* **6** 3220–31
[166] Ryan D M, Doran T M, Anderson S B and Nilsson B L 2011 Effect of C-terminal modification on the self-assembly and hydrogelation of fluorinated Fmoc-Phe derivatives *Langmuir* **27** 4029–39
[167] Kuang Y, Gao Y, Shi J, Li J and Xu B 2014 The first supramolecular peptidic hydrogelator containing taurine *Chem. Commun.* **50** 2772–4
[168] Ou C, Zhang J, Zhang X, Yang Z and Chen M 2013 Phenothiazine as an aromatic capping group to construct a short peptide-based 'super gelator' *Chem. Commun.* **49** 1853–5
[169] Garifullin R and Guler M O 2015 Supramolecular chirality in self-assembled peptide amphiphile nanostructures *Chem. Commun.* **51** 12470–3
[170] Adler-Abramovich L, Kol N, Yanai I, Barlam D, Shneck R Z, Gazit E and Rousso I 2010 Self-assembled organic nanostructures with metallic-like stiffness *Angew. Chem. Int. Ed.* **49** 9939–42
[171] Eakins G L, Gallaher J K, Keyzers R A, Falber A, Webb J E, Laos A, Tidhar Y, Weissman H, Rybtchinski B and Thordarson P 2014 Thermodynamic factors impacting the

peptide-driven self-assembly of perylene diimide nanofibers *J. Phys. Chem.* B **118** 8642–51
[172] Lehrman J A, Cui H, Tsai W-W, Moyer T J and Stupp S I 2012 Supramolecular control of self-assembling terthiophene–peptide conjugates through the amino acid side chain *Chem. Commun.* **48** 9711–3
[173] Ardoña H A M, Besar K, Togninalli M, Katz H E and Tovar J D 2015 Sequence-dependent mechanical, photophysical and electrical properties of pi-conjugated peptide hydrogelators *J. Mater. Chem.* C **3** 6505–14
[174] Matsuura K, Hayashi H, Murasato K and Kimizuka N 2011 Trigonal tryptophane zipper as a novel building block for pH-responsive peptide nano-assemblies *Chem. Commun.* **47** 265–7
[175] Tzokova N, Fernyhough C M, Topham P D, Sandon N, Adams D J, Butler M F, Armes S P and Ryan A J 2009 Soft hydrogels from nanotubes of poly (ethylene oxide)− tetraphenylalanine conjugates prepared by click chemistry *Langmuir* **25** 2479–85
[176] Paira T K, Saha A, Banerjee S, Das T, Das P, Jana N R and Mandal T K 2014 Fluorescent amphiphilic PEG-peptide-PEG triblock conjugate micelles for cell imaging *Macromol. Biosci.* **14** 929–35
[177] Peters D, Kastantin M, Kotamraju V R, Karmali P P, Gujraty K, Tirrell M and Ruoslahti E 2009 Targeting atherosclerosis by using modular, multifunctional micelles *Proc. Natl. Acad. Sci. USA* **106** 9815–9
[178] Guler M O, Pokorski J K, Appella D H and Stupp S I 2005 Enhanced oligonucleotide binding to self-assembled nanofibers *Bioconjugate Chem.* **16** 501–3
[179] Liu L-H, Li Z-Y, Rong L, Qin S-Y, Lei Q, Cheng H, Zhou X, Zhuo R-X and Zhang X-Z 2014 Self-assembly of hybridized peptide nucleic acid amphiphiles *ACS Macro Lett.* **3** 467–71
[180] Li X, Kuang Y, Shi J, Gao Y, Lin H-C and Xu B 2011 Multifunctional, biocompatible supramolecular hydrogelators consist only of nucleobase, amino acid, and glycoside *J. Am. Chem. Soc.* **133** 17513–8
[181] Martinez C R and Iverson B L 2012 Rethinking the term 'pi-stacking' *Chem. Sci* **3** 2191–201
[182] Vegners R, Shestakova I, Kalvinsh I, Ezzell R M and Janmey P A 1995 Use of a gel-forming dipeptide derivative as a carrier for antigen presentation *J. Pept. Sci.* **1** 371–8
[183] Jayawarna V, Ali M, Jowitt T A, Miller A F, Saiani A, Gough J E and Ulijn R V 2006 Nanostructured hydrogels for three-dimensional cell culture through self-assembly of fluorenylmethoxycarbonyl–dipeptides *Adv. Mater.* **18** 611–4
[184] Reches M and Gazit E 2005 Self-assembly of peptide nanotubes and amyloid-like structures by charged-termini-capped diphenylalanine peptide analogues *Isr. J. Chem.* **45** 363–71
[185] Tang C, Ulijn R V and Saiani A 2013 Self-assembly and gelation properties of glycine/leucine Fmoc-dipeptides *Eur. Phys. J.* E **36** 1–11
[186] Du X, Zhou J and Xu B 2014 Supramolecular hydrogels made of basic biological building blocks *Chem. Asian J.* **9** 1446–72
[187] Cheng G, Castelletto V, Moulton C, Newby G and Hamley I 2010 Hydrogelation and self-assembly of Fmoc-tripeptides: unexpected influence of sequence on self-assembled fibril structure, and hydrogel modulus and anisotropy *Langmuir* **26** 4990–8
[188] Cheng G, Castelletto V, Jones R, Connon C J and Hamley I W 2011 Hydrogelation of self-assembling RGD-based peptides *Soft Matter* **7** 1326–33
[189] Orbach R, Adler-Abramovich L, Zigerson S, Mironi-Harpaz I, Seliktar D and Gazit E 2009 Self-assembled Fmoc-peptides as a platform for the formation of nanostructures and hydrogels *Biomacromolecules* **10** 2646–51
[190] Nakayama T, Sakuraba T, Tomita S, Kaneko A, Takai E, Shiraki K, Tashiro K, Ishii N, Hasegawa Y and Yamada Y 2014 Charge-separated Fmoc-peptide β-sheets: sequence-secondary structure relationship for arranging charged side chains on both sides *Asian J. Org. Chem.* **3** 1182–8
[191] Liyanage W and Nilsson B L 2015 Substituent effects on the self-assembly/coassembly and hydrogelation of phenylalanine derivatives *Langmuir* **32** 787–99
[192] Wang H, Yang C, Tan M, Wang L, Kong D and Yang Z 2011 A structure–gelation ability study in a short peptide-based 'super hydrogelator' system *Soft Matter* **7** 3897–905
[193] Tena-Solsona M, Miravet J F and Escuder B 2014 Tetrapeptidic molecular hydrogels: self-assembly and Co-aggregation with amyloid fragment Aβ1-40 *Chem. Eur. J.* **20** 1023–31
[194] Matsuzawa Y and Tamaoki N 2010 Photoisomerization of azobenzene units controls the reversible dispersion and reorganization of fibrous self-assembled systems *J. Phys. Chem.* B **114** 1586–90
[195] Zeng G, Liu L, Xia D, Li Q, Xin Z, Wang J, Besenbacher F, Skrydstrup T and Dong M 2014 Transition of chemically modified diphenylalanine peptide assemblies revealed by atomic force microscopy *RSC Adv.* **4** 7516–20
[196] Qin S-Y, Jiang H-F, Peng M-Y, Lei Q, Zhuo R-X and Zhang X-Z 2015 Adjustable nanofibers self-assembled from an irregular conformational peptide amphiphile *Polym. Chem.* **6** 519–24
[197] Martin A D, Wojciechowski J, Bhadbhade M and Thordarson P 2016 A capped dipeptide which simultaneously exhibits gelation and crystallization behavior *Langmuir* **32** 2245–50
[198] Adler-Abramovich L and Gazit E 2008 Controlled patterning of peptide nanotubes and nanospheres using inkjet printing technology *J. Pept. Sci.* **14** 217–23
[199] Amit M, Appel S, Cohen R, Cheng G, Hamley I W and Ashkenasy N 2014 Hybrid proton and electron transport in peptide fibrils *Adv. Funct. Mater.* **24** 5873–80
[200] Stone D A, Hsu L and Stupp S I 2009 Self-assembling quinquethiophene-oligopeptide hydrogelators *Soft Matter* **5** 1990–3
[201] Matmour R, De Cat I, George S J, Adriaens W, Leclère P, Bomans P H, Sommerdijk N A, Gielen J C, Christianen P C and Heldens J T 2008 Oligo (p-phenylenevinylene)− peptide conjugates: synthesis and self-assembly in solution and at the solid− liquid interface *J. Am. Chem. Soc.* **130** 14576–83
[202] González-Rodríguez D and Schenning A P 2010 Hydrogen-bonded supramolecular π-functional materials *Chem. Mater.* **23** 310–25
[203] Ardoña H A M and Tovar J D 2015 Peptide π-electron conjugates: organic electronics for biology? *Bioconjugate Chem.* **26** 2290–302
[204] Tovar J D 2013 Supramolecular construction of optoelectronic biomaterials *Acc. Chem. Res.* **46** 1527–37
[205] Ghosh S, Reches M, Gazit E and Verma S 2007 Bioinspired design of nanocages by self-assembling triskelion peptide elements *Angew. Chem. Int. Ed.* **119** 2048–50
[206] Matsuura K, Fujino K, Teramoto T, Murasato K and Kimizuka N 2010 Glutathione nanosphere: self-assembly of conformation-regulated trigonal-glutathiones in water *Bull. Chem. Soc. Jpn* **83** 880–6
[207] Matsuura K, Murasato K and Kimizuka N 2011 Syntheses and self-assembling behaviors of pentagonal conjugates of tryptophane zipper-forming peptide *Int. J. Mol. Sci.* **12** 5187–99
[208] Wilson P, Nicolas J and Haddleton D M 2015 Polymer–protein/peptide bioconjugates *Chemistry of Organo-Hybrids: Synthesis and Characterization of Functional*

Nano-Objects (New Jersey: John Wiley & Sons) pp 466–502
[209] Shu J Y, Panganiban B and Xu T 2013 Peptide-polymer conjugates: from fundamental science to application *Annu. Rev. Phys. Chem.* **64** 631–57
[210] Adams D J and Topham P D 2010 Peptide conjugate hydrogelators *Soft Matter* **6** 3707–21
[211] Cavalli S, Popescu D C, Tellers E E, Vos M R, Pichon B P, Overhand M, Rapaport H, Sommerdijk N A and Kros A 2006 Self-organizing β-sheet lipopeptide monolayers as template for the mineralization of $CaCO_3$ *Angew. Chem. Int. Ed.* **45** 739–44
[212] Robson Marsden H, Elbers N A, Bomans P H, Sommerdijk N A and Kros A 2009 A reduced SNARE model for membrane fusion *Angew. Chem. Int. Ed.* **48** 2330–3
[213] Cavalli S, Handgraaf J-W, Tellers E E, Popescu D C, Overhand M, Kjaer K, Vaiser V, Sommerdijk N A, Rapaport H and Kros A 2006 Two-dimensional ordered β-sheet lipopeptide monolayers *J. Am. Chem. Soc.* **128** 13959–66
[214] Ustun Yaylaci S, Sardan Ekiz M, Arslan E, Can N, Kilic E, Ozkan H, Orujalipoor I, İde S, Tekinay A B and Guler M O 2015 Supramolecular GAG-like self-assembled glycopeptide nanofibers induce chondrogenesis and cartilage regeneration *Biomacromolecules* **17** 679–89
[215] Yuan D, Shi J, Du X, Zhou N and Xu B 2015 Supramolecular glycosylation accelerates proteolytic degradation of peptide nanofibrils *J. Am. Chem. Soc.* 10092–5
[216] Zhao F, Heesters B A, Chiu I, Gao Y, Shi J, Zhou N, Carroll M C and Xu B 2014 l-Rhamnose-containing supramolecular nanofibrils as potential immunosuppressive materials *Org. Biomol. Chem.* **12** 6816–9
[217] Lim Y-B, Park S, Lee E, Jeong H, Ryu J-H, Lee M S and Lee M 2007 Glycoconjugate nanoribbons from the self-assembly of carbohydrate-peptide block molecules for controllable bacterial cell cluster formation *Biomacromolecules* **8** 1404–8
[218] Williamson M P and Waltho J P 1992 Peptide structure from NMR *Chem. Soc. Rev.* **21** 227–36
[219] Singh V, Snigdha K, Singh C, Sinha N and Thakur A K 2015 Understanding the self-assembly of Fmoc-phenylalanine to hydrogel formation *Soft Matter* **11** 5353–64
[220] Cohen Y, Avram L and Frish L 2005 Diffusion NMR spectroscopy in supramolecular and combinatorial chemistry: an old parameter—new insights *Angew. Chem. Int. Ed.* **44** 520–54
[221] Pappas C G, Sasselli I R and Ulijn R V 2015 Biocatalytic Pathway Selection in Transient Tripeptide Nanostructures *Angew. Chem. Int. Ed.* **54** 8119–23
[222] Rienstra C M, Tucker-Kellogg L, Jaroniec C P, Hohwy M, Reif B, McMahon M T, Tidor B, Lozano-Pérez T and Griffin R G 2002 *De novo* determination of peptide structure with solid-state magic-angle spinning NMR spectroscopy *Proc. Natl. Acad. Sci. USA* **99** 10260–5
[223] Jaroniec C P, MacPhee C E, Bajaj V S, McMahon M T, Dobson C M and Griffin R G 2004 High-resolution molecular structure of a peptide in an amyloid fibril determined by magic angle spinning NMR spectroscopy *Proc. Natl. Acad. Sci. USA* **101** 711–6
[224] Middleton D A, Madine J, Castelletto V and Hamley I W 2013 Insights into the molecular architecture of a peptide nanotube using FTIR and solid-state NMR spectroscopic measurements on an aligned sample *Angew. Chem. Int. Ed.* **125** 10731–4
[225] Jaroniec C P, MacPhee C E, Astrof N S, Dobson C M and Griffin R G 2002 Molecular conformation of a peptide fragment of transthyretin in an amyloid fibril *Proc. Natl. Acad. Sci. USA* **99** 16748–53
[226] Nieuwland M, Ruizendaal L, Brinkmann A, Kroon-Batenburg L, van Hest J and Löwik D 2013 A structural study of the self-assembly of a palmitoyl peptide amphiphile *Farad. Discuss.* **166** 361–79
[227] Cormier A R, Pang X, Zimmerman M I, Zhou H-X and Paravastu A K 2013 Molecular structure of RADA16-I designer self-assembling peptide nanofibers *ACS Nano* **7** 7562–72
[228] Rad-Malekshahi M, Visscher K M, Rodrigues J P, De Vries R, Hennink W E, Baldus M, Bonvin A M, Mastrobattista E and Weingarth M 2015 The supramolecular organization of a peptide-based nanocarrier at high molecular detail *J. Am. Chem. Soc.* **137** 7775–84
[229] Nagy-Smith K, Moore E, Schneider J and Tycko R 2015 Molecular structure of monomorphic peptide fibrils within a kinetically trapped hydrogel network *Proc. Natl. Acad. Sci. USA* **112** 9816–21
[230] Moore W H and Krimm S 1976 Vibrational analysis of peptides, polypeptides, and proteins. II. β-Poly (L-alanine) and β-poly (L-alanylglycine) *Biopolymers* **15** 2465–83
[231] Bakshi K, Liyanage M, Volkin D and Middaugh C R 2014 Fourier transform infrared spectroscopy of peptides *Therapeutic Peptides* ed A E Nixon (New York: Humana Press) pp 255–69
[232] Kong J and Yu S 2007 Fourier transform infrared spectroscopic analysis of protein secondary structures *Acta Biochim. Biophys. Sinica* **39** 549–59
[233] Wei R, Jin C C, Quan J, Nie H l and Zhu L M 2014 A novel self-assembling peptide with UV-responsive properties *Biopolymers* **101** 272–8
[234] Pappas C G, Frederix P W, Mutasa T, Fleming S, Abul-Haija Y M, Kelly S M, Gachagan A, Kalafatovic D, Trevino J and Ulijn R V 2015 Alignment of nanostructured tripeptide gels by directional ultrasonication *Chem. Commun.* **51** 8465–8
[235] Pappas C G, Mutasa T, Frederix P W J M, Fleming S, Bai S, Debnath S, Kelly S M, Gachagan A and Ulijn R V 2015 Transient supramolecular reconfiguration of peptide nanostructures using ultrasound *Mater. Horiz.* **2** 198–202
[236] Zhou M, Smith A M, Das A K, Hodson N W, Collins R F, Ulijn R V and Gough J E 2009 Self-assembled peptide-based hydrogels as scaffolds for anchorage-dependent cells *Biomaterials* **30** 2523–30
[237] Amorín M, Pérez A, Barberá J, Ozores H L, Serrano J L, Granja J R and Sierra T 2014 Liquid crystal organization of self-assembling cyclic peptides *Chem. Commun.* **50** 688–90
[238] Roux S, Zékri E, Rousseau B, Paternostre M, Cintrat J C and Fay N 2008 Elimination and exchange of trifluoroacetate counter-ion from cationic peptides: a critical evaluation of different approaches *J. Pept. Sci.* **14** 354–9
[239] Marchesan S, Easton C, Styan K, Waddington L, Kushkaki F, Goodall L, McLean K, Forsythe J and Hartley P 2014 Chirality effects at each amino acid position on tripeptide self-assembly into hydrogel biomaterials *Nanoscale* **6** 5172–80
[240] Boulmedais F, Ball V, Schwinte P, Frisch B, Schaaf P and Voegel J-C 2003 Buildup of exponentially growing multilayer polypeptide films with internal secondary structure *Langmuir* **19** 440–5
[241] Nowinski A K, Sun F, White A D, Keefe A J and Jiang S 2012 Sequence, structure, and function of peptide self-assembled monolayers *J. Am. Chem. Soc.* **134** 6000–5
[242] Ramaswamy K, Kumaraswamy P, Sethuraman S and Krishnan U M 2014 Self-assembly characteristics of a structural analogue of Tjernberg peptide *RSC Adv.* **4** 16517–23
[243] Venyaminov S Y and Prendergast F G 1997 Water (H_2O and D_2O) molar absorptivity in the 1000–4000 cm^{-1} range and

quantitative infrared spectroscopy of aqueous solutions *Anal. Biochem.* **248** 234–45
[244] Barth A 2007 Infrared spectroscopy of proteins *BBA Bioenergetics* **1767** 1073–101
[245] Anderson B A, Literati A, Ball B and Kubelka J 2014 Temperature dependence of amino acid side chain IR absorptions in the amide I'region *Biopolymers* **101** 536–48
[246] Das A K, Maity I, Parmar H S, McDonald T O and Konda M 2015 Lipase-catalyzed dissipative self-assembly of a thixotropic peptide bolaamphiphile hydrogel for human umbilical cord stem-cell proliferation *Biomacromolecules* **16** 1157–68
[247] Decatur S M 2006 Elucidation of residue-level structure and dynamics of polypeptides via isotope-edited infrared spectroscopy *Acc. Chem. Res.* **39** 169–75
[248] Swanekamp R J, DiMaio J T, Bowerman C J and Nilsson B L 2012 Coassembly of enantiomeric amphipathic peptides into amyloid-inspired rippled β-sheet fibrils *J. Am. Chem. Soc.* **134** 5556–9
[249] Moran S D, Woys A M, Buchanan L E, Bixby E, Decatur S M and Zanni M T 2012 Two-dimensional IR spectroscopy and segmental 13C labeling reveals the domain structure of human γD-crystallin amyloid fibrils *Proc. Natl. Acad. Sci. USA* **109** 3329–34
[250] Remorino A and Hochstrasser R M 2012 Three-dimensional structures by two-dimensional vibrational spectroscopy *Acc. Chem. Res.* **45** 1896–905
[251] Smith A W and Tokmakoff A 2007 Probing local structural events in β-hairpin unfolding with transient nonlinear infrared spectroscopy *Angew. Chem. Int. Ed.* **119** 8130–3
[252] Kolano C, Helbing J, Kozinski M, Sander W and Hamm P 2006 Watching hydrogen-bond dynamics in a β-turn by transient two-dimensional infrared spectroscopy *Nature* **444** 469–72
[253] Huerta-Viga A, Amirjalayer S, Domingos S R, Meuzelaar H, Rupenyan A and Woutersen S 2015 The structure of salt bridges between Arg+ and Glu− in peptides investigated with 2D-IR spectroscopy: Evidence for two distinct hydrogen-bond geometries *J. Chem. Phys.* **142** 212444
[254] Tuma R 2005 Raman spectroscopy of proteins: from peptides to large assemblies *J. Raman Spectrosc.* **36** 307–19
[255] Mikhonin A V, Ahmed Z, Ianoul A and Asher S A 2004 Assignments and conformational dependencies of the amide III peptide backbone UV resonance Raman bands *J. Phys. Chem.* B **108** 19020–8
[256] Oladepo S A, Xiong K, Hong Z and Asher S A 2011 Elucidating peptide and protein structure and dynamics: UV resonance Raman spectroscopy *J. Phys. Chem. Lett.* **2** 334–44
[257] Roach C A, Simpson J V and JiJi R D 2012 Evolution of quantitative methods in protein secondary structure determination via deep-ultraviolet resonance Raman spectroscopy *Analyst* **137** 555–62
[258] Oshokoya O O, Roach C A and JiJi R D 2014 Quantification of protein secondary structure content by multivariate analysis of deep-ultraviolet resonance Raman and circular dichroism spectroscopies *Anal. Methods* **6** 1691–9
[259] Ayas S, Cinar G, Ozkan A D, Soran Z, Ekiz O, Kocaay D, Tomak A, Toren P, Kaya Y and Tunc I 2013 Label-free nanometer-resolution imaging of biological architectures through surface enhanced raman scattering *Sci. Rep.* **3** 1–7
[260] Stewart S and Fredericks P M 1999 Surface-enhanced Raman spectroscopy of peptides and proteins adsorbed on an electrochemically prepared silver surface *Spectrochim. Acta Mol. Biomol. Spectrosc.* **55** 1615–40
[261] Paulite M, Blum C, Schmid T, Opilik L, Eyer K, Walker G C and Zenobi R 2013 Full spectroscopic tip-enhanced raman imaging of single nanotapes formed from β-amyloid(1–40) peptide fragments *ACS Nano* **7** 911–20
[262] Sonntag M D, Pozzi E A, Jiang N, Hersam M C and Van Duyne R P 2014 Recent advances in tip-enhanced Raman spectroscopy *J. Phys. Chem. Lett.* **5** 3125–30
[263] Fan Z and Govorov A O 2010 Plasmonic circular dichroism of chiral metal nanoparticle assemblies *Nano Lett.* **10** 2580–7
[264] Bakshi K, Liyanage M R, Volkin D B and Middaugh C R 2014 Circular dichroism of peptides *Therapeutic Peptides* (New York: Humana Press) pp 247–53
[265] Singh N, Conte M P, Ulijn R, Miravet J F and Escuder B 2015 Insight into the esterase like activity demonstrated by an imidazole appended self-assembling hydrogelator *Chem. Commun.* **51** 13213–6
[266] Tidhar Y, Weissman H, Wolf S G, Gulino A and Rybtchinski B 2011 Pathway-dependent self-assembly of perylene diimide/peptide conjugates in aqueous medium *Chem. Eur. J.* **17** 6068–75
[267] Liebes-Peer Y, Rapaport H and Ashkenasy N 2014 Amplification of single molecule translocation signal using β-strand peptide functionalized nanopores *ACS Nano* **8** 6822–32
[268] Punzi P, Giordano C, Marino F, Morosetti S, De Santis P and Scipioni A 2012 Metal chelates anchored to poly-l-peptides and linear d, l-α-peptides with promising nanotechnological applications *Nanotechnology* **23** 395703
[269] Van Gough D, Wheeler J S, Cheng S, Stevens M J and Spoerke E D 2014 Supramolecular assembly of asymmetric self-neutralizing amphiphilic peptide wedges *Langmuir* **30** 9201–9
[270] Mondal S, Adler-Abramovich L, Lampel A, Bram Y, Lipstman S and Gazit E 2015 Formation of functional super-helical assemblies by constrained single heptad repeat *Nat. Commun.* **6** 1–8
[271] Pashuck E T, Cui H and Stupp S I 2010 Tuning supramolecular rigidity of peptide fibers through molecular structure *J. Am. Chem. Soc.* **132** 6041–6
[272] Kumar R J, MacDonald J M, Singh T B, Waddington L J and Holmes A B 2011 Hierarchical self-assembly of semiconductor functionalized peptide α-helices and optoelectronic properties *J. Am. Chem. Soc.* **133** 8564–73
[273] Luo T and Kiick K L 2015 Noncovalent modulation of the inverse temperature transition and self-assembly of elastin-b-collagen-like peptide bioconjugates *J. Am. Chem. Soc.* **137** 15362–5
[274] Micsonai A, Wien F, Kernya L, Lee Y-H, Goto Y, Réfrégiers M and Kardos J 2015 Accurate secondary structure prediction and fold recognition for circular dichroism spectroscopy *Proc. Natl. Acad. Sci. USA* **112** E3095–103
[275] Bortolini C, Jones N C, Hoffmann S V, Besenbacher F and Dong M 2016 The influence of the localised charge of C-and N-termini on peptide self-assembly *Soft Matter* **12** 373–7
[276] Bowerman C J, Liyanage W, Federation A J and Nilsson B L 2011 Tuning β-sheet peptide self-assembly and hydrogelation behavior by modification of sequence hydrophobicity and aromaticity *Biomacromolecules* **12** 2735–45
[277] Murphy R M 1997 Static and dynamic light scattering of biological macromolecules: what can we learn? *Curr. Opin. Biotechnol.* **8** 25–30
[278] Kaszuba M, McKnight D, Connah M, McNeil-Watson F and Nobbmann U 2008 Measuring sub nanometre sizes using dynamic light scattering *J. Nanopart. Res.* **10** 823–9
[279] Papish A L, Tari L W and Vogel H J 2002 Dynamic light scattering study of calmodulin–target peptide complexes *Biophys. J.* **83** 1455–64
[280] Aggeli A, Fytas G, Vlassopoulos D, McLeish T C B, Mawer P J and Boden N 2001 Structure and dynamics of

self-assembling β-sheet peptide tapes by dynamic light scattering *Biomacromolecules* **2** 378–88
[281] Yucel T, Micklitsch C M, Schneider J P and Pochan D J 2008 Direct observation of early-time hydrogelation in β-hairpin peptide self-assembly *Macromolecules* **41** 5763–72
[282] Herrera M, Benedini L, Lonez C, Schilardi P, Hellweg T, Ruysschaert J-M and Dodero V 2015 Self-assembly of 33-mer gliadin peptide oligomers *Soft Matter* **11** 8648–60
[283] Kotch F W and Raines R T 2006 Self-assembly of synthetic collagen triple helices *Proc. Natl. Acad. Sci. USA* **103** 3028–33
[284] Zhang Q, Li M, Zhu C, Nurumbetov G, Li Z, Wilson P, Kempe K and Haddleton D M 2015 Well-defined protein/peptide–polymer conjugates by aqueous Cu-LRP: synthesis and controlled self-assembly *J. Am. Chem. Soc.* **137** 9344–53
[285] Xiang X, Ding X, Moser T, Gao Q, Shokuhfar T and Heiden P A 2015 Peptide-directed self-assembly of functionalized polymeric nanoparticles. Part II: Effects of nanoparticle composition on assembly behavior and multiple drug loading ability *Macromol. Biosci.* **15** 568–82
[286] Lim Y B, Lee E and Lee M 2007 Controlled bioactive nanostructures from self-assembly of peptide building blocks *Angew. Chem. Int. Ed.* **46** 9011–4
[287] Choi I, Park I-S, Ryu J-H and Lee M 2012 Control of peptide assembly through directional interactions *Chem. Commun.* **48** 8481–3
[288] Berdugo C, Nalluri S K M, Javid N, Escuder B, Miravet J F and Ulijn R V 2015 Dynamic peptide library for the discovery of charge transfer hydrogels *ACS Appl. Mater. Interfaces* **7** 25946–54
[289] Han T H, Ok T, Kim J, Shin D O, Ihee H, Lee H S and Kim S O 2010 Bionanosphere lithography via hierarchical peptide self-assembly of aromatic triphenylalanine *Small* **6** 945–51
[290] Sadownik J W, Leckie J and Ulijn R V 2011 Micelle to fibre biocatalytic supramolecular transformation of an aromatic peptide amphiphile *Chem. Commun.* **47** 728–30
[291] Ivnitski D, Amit M, Rubinov B, Cohen-Luria R, Ashkenasy N and Ashkenasy G 2014 Introducing charge transfer functionality into prebiotically relevant β-sheet peptide fibrils *Chem. Commun.* **50** 6733–6
[292] Ren C, Wang H, Mao D, Zhang X, Fengzhao Q, Shi Y, Ding D, Kong D, Wang L and Yang Z 2015 When molecular probes meet self-assembly: an enhanced quenching effect *Angew. Chem. Int. Ed.* **54** 4823–7
[293] Cai Y, Zhan J, Shen H, Mao D, Ji S, Liu R, Yang B, Kong D, Wang L and Yang Z 2015 Optimized ratiometric fluorescent probes by peptide self-assembly *Anal. Chem.* **88** 740–5
[294] Mermut O, Phillips D C, York R L, McCrea K R, Ward R S and Somorjai G A 2006 *In situ* adsorption studies of a 14-amino acid leucine-lysine peptide onto hydrophobic polystyrene and hydrophilic silica surfaces using quartz crystal microbalance, atomic force microscopy, and sum frequency generation vibrational spectroscopy *J. Am. Chem. Soc.* **128** 3598–607
[295] Fu L, Wang Z, Psciuk B T, Xiao D, Batista V S and Yan E C 2015 Characterization of parallel β-sheets at interfaces by chiral sum frequency generation spectroscopy *J. Phys. Chem. Lett.* **6** 1310–5
[296] Laaser J E, Skoff D R, Ho J-J, Joo Y, Serrano A L, Steinkruger J D, Gopalan P, Gellman S H and Zanni M T 2014 Two-dimensional sum-frequency generation reveals structure and dynamics of a surface-bound peptide *J. Am. Chem. Soc.* **136** 956–62
[297] Ortony J H, Newcomb C J, Matson J B, Palmer L C, Doan P E, Hoffman B M and Stupp S I 2014 Internal dynamics of a supramolecular nanofibre *Nat. Mater.* **13** 812–6
[298] Newcomb C J, Sur S, Ortony J H, Lee O-S, Matson J B, Boekhoven J, Yu J M, Schatz G C and Stupp S I 2014 Cell death versus cell survival instructed by supramolecular cohesion of nanostructures *Nat. Commun.* **5** 1–10
[299] Fishwick C W, Beevers A J, Carrick L M, Whitehouse C D, Aggeli A and Boden N 2003 Structures of helical β-tapes and twisted ribbons: the role of side-chain interactions on twist and bend behavior *Nano Lett.* **3** 1475–9
[300] Emamyari S and Fazli H 2014 pH-dependent self-assembly of EAK16 peptides in the presence of a hydrophobic surface: coarse-grained molecular dynamics simulation *Soft Matter* **10** 4248–57
[301] Yu T, Lee O-S and Schatz G C 2014 Molecular dynamics simulations and electronic excited state properties of a self-assembled peptide amphiphile nanofiber with metalloporphyrin arrays *J. Phys. Chem.* A **118** 8553–62
[302] Fu I W, Markegard C B, Chu B K and Nguyen H D 2014 Role of hydrophobicity on self-assembly by peptide amphiphiles via molecular dynamics simulations *Langmuir* **30** 7745–54
[303] Fu I W and Nguyen H D 2015 Sequence-dependent structural stability of self-assembled cylindrical nanofibers by peptide amphiphiles *Biomacromolecules* **16** 2209–19
[304] Lanza G, Chiacchio U, Motta S, Pellegrino S and Broggini G 2011 On the stability of polyalanine secondary structures: the role of the polyproline II helix *ChemPhysChem.* **12** 2724–7
[305] Perilla J R, Goh B C, Cassidy C K, Liu B, Bernardi R C, Rudack T, Yu H, Wu Z and Schulten K 2015 Molecular dynamics simulations of large macromolecular complexes *Curr. Opin. Struct. Biol.* **31** 64–74
[306] Tamamis P, Terzaki K, Kassinopoulos M, Mastrogiannis L, Mossou E, Forsyth V T, Mitchell E P, Mitraki A and Archontis G 2014 Self-assembly of an aspartate-rich sequence from the adenovirus fiber shaft: insights from molecular dynamics simulations and experiments *J. Phys. Chem.* B **118** 1765–74
[307] Lange S C, Unsleber J, Drücker P, Galla H-J, Waller M P and Ravoo B J 2015 pH response and molecular recognition in a low molecular weight peptide hydrogel *Org. Biomol. Chem.* **13** 561–9
[308] Frederix P W, Scott G G, Abul-Haija Y M, Kalafatovic D, Pappas C G, Javid N, Hunt N T, Ulijn R V and Tuttle T 2014 Exploring the sequence space for (tri-) peptide self-assembly to design and discover new hydrogels *Nat. Chem.* **7** 30–7
[309] Hamley I W, Nutt D R, Brown G D, Miravet J F, Escuder B and Rodríguez-Llansola F 2010 Influence of the solvent on the self-assembly of a modified amyloid beta peptide fragment: II. NMR and computer simulation investigation *J. Phys. Chem.* B **114** 940–51
[310] Schweitzer-Stenner R 2012 Simulated IR, isotropic and anisotropic Raman, and vibrational circular dichroism amide I band profiles of stacked β-sheets *J. Phys. Chem.* B **116** 4141–53
[311] Welch W R, Kubelka J and Keiderling T A 2013 Infrared, vibrational circular dichroism, and Raman spectral simulations for β-sheet structures with various isotopic labels, interstrand, and stacking arrangements using density functional theory *J. Phys. Chem.* B **117** 10343–58
[312] Baral A, Roy S, Dehsorkhi A, Hamley I W, Mohapatra S, Ghosh S and Banerjee A 2014 Assembly of an injectable noncytotoxic peptide-based hydrogelator for sustained release of drugs *Langmuir* **30** 929–36
[313] Castelletto V, Hamley I W, Hule R A and Pochan D 2009 Helical-ribbon formation by a β-amino acid modified amyloid β-peptide fragment *Angew. Chem. Int. Ed.* **48** 2317–20

[314] Houton K A, Morris K L, Chen L, Schmidtmann M, Jones J T, Serpell L C, Lloyd G O and Adams D J 2012 On crystal versus fiber formation in dipeptide hydrogelator systems *Langmuir* **28** 9797–806

[315] Bernadó P, Mylonas E, Petoukhov M V, Blackledge M and Svergun D I 2007 Structural characterization of flexible proteins using small-angle x-ray scattering *J. Am. Chem. Soc.* **129** 5656–64

[316] Guilbaud J-B and Saiani A 2011 Using small angle scattering (SAS) to structurally characterise peptide and protein self-assembled materials *Chem. Soc. Rev.* **40** 1200–10

[317] Zha R H, Sur S, Boekhoven J, Shi H Y, Zhang M and Stupp S I 2015 Supramolecular assembly of multifunctional maspin-mimetic nanostructures as a potent peptide-based angiogenesis inhibitor *Acta Biomater.* **12** 1–10

[318] Cui H, Pashuck E T, Velichko Y S, Weigand S J, Cheetham A G, Newcomb C J and Stupp S I 2010 Spontaneous and x-ray–triggered crystallization at long range in self-assembling filament networks *Science* **327** 555–9

[319] Mammadov R, Tekinay A B, Dana A and Guler M O 2012 Microscopic characterization of peptide nanostructures *Micron* **43** 69–84

[320] Thomas F, Burgess N C, Thomson A R and Woolfson D N 2015 Controlling the assembly of coiled–coil peptide nanotubes *Angew. Chem. Int. Ed.* **128** 999–1003

[321] Wang Y, Qi W, Huang R, Yang X, Wang M, Su R and He Z 2015 Rational design of chiral nanostructures from self-assembly of a ferrocene-modified dipeptide *J. Am. Chem. Soc.* **137** 7869–80

[322] Newcomb C J, Moyer T J, Lee S S and Stupp S I 2012 Advances in cryogenic transmission electron microscopy for the characterization of dynamic self-assembling nanostructures *Curr. Opin. Colloid Interface Sci.* **17** 350–9

[323] Danino D 2012 Cryo-TEM of soft molecular assemblies *Curr. Opin. Colloid Interface Sci.* **17** 316–29

[324] Chen Y, Gan H X and Tong Y W 2015 pH-controlled hierarchical self-assembly of peptide amphiphile *Macromolecules* **48** 2647–53

[325] Sharp T H, Bruning M, Mantell J, Sessions R B, Thomson A R, Zaccai N R, Brady R L, Verkade P and Woolfson D N 2012 Cryo-transmission electron microscopy structure of a gigadalton peptide fiber of *de novo* design *Proc. Natl. Acad. Sci. USA* **109** 13266–71

[326] Castelletto V, Hamley I W, Cenker C E, Olsson U, Adamcik J, Mezzenga R, Miravet J F, Escuder B and Rodríguez-Llansola F 2011 Influence of end-capping on the self-assembly of model amyloid peptide fragments *J. Phys. Chem.* B **115** 2107–16

[327] Goldsbury C, Kistler J, Aebi U, Arvinte T and Cooper G J 1999 Watching amyloid fibrils grow by time-lapse atomic force microscopy *J. Mol. Biol.* **285** 33–9

[328] Bracalello A, Santopietro V, Vassalli M, Marletta G, Del Gaudio R, Bochicchio B and Pepe A 2011 Design and production of a chimeric resilin-, elastin-, and collagen-like engineered polypeptide *Biomacromolecules* **12** 2957–65

[329] Lara C, Reynolds N P, Berryman J T, Xu A, Zhang A and Mezzenga R 2014 ILQINS hexapeptide, identified in lysozyme left-handed helical ribbons and nanotubes, forms right-handed helical ribbons and crystals *J. Am. Chem. Soc.* **136** 4732–9

[330] Pinotsi D, Buell A K, Galvagnion C, Dobson C M, Kaminski Schierle G S and Kaminski C F 2013 Direct observation of heterogeneous amyloid fibril growth kinetics via two-color super-resolution microscopy *Nano Lett.* **14** 339–45

[331] del Mercato L L, Pompa P P, Maruccio G, Della Torre A, Sabella S, Tamburro A M, Cingolani R and Rinaldi R 2007 Charge transport and intrinsic fluorescence in amyloid-like fibrils *Proc. Natl. Acad. Sci. USA* **104** 18019–24

[332] Pinotsi D, Buell A K, Dobson C M, Kaminski Schierle G S and Kaminski C F 2013 A label-free, quantitative assay of amyloid fibril growth based on intrinsic fluorescence *Chem. Bio. Chem.* **14** 846–50

[333] Petry R, Schmitt M and Popp J 2003 Raman spectroscopy—a prospective tool in the life sciences *Chem. Phys. Chem.* **4** 14–30

[334] Antonio K A and Schultz Z D 2013 Advances in biomedical Raman microscopy *Anal. Chem.* **86** 30–46

[335] Pozzi E A, Sonntag M D, Jiang N, Klingsporn J M, Hersam M C and Van Duyne R P 2013 Tip-enhanced Raman imaging: An emergent tool for probing biology at the nanoscale *ACS Nano* **7** 885–8

[336] Acar H, Genc R, Urel M, Erkal T S, Dana A and Guler M O 2012 Self-assembled peptide nanofiber templated one-dimensional gold nanostructures exhibiting resistive switching *Langmuir* **28** 16347–54

[337] Amit M, Cheng G, Hamley I W and Ashkenasy N 2012 Conductance of amyloid beta based peptide filaments: structure-function relations *Soft Matter* **8** 8690–6

[338] Amit M and Ashkenasy N 2014 Electronic properties of amyloid β-based peptide filaments with different non-natural heterocyclic side chains *Isr. J. Chem.* **54** 703–7

[339] Mizrahi M, Zakrassov A, Lerner-Yardeni J and Ashkenasy N 2012 Charge transport in vertically aligned, self-assembled peptide nanotube junctions *Nanoscale* **4** 518–24

[340] Frederix P L, Gullo M R, Akiyama T, Tonin A, de Rooij N F, Staufer U and Engel A 2005 Assessment of insulated conductive cantilevers for biology and electrochemistry *Nanotechnology* **16** 997–1005

[341] Juhaniewicz J, Pawlowski J and Sek S 2015 Electron transport mediated by peptides immobilized on surfaces *Isr. J. Chem.* **55** 645–60

[342] Kelley T W, Granstrom E and Frisbie C D 1999 Conducting probe atomic force microscopy: a characterization tool for molecular electronics *Adv. Mater.* **11** 261–4

[343] Wold D J and Frisbie C D 2001 Fabrication and characterization of metal-molecule-metal junctions by conducting probe atomic force microscopy *J. Am. Chem. Soc.* **123** 5549–56

[344] Atanassov A, Hendler Z, Berkovich I, Ashkenasy G and Ashkenasy N 2013 Force modulated conductance of artificial coiled-coil protein monolayers *Biopolymers* **100** 93–9

[345] Pawlowski J, Juhaniewicz J, Tymecka D and Sek S 2012 Electron transfer across α-helical peptide monolayers: importance of interchain coupling *Langmuir* **28** 17287–94

[346] Amdursky N 2013 Enhanced solid-state electron transport via tryptophan containing peptide networks *Phys. Chem. Chem. Phys.* **15** 13479–82

[347] Girard P 2001 Electrostatic force microscopy: principles and some applications to semiconductors *Nanotechnology* **12** 485–90

[348] Clausen C H, Dimaki M, Panagos S P, Kasotakis E, Mitraki A, Svendsen W E and Castillo-León J 2011 Electrostatic force microscopy of self-assembled peptide structures *Scanning* **33** 201–7

[349] Clausen C H, Jensen J, Castillo J, Dimaki M and Svendsen W E 2008 Qualitative mapping of structurally different dipeptide nanotubes *Nano Lett.* **8** 4066–9

[350] Du H, Li D, Wang Y, Wang C, Li P, Yang Y-l and Wang C 2014 Peptide-assisted directional adsorption of purple membrane at the liquid–solid interface *J. Phys. Chem.* C **118** 29770–6

[351] Sheikholeslam M, Pritzker M and Chen P 2014 Hybrid peptide–carbon nanotube dispersions and hydrogels *Carbon* **71** 284–93

[352] Melitz W, Shen J, Kummel A C and Lee S 2011 Kelvin probe force microscopy and its application *Surf. Sci. Rep.* **66** 1–27
[353] Shlizerman C, Atanassov A, Berkovich I, Ashkenasy G and Ashkenasy N 2010 *De novo* designed coiled-coil proteins with variable conformations as components of molecular electronic devices *J. Am. Chem. Soc.* **132** 5070–6
[354] Handelman A, Shalev G and Rosenman G 2015 Symmetry of bioinspired short peptide nanostructures and their basic physical properties *Isr. J. Chem.* **55** 637–44
[355] Cui X, Wiler J, Dzaman M, Altschuler R A and Martin D C 2003 *In vivo* studies of polypyrrole/peptide coated neural probes *Biomaterials* **24** 777–87
[356] Park B-W, Zheng R, Ko K-A, Cameron B D, Yoon D-Y and Kim D-S 2012 A novel glucose biosensor using bi-enzyme incorporated with peptide nanotubes *Biosens. Bioelectron.* **38** 295–301
[357] Chang W K, Wimley W C, Searson P C, Hristova K and Merzlyakov M 2008 Characterization of antimicrobial peptide activity by electrochemical impedance spectroscopy *BBA Biomembranes* **1778** 2430–6
[358] Xu H, Das A K, Horie M, Shaik M S, Smith A M, Luo Y, Lu X, Collins R, Liem S Y and Song A 2010 An investigation of the conductivity of peptide nanotube networks prepared by enzyme-triggered self-assembly *Nanoscale* **2** 960–6
[359] Viguier B, Zór K, Kasotakis E, Mitraki A, Clausen C H, Svendsen W E and Castillo-León J 2011 Development of an electrochemical metal-ion biosensor using self-assembled peptide nanofibrils *ACS Appl. Mater. Interfaces* **3** 1594–600
[360] Kurland N E, Drira Z and Yadavalli V K 2012 Measurement of nanomechanical properties of biomolecules using atomic force microscopy *Micron* **43** 116–28
[361] Zhang S, Aslan H, Besenbacher F and Dong M 2014 Quantitative biomolecular imaging by dynamic nanomechanical mapping *Chem. Soc. Rev.* **43** 7412–29
[362] Tranchida D, Piccarolo S and Deblieck R A C 2006 Some experimental issues of AFM tip blind estimation: the effect of noise and resolution *Meas. Sci. Technol.* **17** 2630–6
[363] Calabri L, Pugno N, Menozzi C and Valeri S 2008 AFM nanoindentation: tip shape and tip radius of curvature effect on the hardness measurement *J. Phys. Condens. Matter* **20** 474208
[364] Li X and Bhushan B 2002 A review of nanoindentation continuous stiffness measurement technique and its applications *Mater. Charact.* **48** 11–36
[365] Dagdas Y S, Tombuloglu A, Tekinay A B, Dana A and Guler M O 2011 Interfiber interactions alter the stiffness of gels formed by supramolecular self-assembled nanofibers *Soft Matter* **7** 3524–32
[366] Yuran S, Razvag Y, Das P and Reches M 2014 Self-assembly of azide containing dipeptides *J. Pept. Sci.* **20** 479–86
[367] Dagdas Y S, Aslan M N, Tekinay A B, Guler M O and Dâna A 2011 Nanomechanical characterization by double-pass force–distance mapping *Nanotechnology* **22** 295704
[368] Bolisetty S, Adamcik J, Heier J and Mezzenga R 2012 Amyloid directed synthesis of titanium dioxide nanowires and their applications in hybrid photovoltaic devices *Adv. Funct. Mater.* **22** 3424–8
[369] Sakai H, Watanabe K, Asanomi Y, Kobayashi Y, Chuman Y, Shi L, Masuda T, Wyttenbach T, Bowers M T and Uosaki K 2013 Formation of functionalized nanowires by control of self-assembly using multiple modified amyloid peptides *Adv. Funct. Mater.* **23** 4881–7
[370] Li D, Furukawa H, Deng H, Liu C, Yaghi O M and Eisenberg D S 2014 Designed amyloid fibers as materials for selective carbon dioxide capture *Proc. Natl. Acad. Sci. USA* **111** 191–6
[371] Shimanovich U, Efimov I, Mason T O, Flagmeier P, Buell A K, Gedanken A, Linse S, Åkerfeldt K S, Dobson C M and Weitz D A 2015 Protein microgels from amyloid fibril networks *ACS Nano* **9** 43–51
[372] Reynolds N P, Charnley M, Bongiovanni M N, Hartley P G and Gras S L 2015 Biomimetic topography and chemistry control cell attachment to amyloid fibrils *Biomacromolecules* **16** 1556–65
[373] Knowles T P and Buehler M J 2011 Nanomechanics of functional and pathological amyloid materials *Nat. Nanotechnol.* **6** 469–79
[374] Bortolini C, Jones N C, Hoffmann S V, Wang C, Besenbacher F and Dong M 2015 Mechanical properties of amyloid-like fibrils defined by secondary structures *Nanoscale* **7** 7745–52
[375] Rubin D J, Nia H T, Desire T, Nguyen P Q, Gevelber M, Ortiz C and Joshi N S 2013 Mechanical reinforcement of polymeric fibers through peptide nanotube incorporation *Biomacromolecules* **14** 3370–5
[376] Sathaye S, Mbi A, Sonmez C, Chen Y, Blair D L, Schneider J P and Pochan D J 2015 Rheology of peptide- and protein-based physical hydrogels: are everyday measurements just scratching the surface? *Interdiscip. Rev. Nanomed. Nanobiotechnol.* **7** 34–68
[377] Jones B H, Martinez A M, Wheeler J S and Spoerke E D 2015 Surfactant-induced assembly of enzymatically-stable peptide hydrogels *Soft Matter* **11** 3572–80
[378] King P J, Lizio M G, Booth A, Collins R F, Gough J E, Miller A F and Webb S J 2016 A modular self-assembly approach to functionalised β-sheet peptide hydrogel biomaterials *Soft Matter* **12** 1915–23
[379] Veerman C, Rajagopal K, Palla C S, Pochan D J, Schneider J P and Furst E M 2006 Gelation kinetics of β-hairpin peptide hydrogel networks *Macromolecules* **39** 6608–14
[380] Owczarz M, Bolisetty S, Mezzenga R and Arosio P 2015 Sol–gel transition of charged fibrils composed of a model amphiphilic peptide *J. Colloid Interface Sci.* **437** 244–51
[381] Chu T-W, Feng J, Yang J and Kopeček J 2015 Hybrid polymeric hydrogels via peptide nucleic acid (PNA)/DNA complexation *J. Control Release* **220** 608–16
[382] Herling T W, Garcia G A, Michaels T C, Grentz W, Dean J, Shimanovich U, Gang H, Müller T, Kav B and Terentjev E M 2015 Force generation by the growth of amyloid aggregates *Proc. Natl. Acad. Sci. USA* **112** 9524–9
[383] Wiester M J, Ulmann P A and Mirkin C A 2011 Enzyme mimics based upon supramolecular coordination chemistry *Angew. Chem. Int. Ed.* **50** 114–37
[384] Guler M O and Stupp S I 2007 A self-assembled nanofiber catalyst for ester hydrolysis *J. Am. Chem. Soc.* **129** 12082–3
[385] Singh N, Tena-Solsona M, Miravet J F and Escuder B 2015 Towards supramolecular catalysis with small self-assembled peptides *Isr. J. Chem.* **55** 711–23
[386] Enders D, Huttl M R M, Grondal C and Raabe G 2006 Control of four stereocentres in a triple cascade organocatalytic reaction *Nature* **441** 861–3
[387] Rodriguez-Llansola F, Escuder B and Miravet J F 2009 Remarkable increase in basicity associated with supramolecular gelation *Org. Biomol. Chem.* **7** 3091–4
[388] Rodriguez-Llansola F, Escuder B and Miravet J F 2009 Switchable perfomance of an L-proline-derived basic catalyst controlled by supramolecular gelation *J. Am. Chem. Soc.* **131** 11478–84
[389] Rodriguez-Llansola F, Miravet J F and Escuder B 2009 A supramolecular hydrogel as a reusable heterogeneous catalyst for the direct aldol reaction *Chem. Commun.* **2009** 7303–5
[390] Huang Z P, Guan S W, Wang Y G, Shi G N, Cao L N, Gao Y Z, Dong Z Y, Xu J Y, Luo Q and Liu J Q 2013 Self-assembly of amphiphilic peptides into bio-functionalized

nanotubes: a novel hydrolase model *J. Mater. Chem.* B **1** 2297–304
[391] Zhang C Q *et al* 2014 Self-assembled peptide nanofibers designed as biological enzymes for catalyzing ester hydrolysis *ACS Nano* **8** 11715–23
[392] Yu F T, Cangelosi V M, Zastrow M L, Tegoni M, Plegaria J S, Tebo A G, Mocny C S, Ruckthong L, Qayyum H and Pecoraro V L 2014 Protein design: toward functional metalloenzymes *Chem. Rev.* **114** 3495–578
[393] Jin Q X, Zhang L, Cao H, Wang T Y, Zhu X F, Jiang J and Liu M H 2011 Self-assembly of copper(II) ion-mediated nanotube and its supramolecular chiral catalytic behavior *Langmuir* **27** 13847–53
[394] Rufo C M, Moroz Y S, Moroz O V, Stohr J, Smith T A, Hu X Z, DeGrado W F and Korendovych I V 2014 Short peptides self-assemble to produce catalytic amyloids *Nat. Chem.* **6** 303–9
[395] Khalily M A, Gulseren G, Tekinay A B and Guler M O 2015 Biocompatible supramolecular catalytic one-dimensional nanofibers for efficient labeling of live cells *Bioconjugate Chem.* **26** 2371–5
[396] Schenning A P H J and Meijer E W 2005 Supramolecular electronics; nanowires from self-assembled pi-conjugated systems *Chem. Commun.* **26** 3245–58
[397] Kim S, Kim J H, Lee J S and Park C B 2015 Beta-sheet-forming, self-assembled peptide nanomaterials towards optical, energy, and healthcare applications *Small* **11** 3623–40
[398] Hauser C A E, Maurer-Stroh S and Martins I C 2014 Amyloid-based nanosensors and nanodevices *Chem. Soc. Rev.* **43** 5326–45
[399] Shao H, Nguyen T, Romano N C, Modarelli D A and Parquette J R 2009 Self-assembly of 1D n-type nanostructures based on naphthalene diimide-appended dipeptides *J. Am. Chem. Soc.* **131** 16374–6
[400] Shao H, Seifert J, Romano N C, Gao M, Helmus J J, Jaroniec C P, Modarelli D A and Parquette J R 2010 Amphiphilic self-assembly of an n-type nanotube *Angew. Chem. Int. Ed.* **49** 7688–91
[401] Diegelmann S R, Gorham J M and Tovar J D 2008 One-dimensional optoelectronic nanostructures derived from the aqueous self-assembly of pi-conjugated oligopeptides *J. Am. Chem. Soc.* **130** 13840–1
[402] Sanders A M, Dawidczyk T J, Katz H E and Tovar J D 2012 Peptide-based supramolecular semiconductor nanomaterials via Pd-catalyzed solid-phase 'Dimerizations' *ACS Macro Lett.* **1** 1326–9
[403] Wall B D, Diegelmann S R, Zhang S M, Dawidczyk T J, Wilson W L, Katz H E, Mao H Q and Tovar J D 2011 Aligned macroscopic domains of optoelectronic nanostructures prepared via shear-flow assembly of peptide hydrogels *Adv. Mater.* **23** 5009–14
[404] Vadehra G S, Wall B D, Diegelmann S R and Tovar J D 2010 On-resin dimerization incorporates a diverse array of pi-conjugated functionality within aqueous self-assembling peptide backbones *Chem. Commun.* **46** 3947–9
[405] Sun Y H, Jiang L, Schuermann K C, Adriaens W, Zhang L, Boey F Y C, De Cola L, Brunsveld L and Chen X D 2011 Semiconductive, one-dimensional, self-assembled nanostructures based on oligopeptides with pi-conjugated segments *Chem. Eur. J.* **17** 4746–9
[406] Schillinger E K, Mena-Osteritz E, Hentschel J, Borner H G and Bauerle P 2009 Oligothiophene versus beta-sheet peptide: synthesis and self-assembly of an organic semiconductor-peptide hybrid *Adv. Mater.* **21** 1562–7
[407] Eakins G L, Pandey R, Wojciechowski J P, Zheng H Y, Webb J E A, Valery C, Thordarson P, Plank N O V, Gerrard J A and Hodgkiss J M 2015 Functional organic semiconductors assembled via natural aggregating peptides *Adv. Funct. Mater.* **25** 5640–9
[408] Berdugo C, Nalluri S K M, Javid N, Escuder B, Miravet J F and Ulijn R V 2015 Dynamic peptide library for the discovery of charge transfer hydrogels *ACS Appl. Mater. Interfaces* **7** 25946–54
[409] Nalluri S K M, Berdugo C, Javid N, Frederix P W J M and Ulijn R V 2014 Biocatalytic self-assembly of supramolecular charge-transfer nanostructures based on n-type semiconductor-appended peptides *Angew. Chem. Int. Ed.* **53** 5882–7
[410] Nalluri S K M and Ulijn R V 2013 Discovery of energy transfer nanostructures using gelation-driven dynamic combinatorial libraries *Chem. Sci.* **4** 3699–705
[411] Nalluri S K M, Shivarova N, Kanibolotsky A L, Zelzer M, Gupta S, Frederix P W J M, Skabara P J, Gleskova H and Ulijn R V 2014 Conducting nanofibers and organogels derived from the self-assembly of tetrathiafulvalene-appended dipeptides *Langmuir* **30** 12429–37
[412] Ardona H A M and Tovar J D 2015 Energy transfer within responsive pi-conjugated coassembled peptide-based nanostructures in aqueous environments *Chem. Sci.* **6** 1474–84
[413] Chen L, Revel S, Morris K and Adams D J 2010 Energy transfer in self-assembled dipeptide hydrogels *Chem. Commun.* **46** 4267–9
[414] Lopez-Andarias J, Rodriguez M J, Atienza C, Lopez J L, Mikie T, Casado S, Seki S, Carrascosa J L and Martin N 2015 Highly ordered n/p-Co-assembled materials with remarkable charge mobilities *J. Am. Chem. Soc.* **137** 893–7
[415] Huang J L, Lin L Q, Sun D H, Chen H M, Yang D P and Li Q B 2015 Bio-inspired synthesis of metal nanomaterials and applications *Chem. Soc. Rev.* **44** 6330–74
[416] Cung K *et al* 2013 Biotemplated synthesis of PZT nanowires *Nano Lett.* **13** 6197–202
[417] Lee S Y, Lim J S and Harris M T 2012 Synthesis and application of virus-based hybrid nanomaterials *Biotechnol. Bioeng.* **109** 16–30
[418] Nuraje N, Dang X N, Qi J F, Allen M A, Lei Y and Belcher A M 2012 Biotemplated synthesis of perovskite nanomaterials for solar energy conversion *Adv. Mater.* **24** 2885–9
[419] Beznosov S N, Veluri P S, Pyatibratov M G, Chatterjee A, MacFarlane D R, Fedorov O V and Mitra S 2015 Flagellar filament bio-templated inorganic oxide materials—towards an efficient lithium battery anode *Sci. Rep.* **5** 1–7
[420] Zhang T J, Wang W, Zhang D Y, Zhang X X, Ma Y R, Zhou Y L and Qi L M 2010 Biotemplated synthesis of gold nanoparticle-bacteria cellulose nanofiber nanocomposites and their application in biosensing *Adv. Funct. Mater.* **20** 1152–60
[421] Liu J F, Uprety B, Gyawali S, Woolley A T, Myung N V and Harb J N 2013 Fabrication of DNA-templated Te and Bi_2Te_3 nanowires by galvanic displacement *Langmuir* **29** 11176–84
[422] Jackson E, Ferrari M, Cuestas-Ayllon C, Fernandez-Pacheco R, Perez-Carvajal J, de la Fuente J M, Grazu V and Betancor L 2015 Protein-templated biomimetic silica nanoparticles *Langmuir* **31** 3687–95
[423] McMillan R A, Howard J, Zaluzec N J, Kagawa H K, Mogul R, Li Y F, Paavola C D and Trent J D 2005 A self-assembling protein template for constrained synthesis and patterning of nanoparticle arrays *J. Am. Chem. Soc.* **127** 2800–1
[424] Matsui H, Pan S, Gologan B and Jonas S H 2000 Bolaamphiphile nanotube-templated metallized wires *J. Phys. Chem.* B **104** 9576–9
[425] Djalali R, Chen Y and Matsui H 2002 Au nanowire fabrication from sequenced histidine-rich peptide *J. Am. Chem. Soc.* **124** 13660–1

[426] Rabatic B M, Claussen R C and Stupp S I 2005 Templated mineralization of peptide-based unsymmetric bolaamphiphiles *Chem. Mater.* **17** 5877–9
[427] Sone E D and Stupp S I 2011 Bioinspired magnetite mineralization of peptide-amphiphile nanofibers *Chem. Mater.* **23** 2005–7
[428] Acar H, Garifullin R and Guler M O 2011 Self-assembled template-directed synthesis of one-dimensional silica and titania nanostructures *Langmuir* **27** 1079–84
[429] Yildirim A, Acar H, Erkal T S, Bayindir M and Guler M O 2011 Template-directed synthesis of silica nanotubes for explosive detection *ACS Appl. Mater. Interfaces* **3** 4159–64
[430] Acar H, Garifullin R, Aygun L E, Okyay A K and Guler M O 2013 Amyloid-like peptide nanofiber templated titania nanostructures as dye sensitized solar cell anodic materials *J. Mater. Chem.* A **1** 10979–84
[431] Khalily M A, Ustahuseyin O, Garifullin R, Genc R and Guler M O 2012 A supramolecular peptide nanofiber templated Pd nanocatalyst for efficient Suzuki coupling reactions under aqueous conditions *Chem. Commun.* **48** 11358–60
[432] Ceylan H, Ozgit-Akgun C, Erkal T S, Donmez I, Garifullin R, Tekinay A B, Usta H, Biyikli N and Guler M O 2013 Size-controlled conformal nanofabrication of biotemplated three-dimensional TiO_2 and ZnO nanonetworks *Sci. Rep.* **3** 1–7
[433] Tao K, Wang J Q, Li Y P, Xia D H, Shan H H, Xu H and Lu J R 2013 Short peptide-directed synthesis of one-dimensional platinum nanostructures with controllable morphologies *Sci. Rep.* **3** 1–6
[434] Zhou B B, Sun Z F, Li D, Zhang T, Deng L and Liu Y N 2013 Platinum nanostructures via self-assembly of an amyloid-like peptide: a novel electrocatalyst for the oxygen reduction *Nanoscale* **5** 2669–73
[435] Chen C L, Zhang P J and Rosi N L 2008 A new peptide-based method for the design and synthesis of nanoparticle superstructures: construction of highly ordered gold nanoparticle double helices *J. Am. Chem. Soc.* **130** 13555–7
[436] Jiang J A, Wang T Y and Liu M H 2010 Creating chirality in the inner walls of silica nanotubes through a hydrogel template: chiral transcription and chiroptical switch *Chem. Commun.* **46** 7178–80